FORECASTING OF PHOTOVOLTAIC
POWER SYSTEM PRODUCTION
USING THE METEOROLOGICAL INFORMATION

BY

PETI MEEBUNSMER

**A THESIS SUBMITTED IN PARTIAL FULFILLMENT OF
THE REQUIREMENTS FOR THE DEGREE OF MASTER OF
ENGINEERING IN ENGINEERING TECHNOLOGY
SIRINDHORN INTERNATIONAL INSTITUTE OF TECHNOLOGY
THAMMASAT UNIVERSITY
ACADEMIC YEAR 2014**

FORECASTING OF PHOTOVOLTAIC
POWER SYSTEM PRODUCTION
USING THE METEOROLOGICAL INFORMATION

BY

PETI MEEBUNSMER

**A THESIS SUBMITTED IN PARTIAL FULFILLMENT OF
THE REQUIREMENTS FOR THE DEGREE OF MASTER OF
ENGINEERING IN ENGINEERING TECHNOLOGY
SIRINDHORN INTERNATIONAL INSTITUTE OF TECHNOLOGY
THAMMASAT UNIVERSITY
ACADEMIC YEAR 2014**

FORECASTING OF PHOTOVOLTAIC POWER SYSTEM PRODUCTION
USING THE METEOROLOGICAL INFORMATION

A Thesis Presented

By

PETI MEEBUNSMER

Submitted to

Sirindhorn International Institute of Technology

Thammasat University

In partial fulfillment of the requirements for the degree of

MASTER OF ENGINEERING (ENGINEERING TECHNOLOGY)

Approved as to style and content by

Advisor and Chairperson of Thesis Committee _____ *chili C.* _____

(Assoc.Prof.Chalie Charoenlarpnopparut, Ph.D.)

Co-Advisor _____

( )

Committee Member and
Chairperson of Examination Committee _____

(Asst.Prof. Prapun Suksompong, Ph.D.)

Committee Member _____

(Asst.Prof. Thavatchai Tayjasanat, Ph.D.)

Committee Member _____

(Attaphongse Taparugssanagorn, Ph.D.)

MAY 2015

i

Acknowledgements

Abstract

FORECASTING PHOTOVOLTAIC POWER SYSTEM PRODUCTION
USING THE METEOROLOGICAL INFORMATION

by

PETI MEEBUNSMER

B.Eng., Chulalongkorn University, 2004

Solar power is one of the effective renewable energy resources used to generate electricity in Thailand which affect to the rapid increasing number of photovoltaic (PV) power plants. However, the main disadvantages in using PV power system are that the production can produce only in the daytime, and it has high variations subject to different weather conditions impacting to the stability and power quality of connected power grid system. The accurate power output forecasting is an important solution to help grid operators to efficiently manage and plan the schedule to work with the power system, as well as increasing the customer confidence on the power system reliability and stability. This study presents methods to forecast the PV power plant output using linear and non-linear algorithm, Multiple Linear Regression and Artificial Neural Network (ANN), respectively. Linear Regression Analysis is used to evaluate the daily generated energy prediction performance of three models. It provides the acceptable errors but solar radiation which is the main factor affected to the output is not automatically obtained. In the new model, it is designed by using calculated solar radiation and the meteorological information from the public website as input. Two ANN approaches are employed to predict the actual solar radiation in the first step before applying the estimated to forecast the hourly PV power system production. The accuracy performance of the model will be compared to other models in Thailand.

Keywords: Renewable Energy; Photovoltaic power plant output forecasting; Multiple Linear Regression; Artificial Neural Network

Table of Contents

List of Figures

List of Tables

Chapter 1

Introduction

1.1 Background

Energy crisis is currently one of the most important issues in Thailand as it affects throughout the country. It generates more and more serious problems that would rather leading to country development. The reason why energy crisis important is Thailand still import energy, including electrical energy, in a large amount from outside country for customer demand responding. However, Thailand also generates electricity from renewable and non-renewable energy resources which shown the details in Fig. 1.1 Unfortunately, the raw material using for generate electricity such as oil , coal , natural gas etc. has decreased in everyday and will be used up in the near future whereas the cost deemed inevitably increase.
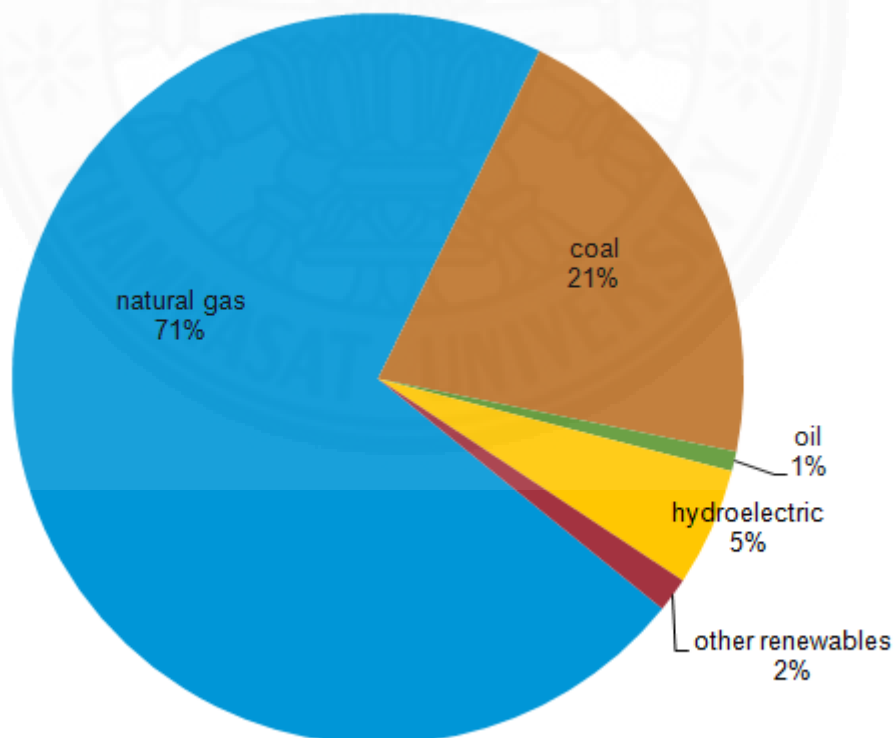
Source: Thailand Ministry of Energy

Figure 1.1: The various sources of Thailand electricity generation in 2011

From those aspects, the government focuses on electricity generation from renewable energy resources, e.g., solar power, wind power, hydro power etc. that will help to lessen greenhouse gas emission which is the factor of global warming issue, and also reduce non-renewable raw material and electricity energy importation. Therefore, the government has announced the policy to support electricity generation from renewable energy resources which cause to a large number of renewable energy resources power plants/distributed generators (DGs) construction.

The Provincial Electricity Authority (PEA) is a Government Enterprise in the utility sector attached to the Interior Ministry. The PEA's responsibility is primarily concerned with the generation, distribution, sales and provision of electric energy services to the business and industrial sectors as well as to the general public in provincial areas, with the exception of Bangkok, Nonthaburi and SamutPrakran provinces [1]. The PEA has declared 'PEA Smart Grid Policy' and 'PEA Smart Grid Roadmap 2012 to 2026' to keep up with the energy crisis issues and support the government policy. Fig. 1.2 shows PEA Smart Grid Roadmap.
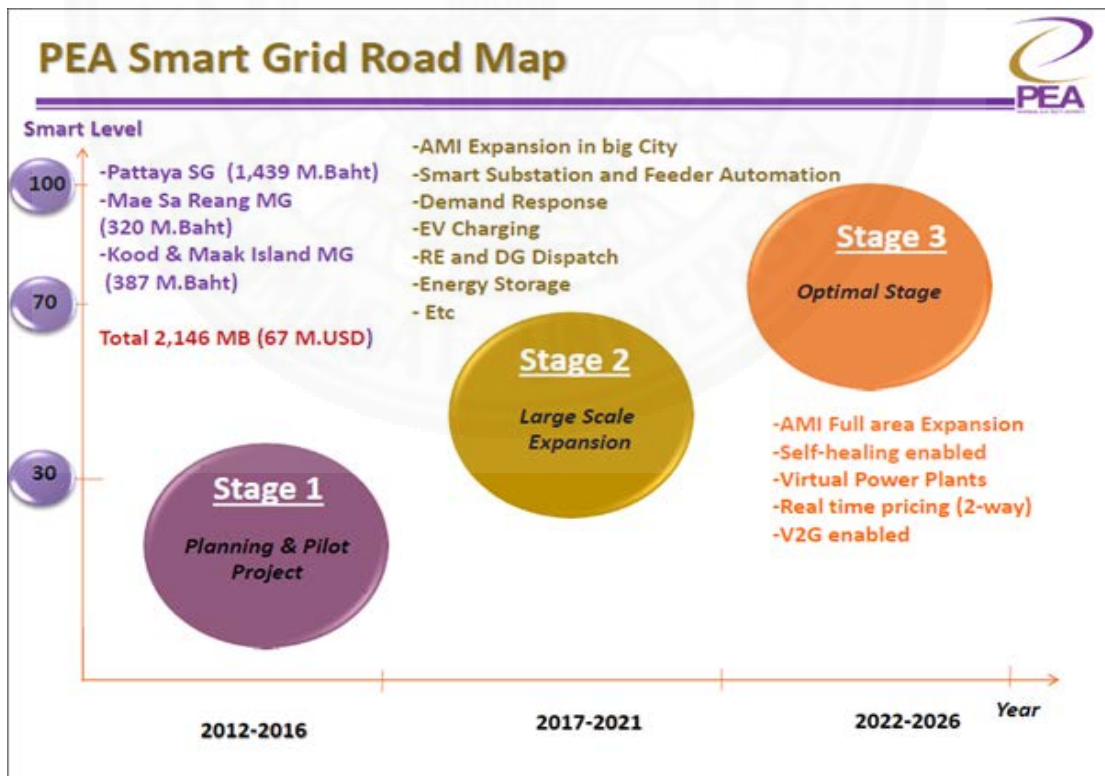
Source: Provincial Electricity Authority (PEA)

Figure 1.2: PEA Smart Grid Roadmap 2012 to 2026

2

PEA Smart Grid is the combination of information, communication and computer technologies (ICTs) and the PEA power grid system which using to effectively manage, monitor and control the generation system, including the distribution and transmission system. It will improve reliability, security, power quality of the power system to respond the growing of customers demand. One driver in the development of PEA Smart Grid which conform to the government policy is the safe and friendly power system for the environment. Hence, the penetration of DGs that use renewable energy resources to generate electricity is supported and contained in PEA Smart Grid Roadmap 2012 to 2026 [28].

DGs are electrical generators that diffusely located in the communities and directly connected to power system network. They are designed to support parallel operation with the utility power system and they have ability to feed electricity to a load by separate operation from the utility power system [2]. Moreover, they are installed throughout Thailand, including the rural area, by using various types of renewable energy as fuel sources to improve stability, continuity and reliability of the power system to maintain its power quality including reduce the distribution network power losses.

1.2 Statement of Problem

Solar power is one of the effective renewable energy resources because it can be applied to use in many applications such as thermal form, active solar or photovoltaic and passive solar (directly use solar intensity). Due to the environmental and energy crisis, solar power plays important roles to generate electricity because it is clean, free of charge, unlimited using and does not emit the pollution [3].

Thailand has rather high potential to generate electricity from solar power because its topography located at equator area that makes it got high intensity of solar radiation whole all the year. Fig. 1.3 which displays Thailand solar energy potential in average value and solar insolation potential when compare to the other countries also supports the above issue. The installation of solar panels connected to power grid system, solar rooftop or photovoltaic (PV) power plant, has been rapidly increased for electricity generation related to solar intensity potential [4].
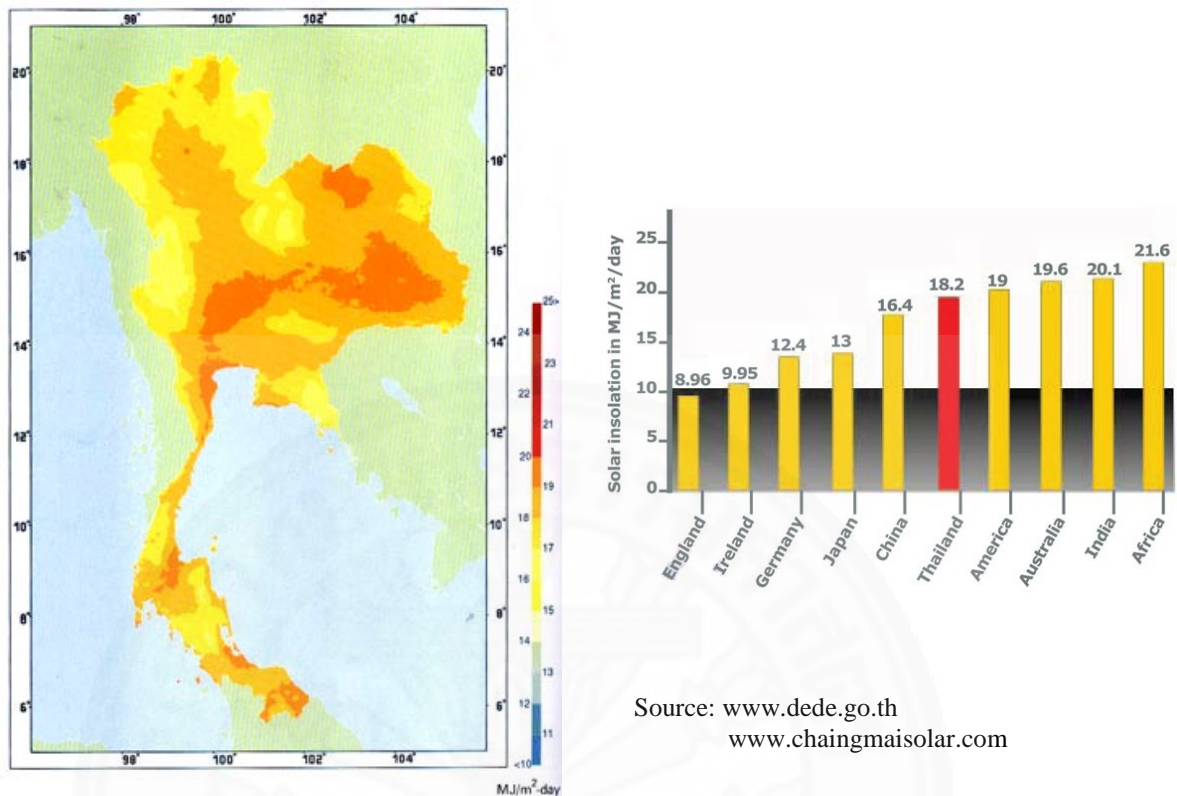
Figure 1.3: Map and graph of Thailand solar energy potential

However, the main disadvantages in using PV power system are the production cannot be generated whole day, it can produce only in the daytime, and it has high variations subjecting to different weather conditions. The fluctuation and intermittence of the outcome affect to the stability and power quality of connected power grid system. A grid operator who is also affected from them is difficult to schedule and manage the power system efficiently. In order to cooperate with demand side management, distribution automation and power system operation, developing an accurate algorithm for the forecasting of PV power system production has become essential.

1.3 Purpose of Study

The main objective of this study is to present the methods used to estimate the future production generated by PV power system under the weather information consideration. Furthermore, the suitable model applied for the output prediction is especially designed

4

for Thailand by using known weather parameters and solar radiation from the calculation.

1.4 Significance of Study

This study would like to present accurate approaches according to the designed model to predict the outcome from solar power system. They can help grid operator to schedule the spinning reserve capacity in energy storage system, administrate the variable of distributed generators in microgrid system for dispatching, planning and control including maintain power quality in standard level. Moreover, they are used to minimize electricity generation cost in microgrid system. In the case of investors, it would be easy to merchandise and make decision on energy planning if they know the production in the future.

1.5 Review of Literature

This section provides a review of the work relevant to this research. There are many techniques used for modelling the solar radiation or the PV power system production. Linear and non-linear models are introduced and applied to typical time series collected from PV systems.

Two methods forecasting the output from PV stations, physical method and statistical method, were compared in [5]. A physical model combined the sun position model and the diode model which related to the temperature and solar irradiance. Artificial Neural network (ANN) was applied to statistical model by using weather information, obtained from a numerical weather prediction (NWP), as input variable same as physical model. This study illustrated statistical model provided better performance than physical model in the prediction.

In Linear Regression model, [6] predicted the morning hours solar radiation. It applied the first and second order regression and multiple correlation analysis method. The forecast error by using both humidity and temperature in the first order equation was minimal.

Statistical methods based on Linear Regression Analysis and ANN have been developed in [7] to predict the output of PV power generation for one week ahead using global solar radiation and environmental temperature. The strength of correlation between weather parameters and the production affected to the forecast error of model

5

[8] also underlined the several weather parameters influenced to the accuracy of PV power prediction. Thus, the number and category of input data are important data in the estimation.

Solar radiation and ambient temperature were the basic factors which used to predict the production. Moreover, humidity and wind velocity also influenced to the efficiency of PV cells. In analyzing the effect of humidity, the effect of water vapor particles on the irradiance level of sunlight and humidity ingression to the solar cell enclosure need to be considered. Wind velocity is one factor impacted to PV cell temperature which sharply respond to the PV cell performance. By increasing of humidity, it always caused to degrade the efficiency of solar cells. While wind velocity increased, it can remove heat from solar cell surface which lead to the better performance [9].

Linear time-series models were reported in [10] where forecasted accuracy of autoregressive (AR) and autoregressive with exogenous input (ARX) models. These two models were used to predict hourly values of solar power up to 36 hours ahead. The results indicated that ARX performed better than AR and exogenous input (solar irradiance forecast from NWP models) was significant when the horizon is longer than 2 hours.

In [11], a review of solar radiation prediction using different ANN technique was presented. The ANN models were found to estimate solar radiation more accurately than Angstrom model, conventional, linear, non-linear and fuzzy logic models. It also indicated that the appropriate selection of input parameters was important for predicting with better accuracy. ANN model has been proposed in [12] to predict diffuse fraction in hourly and daily scale to compare the performance of ANN model with two linear regression models. The results hint that the ANN model is more suitable to predict diffuse fraction in hourly and daily scales than the regression models. Besides [13] and [14] applied ANN to confirm the higher performance and more suitable to predict than various proposed approaches: polynomial regression, multiple linear regression, analytical and one-diode models.

In [15], the applicability neural networks for 24 hours ahead solar power generation forecasting was presented. Three conventional neural network, Multi-layered Perceptron Neural Network (MLPNN), Radial Basis Function Neural Network

(RBFNN) and Recurrent Neural Network (RNN), were proposed in this study and they fulfilled an acceptable forecasting accuracy. In comparison, the great performance was displayed by RBFNN while MLPNN achieved the lowest estimation accuracy. Moreover, the work of [16] presented two ANN structures, General Regression Neural Network (GRNN) and Feedforward Back Propagation (FFBP), used to approximate the generated PV panels output. At the end, both of these networks have shown good modelling performance; however, FFBP has displayed a better performance comparing with GRNN.

Additionally, the estimation and forecast of daily solar radiation using Focused Time-Delay Neural Network (FTDNN) and NARX Network was proposed in [17]. Both of these models showed the good performance and can simplify energy management system when energy storage system are adopted. However, the error on estimated energy generated by PV field of NARX model is lower.

In the literatures, various forecasting models automatically achieved solar intensity on the forecasted day. However, in reality radiation models of inclined surfaces were a perquisite input which was not always available. The work of [18] proposed a low-cost method based on a NARX in order to forecast hourly power output on 24 hours ahead for PV power system. Solar radiation calculated in the clear sky condition and meteorological forecasting reports coming from online provider were taken as the input. NARX and MLP were compared to forecast the daily power output of PV. NARX displayed outperform and also can be employed to forecast precisely.

All of the previous literatures have an essential role in the development of this thesis. Although the parameters used in each study may be different, there are some important details to retrieve from the results, the algorithm, type of ANN or even the horizon for PV power system production prediction. This study will display linear and non-linear algorithm to achieve more accurate estimated results of photovoltaic power system production by modifying the previous model format.

1.6 Thesis Structure

The rest of this thesis is arranged as follows. Chapter 2 provides a review of a brief related background theory according to the basic knowledge of PV cell and forecasting methodologies. In Chapter 3, the implementation of linear algorithm is presented. In

particular, section 3.1 describes the detail of data source and algorithm guideline. Linear models are displayed in section 3.2 and the correlations between weather parameter and PV power system production are presented in section 3.3. Linear regression analysis applied on the models is explained in section 3.4 following with experiment results including discussion in section 3.5.

Non-linear algorithm is shown in Chapter 4. The detail of data source and process guideline is described in section 4.1 and section 4.2 shows the models used in non-linear algorithm. Section 4.3 presents the relationship between weather parameter that not contained in linear algorithm and PV power system production. In section 4.4, Artificial Neural Network (ANN), Feedforward Neural Network and Nonlinear autoregressive network with exogenous inputs (NARX), applied on the models in section 4.2 is illustrated. The experiment results and discussion are followed in the last section.

Finally, the main conclusions of this study from the experiment results are presented in Chapter 5.

Chapter 2

Background Theory

2.1 Photovoltaic Cells

Solar cells, also called PV cells, are the photovoltaic system fundamental unit which are applied to convert power. They use their organic molecules to convert light to electricity when a source of light shines on it. When the solar cell gets connected to a circuit via wires, the electrical current flows through the wire, as a result work will be produced.

There are four major types of PV cells namely, mono-crystalline (or single crystalline), poly-crystalline, amorphous and organic cells. Nano PV is also a newly introduced kind of solar cells. They are mostly produced out of copper, cadmium sulphide, gallium arsenide and cadmium telluride and etc. while optical properties silicon holds the top position among these materials.

The operation of a shaded PV cell can be described by diode equation. An I–V characteristic can clearly describe the performance of PV cell under different environmental conditions such as temperature and illumination. Then, the output current I is the difference between the light-generated current, I_l, and the diode current, I_s, the equation of I-V characteristic is presented below:

$$I = I_l - I_s(e^{(qv/kT)} - 1)$$

(1)

where q is an electron charge, $q = 1.6x10^{-19}$ C, k is the Boltzmann's constant $k = 1.38x10^{-23}$ J/K. T_C is the cell temperature and V is the terminal voltage of the cell. I_s is the diode saturation current, and this current indicates that PV cells function as a semiconductor current rectifier or diode when there is no sunlight hitting the cells.
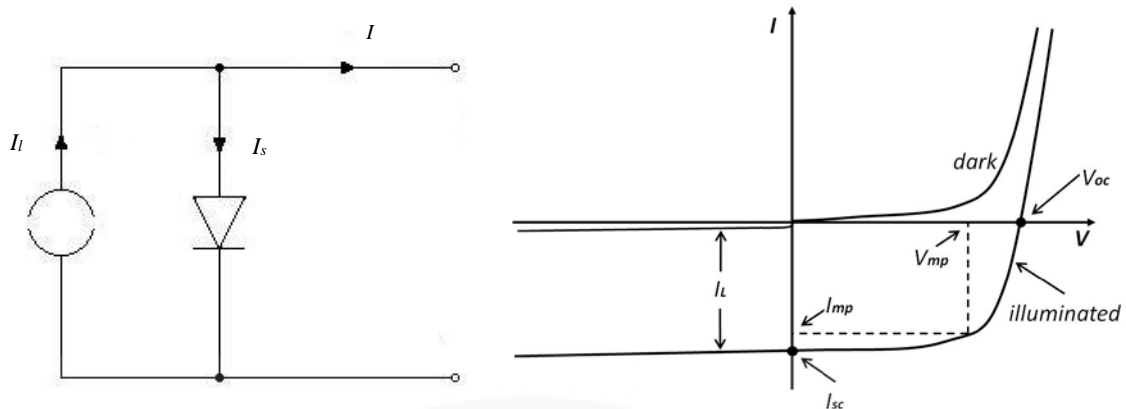
Figure 2.1: The equivalent circuit and *I-V* characteristics of a solar cell compared to diode

The equivalent circuit is shown in above. Under open circuit, $I = 0$, all the light-generated current passes through the diode. Whereas under short circuit ($V = 0$), all this current passes through the external load. An *I-V* characteristic in (1) and the relationship between it and diode characteristic are show in Fig. 2.1. The important points are considered. One is short-circuit current, I_{SC}, which is simply the light-generated current I_l. The second is the open-circuit voltage, V_{OC}, gathered by setting $I = 0$.

$$V_{OC} = \frac{kT}{q} \ln(\frac{I_l}{I_o} + 1) \qquad (2)$$

Both I_l and I_o depend on the structure of the device. No power is generated under short or open circuit. The maximum power P_{max} produced by the device is reached at a point on the characteristic where the product *IV* is maximum. This is displayed in Fig. 2.2 where the position of the *maximum power point* represents the largest area of rectangle shown. One usually defines the fill factor FF by

$$P_{max} = V_m * I_m = FF * V_{OC} * I_{SC} \qquad (3)$$

where V_m and I_m are the voltage and current at the maximum power point.

10
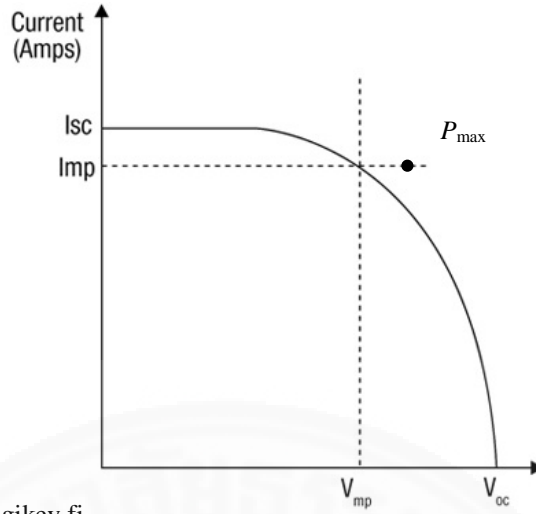
Figure 2.2: The *I-V* characteristics of a solar cell with the maximum power point

The efficiency, η, of a solar cell is expressed as the power generated by the PV module at MPPT under standard test conditions, P_{max}, divided by the power of radiation incident on it, P_{in}. Most frequent conditions are irradiance 100 mW/cm^2, standard reference AM 1.5 spectrum, and temperature 25 °C. Using this irradiance standard value is especially convenient since the efficiency is in percent form and it is numerically equal to the cell power output.

$$\eta = \frac{P_{max}}{P_{in}} = \frac{FF * V_{OC} * I_{SC}}{P_{in}} \tag{4}$$

2.2 Factors Affecting Production of Photovoltaic System [18]

The maximum DC power output for PV panels that have identical orientation can be clearly defined as

$$P_{PV} = \eta A_{PV} G_T [1 - 0.005(T_C - 25)] \tag{5}$$

where η is the PV array photoelectric conversion efficiency (%), A_{PV} is the total PV array area (m^2), G_T is the solar radiation incident on the modules (kW/m^2), and T_C is the temperature of PV panel (°C). By the way, the grid-connected PV inverters almost operate in the Maximum Power Point Tracking (MPPT) mode with relatively constant power conversion efficiency. From these features, AC power output is mostly defined by the operation temperature and the solar radiation at the area that PV arrays are installed.

It seems that AC power output of PV power system can be exactly predicted whenever the solar radiation and the panel's operation temperature can be estimated accurately. However, it is almost impossible to measure all PV modules temperature for the prediction since many temperature sensors must be used and the limitation in computation. In the fact, the operation temperature is affected from many factors such as ambient temperature, environmental wind speed, humidity, air pressure and etc. Then, the weather conditions are applied as input variables to forecast the PV power production in the previous methods.

From equation (5), it is also shown that solar irradiance is the important factor to estimate the outcome from solar power plant. In any way, solar radiation is influenced by solar position, atmospheric transmittance, cloud cover, and the orientation of PV panels at the same time. Therefore, it can summarize that the production of PV power system associate to its configuration and meteorological conditions.

2.3 Solar Radiation Calculation [18]

The total solar radiation that incidents on an inclined PV panel (G_T) is the combination of three radiation components: beam (G_{bT}), diffuse (G_{dT}) and reflected (G_{rT}) which is displayed in Fig. 2.3 (a) and it can determine as

$$G_T = G_{bT} + G_{dT} + G_{rT} \tag{6}$$
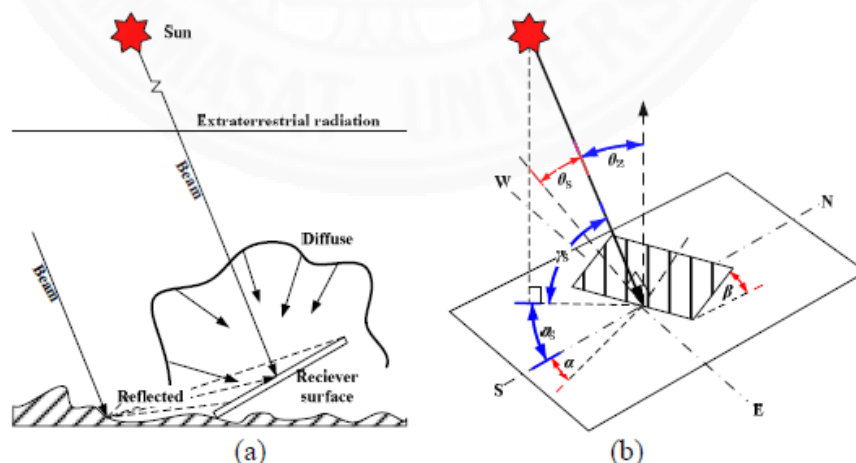
Figure 2.3: (a) Configuration of the total solar radiation on inclined surface
(b) The definition of solar angles and surface orientation

Three radiation components can be calculated from the following equations

$$G_{bT} = G_{on}\tau_b \cos\theta_s \tag{7.a}$$

$$G_{dT} = G_{on}\cos\theta_z \tau_d \left(\frac{1+\cos\beta}{2}\right) \tag{7.b}$$

$$G_{rT} = \rho G_{on}\cos\theta_z \tau_r \left(\frac{1+\cos\beta}{2}\right) \tag{7.c}$$

where G_{on} is the solar radiation which incident on the surface which normal to the radiation and locate outside the earth atmosphere (W/m.^{2}). It can also call "*extraterrestrial solar radiation*". τ_d, τ_b, τ_r are the atmospheric transmittance for three radiation components; beam, diffuse and reflected respectively. θ_S is the angle between the direction to the sun (deg) and the normal to the surface (deg). θ_Z, β and ρ are, respectively, the solar zenith angle (rad), the surface inclination angle (deg) and the ground's average reflectance. G_{on} can be expressed by

$$G_{on} = G_{sc}\left[1+0.033\times\cos(360D/365)\right] \tag{8}$$

where G_{sc} is the solar constant, $G_{sc} = 1{,}367$ W/m^2, and D is the day of year that $1 \leq D \leq 365$.

The beam radiation's atmospheric transmittance, τ_b, can be calculated from Hottel's equation which shows as follow:

$$\tau_b = a_0 + a_1\exp(-k/\cos\theta_z) \tag{9}$$

where a_0, a_1 and k are constants which can be calculated from the following equations also proposed by Hottel:

$$a_0 = r_0\left[0.4237-0.00821(6-A)^2\right] \tag{10.a}$$

$$a_1 = r_1\left[0.5055+0.00595(6.5-A)^2\right] \tag{10.b}$$

$$k = r_k\left[0.2711+0.01858(2.5-A)^2\right] \tag{10.c}$$

where A is the PV module altitude in km, r_0, r_1 and r_k are correction factors for four different types of climate and presented in Table 2.1.

The atmospheric transmittance of diffuse and reflected radiation component, τ_d and τ_r, can be calculated from (11) and (12), respectively.

$$\tau_d = 0.271 - 0.294\tau_b \tag{11}$$

$$\tau_r = 0.271 + 0.706\tau_b \tag{12}$$

Table 2.1: Correction factors for different climate types

Climate Types	r_0	r_1	r_k
Tropical	0.95	0.98	1.02
Midlatitude summer	0.97	0.99	1.02
Midlatitude winter	0.99	0.99	1.01
Subarctic summer	1.03	1.01	1.00

The solar zenith angle, θ_z, and the incident angle, θ_s, can be calculated as following equations

$$\cos\theta_z = \cos\delta\cos\phi\cos\varpi + \sin\delta\sin\phi \tag{13}$$

$$\cos\theta_s = \sin\delta\sin\phi\cos\beta - \sin\delta\cos\phi\sin\beta\cos\alpha + \cos\delta\cos\phi\cos\beta\cos\varpi \tag{14}$$
$$+ \cos\delta\sin\phi\sin\beta\cos\alpha\cos\varpi + \cos\delta\sin\alpha\sin\varpi\sin\beta$$

where δ is the solar declination, ϕ is the PV system location latitude, ϖ is the hour angle and α is the azimuth angle. These five parameters have the same unit; it is degree.

The solar declination, δ, is expressed by

$$\delta = 23.45\sin\left[360(D + 284)/365\right] \tag{15}$$

The apparent or local solar time, *AST*, in the western longitudes is given by

$$AST = LST + (4\min/\deg)(LSTM - Long) + ET \tag{16}$$

where *LST* is local standard time or clock for that time zone, *Long* is local longitude at the position of interest, and *LSTM* is local longitude of standard time meridian

$$LSTM = 15° \times \left[\frac{Long}{15°}\right]_{\text{round to integer}} \tag{17}$$

The equation of time in minute, *ET*, is calculated as follow:

$$ET = 2.292(0.0075 + 0.1868\cos\theta - 3.2077\sin\theta - 1.4615\cos 2\theta - 4.089\sin 2\theta) \qquad (18)$$

where $\theta = 360(D\text{-}1)/365$, θ in degree

The hour angle, ϖ, is an angular measure of time and equivalent to 15° per hour during the morning (+) and afternoon (-). It is expressed as

$$\varpi = \frac{\left(No.\ of\ minutes\ past\ midnight,\ AST\right)\ -\ 720\ \text{mins}}{4\,\text{min}/\deg} \qquad (19)$$

The ground's average reflectance, ρ, is equal to 0.2, 0.8, and 0.15 when solar radiation reflects on normal ground or vegetation, snow covered ground, and gravel roof, respectively.

2.4 Regression Analysis [20]

Regression analysis is a statistical methodology that analyzes the relationship between two or more quantitative variables, dependent and independent variable, so that an outcome variable can be predicted from the other. Linear Regression is the most popular because of its simplicity and it can be applied to estimate the relationship between one dependent variable and one independent variable, called *Simple Linear Regression*. The other one, using for more than one independent variable, is called *Multiple Linear Regression*.

A. Simple Linear Regression

A linear regression model, with a single independent variable, uses ordinary least squares criterion for estimating unknown parameters called *Simple Linear Regression*. The simplest mathematical expression for the straight line given by

$$y = a_0 + a_1 x + e \qquad (20)$$

where x is independent or explanatory variable while y is dependent variable, a_0 and a_1 are coefficients representing the intercept and the slope, respectively, e is the error or residual between the model and the observations.

A strategy, for fitting a best line through the set of n observations and minimizing the sum of the squares of the residuals, is called *least-square algorithm.* The sum of the squares of the residuals can be expressed as

$$Sr = \sum_{i=1}^{n} e_i^2 = \sum_{i=1}^{n} (y_i - a_0 - a_1 x_i)^2 \tag{21}$$

Next, Eq. (21) is differentiated with respect to each unknown coefficient to determine a_0 and a_1. Then, set these derivatives equal to zero to obtain the minimum Sr and so,

$$a_0 = \bar{y} - a_1 \bar{x} \tag{22}$$

$$a_1 = \frac{n \sum x_i y_i - \sum x_i \sum y_i}{n \sum x_i^2 - (\sum x_i)^2} \tag{23}$$

where $\bar{y}$ is mean of y and $\bar{x}$ is mean of x.

The goodness level of variation in the dependent variable y, explained by the explanatory variables x, in the linear regression model, is estimated by the coefficient of determination, R^2. For a perfect fit, $R^2 = 1$, signifying that the line explains 100% of the variability of data but the fit represents no improvement for $R^2 = 0$. An alternative formula for R^2 is given by

$$R^2 = \left(\frac{n \sum (x_i y_i) - (\sum x_i)(\sum y_i)}{\sqrt{n \sum x_i^2 - (\sum x_i)^2} \sqrt{n \sum y_i^2 - (\sum y_i)^2}} \right)^2 \tag{24}$$

B. Multiple Linear Regression

Multiple linear regression is one of general linear least-squares model. It attempts to model the relation between two or more explanatory variables and a dependent variable by fitting a linear equation to observed data. The basic expression of multiple linear regression model of n variables is

$$y = a_0 + a_1 x_1 + a_2 x_2 + \dots + a_n x_n + e \tag{25}$$

To evaluate the best values of the unknown coefficients, the least-squares procedure can be extended to fit the data. For the case of two independent variables, the sum of the squares of the residuals becomes

$$Sr = \sum_{i=1}^{n} (y_i - a_0 - a_1 x_{1,i} - a_2 x_{2,i})^2 \tag{26}$$

We can minimize Sr by differentiating Eq. (26) with respect to each of the unknown coefficients and setting the partial derivatives equal to zero. The following set of normal equations can be generated in matrix form as

$$
\begin{bmatrix}
n & \sum x_{1,i} & \sum x_{2,i} \\
\sum x_{1,i} & \sum x_{1,i}^2 & \sum x_{1,i}x_{2,i} \\
\sum x_{2,i} & \sum x_{1,i}x_{2,i} & \sum x_{2,i}^2
\end{bmatrix}
\begin{bmatrix} a_0 \\ a_1 \\ a_2 \end{bmatrix}
=
\begin{bmatrix}
\sum y_i \\
\sum x_{1,i}y_i \\
\sum x_{2,i}y_i
\end{bmatrix}
\tag{27}
$$

The coefficients yielding the minimum sum of the residuals, a_0, a_1 and a_2 are obtained by solving (27)

The coefficient of determination, R^2, is described by

$$
R^2 = 1 - \frac{St}{Sr}
\tag{28}
$$

St is the square of the residual:

$$
St = \sum_{i=1}^{n}(y_i - \bar{y})^2
\tag{29}
$$

Sr is the sum of the squares of the residuals and its equation is shown in (26)

2.5 Feedforward Neural Network (FFNN)

A simple type of neural network which the information flows in the forward direction is Feedforward Neural Network. It consists of a series of layers; input layer, hidden layer and output layer. In each layer, every node is connected to every node in the previous layer. A typical feedforward neural network is shown in Fig 2.4.
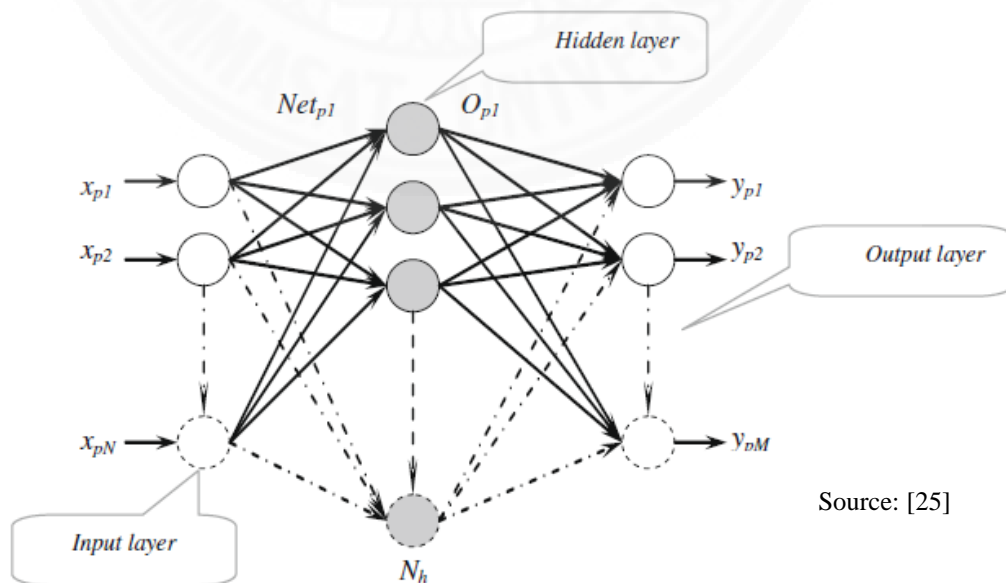
Source: [25]

Figure 2.4: The structure of FFNN model

17

Assumed that the input layer consists of *N* nodes, hidden layers consists of *h* nodes and output layer consists of *M* nodes. The *i*th node output in the output layer is expressed as follow

$$y_i = f(\sum_{j=1}^{h}(w_{ij}f(\sum_{k=1}^{N}v_{jk}x_k + \theta_{vj}) + \theta_{wi})) , i = 1,...,M \tag{30}$$

where y_i is the output of the *i*th node in the output layer, x_k is the input of the *k*th node in the input layer, w_{ij} is the connective weight between nodes in the hidden and output layers, v_{jk} is the connective weight between the nodes in the input and hidden layers, and θ_{wi} (or θ_{vj}) are bias terms that represent the threshold of the transfer function *f* [26].

The hidden layers of feedforward networks often consist of sigmoid neurons followed by an output layer of linear neurons. Network are studied nonlinear relationships between input and output vectors by using multiple layers of neurons with nonlinear transfer functions. The layer number determines the superscript on the weight matrix. The appropriate notation is used in the two-layer tansig/purelin network displayed below.
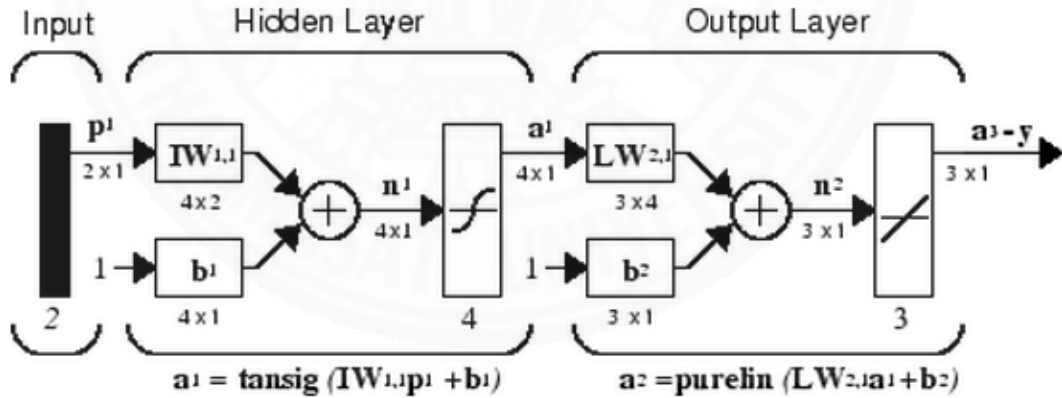
Figure 2.5: A typical of two-layer FFNN model

This network can be applied as a general function to estimate any function with a finite number of discontinuities arbitrarily well. [22]

2.6 Nonlinear Autoregressive Network with Exogenous Inputs (NARX)

The nonlinear autoregressive network with exogenous inputs (NARX) is an important class of discrete-time nonlinear systems. It uses the past values of the actual time series

to be predicted and past values of other inputs to make predictions about the future value of the target series. The defining equation for the NARX model is defined as follow

$$y(t) = f(y(t-1),...y(t-n_y); u(t-1),...,u(t-n_u)) + \varepsilon(t) \tag{31}$$

where $u(t)$ and $y(t)$ respectively represent the input and output of the model at discrete time step t, while $n_u \geq 1$ and $n_y \geq 1$, $n_u \leq n_y$ are the input-memory and output-memory orders, and $\varepsilon(t)$ is a noise term. The structure of NARX is depicted in below [21].
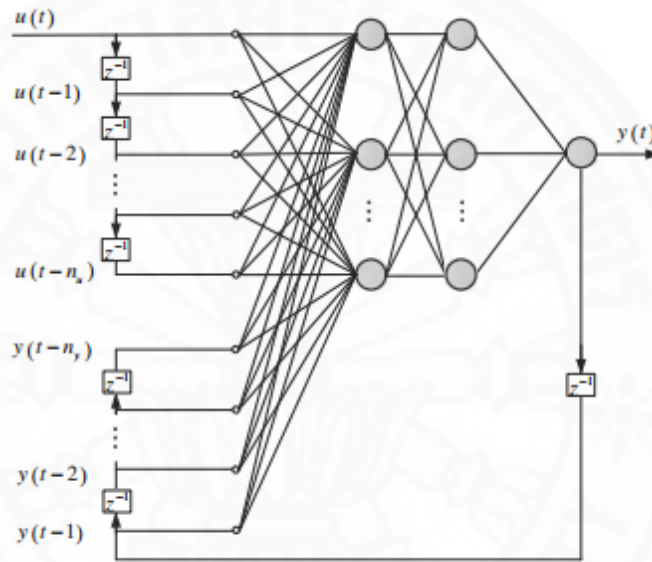
Source: [9]

Figure 2.6: The structure of NARX model

The NARX is a recurrent dynamic network, with feedback connections enclosing several layers of the network. The NARX model is based on the linear ARX model, which is commonly used in time-series modeling. It can be implemented by using a feedforward neural network to approximate the function f. A diagram of the resulting network is shown below, where a two-layer feedforward network is used for the approximation. This implementation also allows for a vector ARX model, where the input and output can be multidimensional [22]. This model is widely used in many applications since it is suitable for nonlinear dynamic model.

19
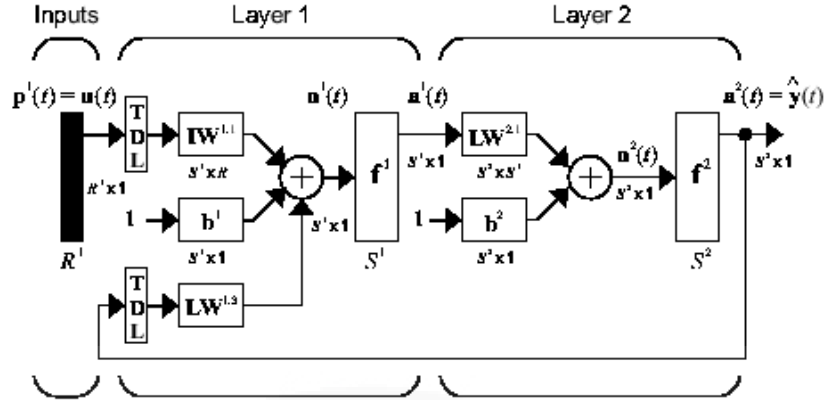
Figure 2.7: A typical NARX model

2.7 Prediction Accuracy Evaluation

2.7.1 Mean Absolute Percentage Error (MAPE) [23]

MAPE is the most common measure of forecast error. When it does not have severe to the data, MAPE functions is the best.

With zero or near-zero data, MAPE can provide a distorted picture of error. The error on a near-zero item can be infinitely high which making a distortion to the total error rate.

MAPE is the average absolute percent error for the difference between the forecasted data and actual data, divided by actual expressed as following:

$$MAPE = \frac{100}{N} \sum_{i=1}^{N} \frac{|P_f^i - P_a^i|}{P_a^i} \% \tag{32}$$

where N is the total number of data, P_f^i is the predicted value, P_a^i is the actual value, i is the index of the data.

2.7.2 Mean Squared Error (MSE) [27]

The mean squared error is the most important criterion used to evaluate the performance of a predictor or an estimator. It is a slight difference between predictors and estimators that predict random variables and estimate constants.

In statistical estimation, the mean squared error is also useful to relay the concepts of bias, precision, and accuracy. An estimation or prediction target, and a predictor or estimator that is a function of the data is needed for MSE investigation.

20

Suppose that $\hat{Y}$ represents a vector of N predictions and Y is denoted as the vector of the true values. The mean squared error (MSE) of the predictor display as following:

$$MSE = \frac{1}{N}\sum_{i=1}^{N}(\hat{Y}_i - Y_i)^2 \tag{33}$$

Chapter 3

Linear Analysis

In this research, the methodology is divided to two algorithms, Linear and Non-linear Analysis, and they are implemented in MATLAB@2013a program which simplify to adopt. This chapter proposes linear algorithm to predict the production generated by solar power plant system. For non-linear algorithm, it is explained in the following chapter.

3.1 Step of Procedure

1. Contact the solar power plant for gathering data used in the experiment: Daily system production and weather parameter
2. Design experimental model and study the strength of correlation between weather parameters and the system output
3. Evaluate performance of the model
4. Apply data only obtained from Thai Meteorological Department to design model and study its performance
5. Summarize the experiment

3.2 Data Description

Experimental data are provide by solar energy power plant, L Solar 1 Co., Ltd., with capacity 8.7 MW. It located at Kabinburi district, Prachinburi province in Thailand (13°57'42.99" N, 101°50'06.61" E). At this site, Amorphous Silicon thin film PV type module manufactured from Du Pont Apollo (Shenzhen) Limited and three-phase inverter supplied by LEONICS would be used. The solar modules incline at a tilt angle of 15° and their average height are 40 cm.

The data acquisition system consists of eight inverters, the solar irradiance sensors, PV module and ambient temperature sensor. The time series data represented by following are conducted to use in this algorithm: ambient temperature (°C), solar irradiance (kWh/m^2) and PV system generated energy (MWh). They are actual data of average values which are gathered whole day by the mentioned power plant over nineteen months between 2012 and 2013. Example of data are shown in Table 3.1.

Date	Solar Irradiance (kWh/m^2)	Ambient Temperature (°C)	PV Temperature (°C)	Energy (MWh)
1	6.46	35.43	48.86	45.13
2	6.66	35.94	50.21	49.34
3	6.44	36.19	50.82	47.94
.	.	.	.	.
.	.	.	.	.
.	.	.	.	.
31	3.68	30.48	41.12	26.72

3.3 Experimental Model

There are three models applied with linear predictor designed to forecast the daily energy of the next day produced by solar power plant. Linear Regression Analysis is a linear predictor applied to these three models due to the simplicity.

The first model uses only one weather parameter as input, solar irradiance or ambient temperature, which is conducted to predict the output by using Simple Linear Regression. Fig. 3.1 displays the first model diagram.
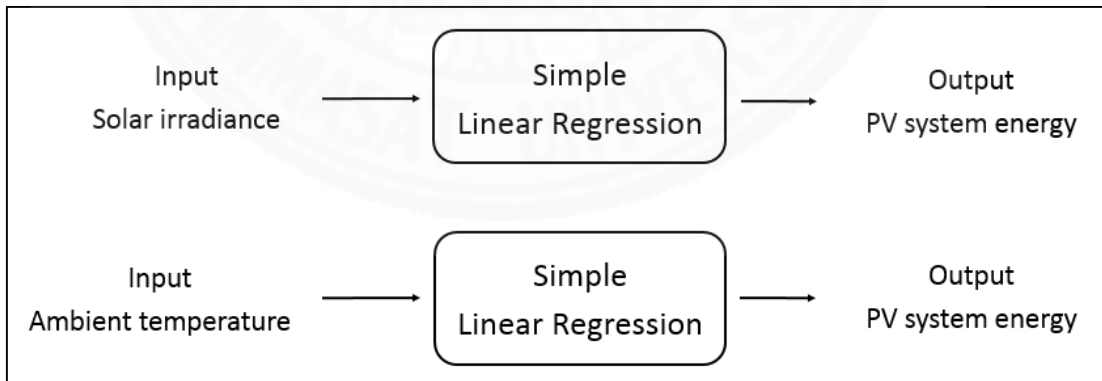
Figure 3.1: Diagram of Model 1

Both weather parameters, solar irradiance and ambient temperature, are combined together for using as independent input variable in the second model. Multiple Linear Regression is applied as a linear predictor to forecast the out in this

model because the number of input variables are more than one. The diagram of model 2 is displayed in Fig. 3.2
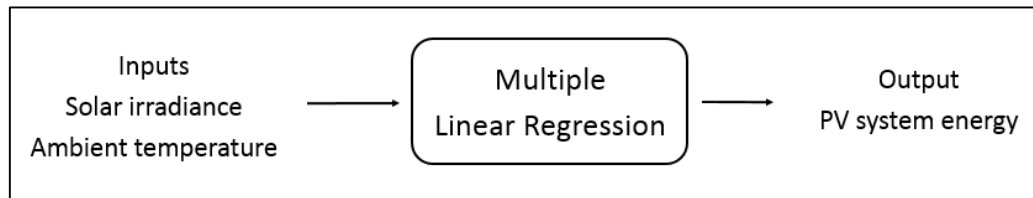
Figure 3.2: Diagram of Model 2

Because weather forecasted information on the forecast day obtained from Thailand Meteorological Department does not cover to solar irradiance that is the useful parameter to predict the production, the 3rd model is designed relate to the obtained information. It is created by applying available weather parameter, ambient temperature, to predict solar irradiance in the first step. After that the forecasted solar irradiance is conducted to predict PV power system production. Both steps use Simple Linear Regression as an approach for the prediction. Diagram of model 3 is shown in Fig. 3.3
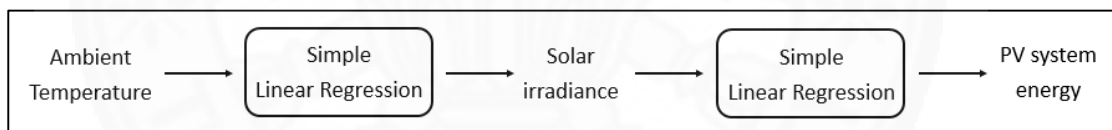
Figure 3.3: Diagram of Model 3

3.4 Relationship between Weather Parameter and PV System Production

Firstly, in order to know which weather parameter has higher effect to the output, data gathered in section 3.2 is conducted to analyze the strength of the correlation between weather parameter and solar power plant outcome. The model used to utilize to find the relationship between solar power plant energy and solar irradiance or ambient temperature by using Simple Linear Regression is similar to Model 1. The correlation between solar irradiance and PV generated energy is shown in Fig. 3.4 and the other one, ambient temperature and PV system output, is displayed in Fig. 3.5.
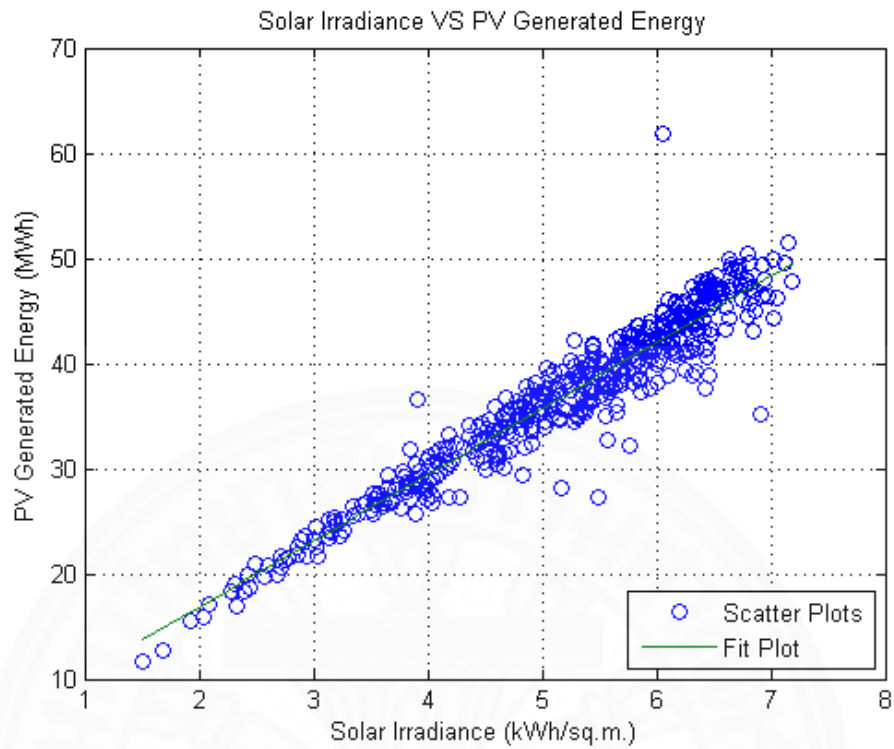
Figure 3.4: The correlation between solar irradiance and PV generated energy
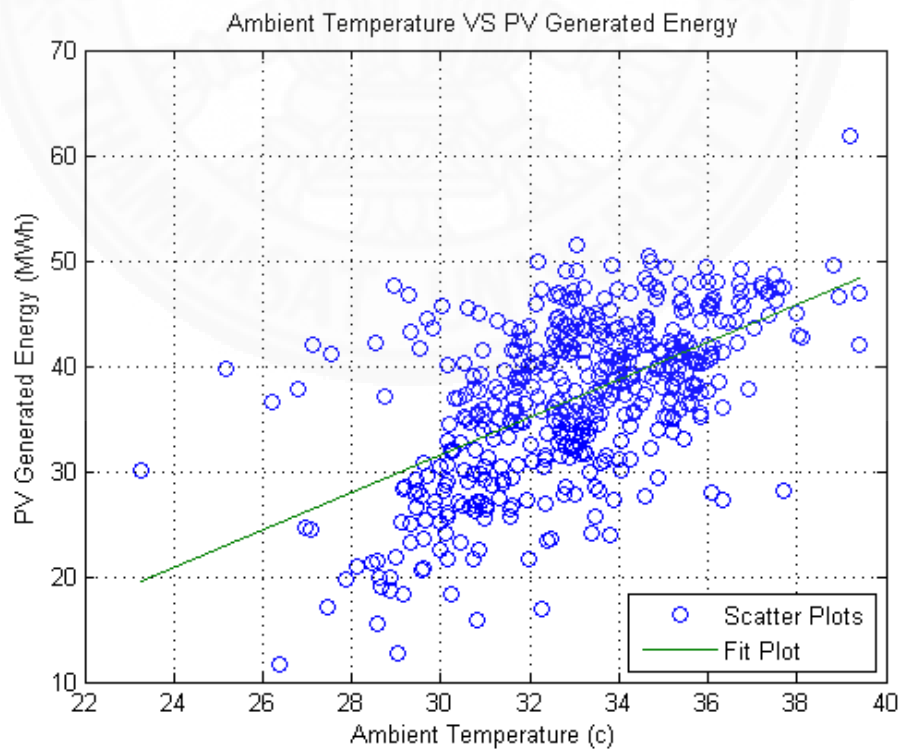
Figure 3.5: The correlation between ambient temperature and PV generated energy

By obviousness, it is indicated that the strength of the relationship between PV power system production and solar irradiance is stronger than the other one, PV power system output and ambient temperature. That means solar irradiance has higher impact to the production generated by PV power system than ambient temperature. Moreover, the coefficient of determination, R^2, from Simple Linear Regression approach is an evidence that also presents the number of outputs generated by PV power system depend on solar irradiance more than ambient temperature as shows in Table 3.2.

Table 3.2: R^2 coefficient between weather parameter and PV system production

Input	Output	R^2 coefficient
Solar Irradiance	PV system generated energy	0.9123
Ambient Temperature	PV system generated energy	0.3274

3.5 Experiment Result and Discussion

Three models in section 3.3 are used in the experiment for evaluation the accuracy of PV power system output prediction.

3.5.1 Model 1

In the first model, data obtained from section 3.2 are divided to two groups, training and test. The first sixteen months of data are conducted to fit the best line for creating forecast equation, while the rest are applied to evaluate the performance of model.

Two regression equations conducted to solve the best line for achieving the future production of solar power plant are obtained by using solar irradiance or ambient temperature. They can be expressed in term of equation (20) as follow:

$$y_1 = 4.2154 + 6.2953x_1 \tag{34}$$

$$y_2 = -21.9426 + 1.7851x_2 \tag{35}$$

Equation (34) is applied by solar irradiance, the rest is applied by ambient temperature. After that the actual output and the predicted one are compared.

The results displayed in Fig. 3.6 and Fig. 3.7 present the correlation between the measured energy production of solar power plant and the predicted production calculated by using solar intensity and ambient temperature, respectively.

Furthermore, Mean Squared Error (MSE) is used to identify the difference between actual and forecasted PV power system energy production to test performance of the model as displayed in Table 3.3.
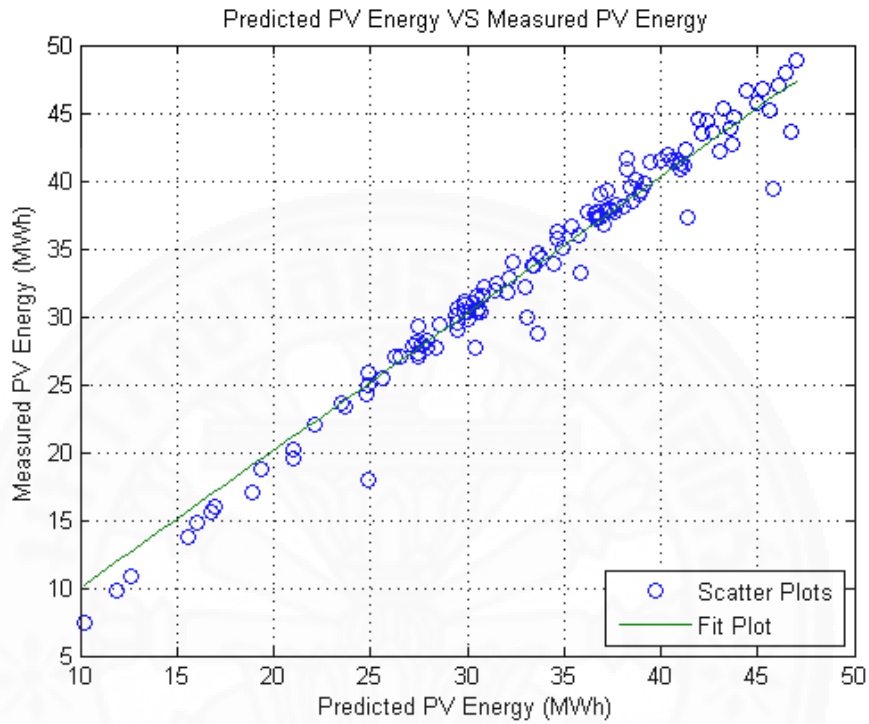
Figure 3.6: The correlation between measured energy production and predicted energy production calculated by using solar irradiance
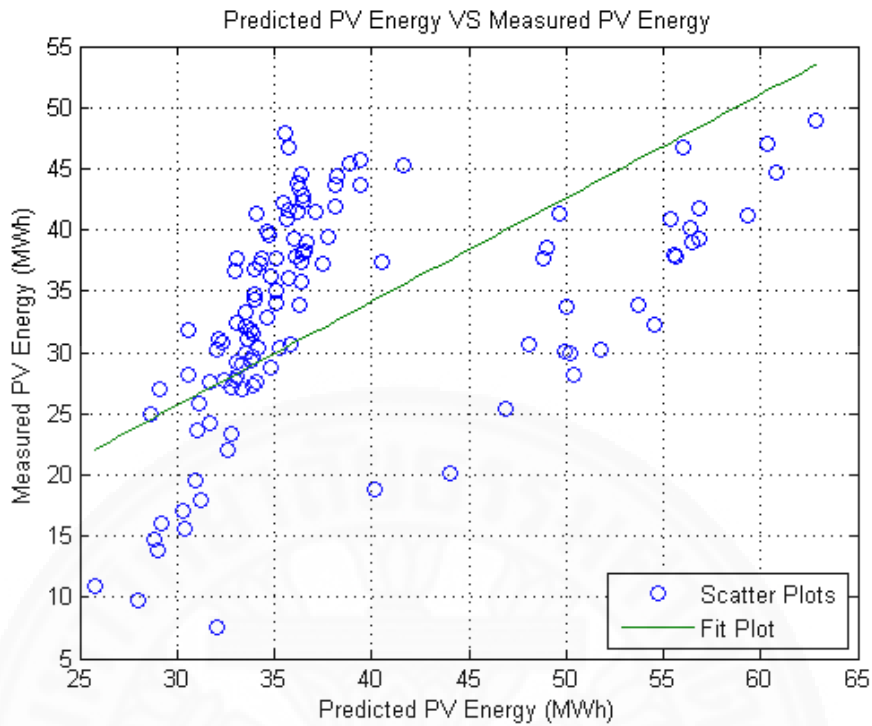
Figure 3.7: The correlation between measured energy production and predicted energy production calculated by using ambient temperature

Table 3.3: MSE of actual and predicted PV system production by using weather parameter

Input	Output	MSE
Solar Irradiance	PV system generated energy	2.5896
Ambient Temperature	PV system generated energy	105.1094

Due to the results in Table 3.2 and Table 3.3, it denotes that the performance of the model is depends on the strength of the correlation between weather parameter and PV generate energy. The prediction error in the model decrease when R^2 coefficient increase, $MSE = 2.5894$ when $R^2 = 0.9123$ and $MSE = 105.1094$ when $R^2 = 0.3274$. The increasing of the strength of the relationship between the actual and predicted PV system generated energy also vary with the strength of the correlation between weather parameter and solar power plant production.

3.5.2 Model 2

Data used in this model are divided to two groups same as model 1 but they are combined together and use as input variable. The multi regression equation is conducted to fit the best line for the production prediction. It using both solar irradiance and ambient temperature is obtained in term of equation (25) as

$$y = 4.5981 + 6.3138x_1 - 0.0145x_2 \qquad (36)$$

The model performance identified by MSE in order to verify the prediction accuracy is displayed in Table 3.4 and the relationship between measured and forecasted PV generated energy by using both weather parameters is presented in Fig. 3.8. It can be realized that this correlation seems to be rather strong.

Table 3.4: MSE of actual and predicted PV system production of Model 2

Input	Output	MSE
Solar Irradiance Ambient Temperature	PV system generated energy	2.5794
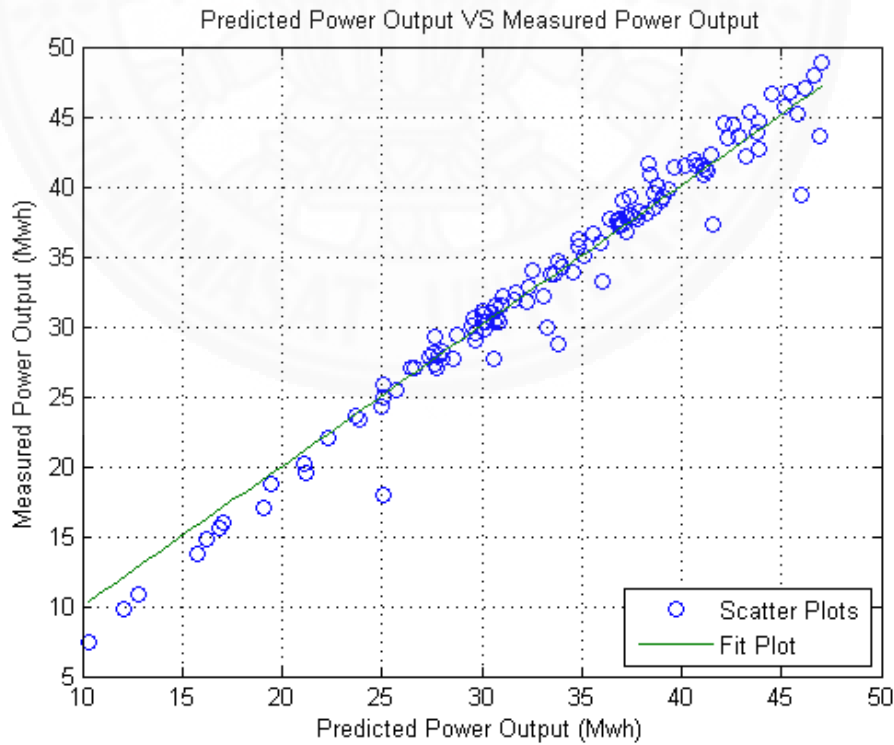
Figure 3.8: The correlation between measured and predicted energy production of Model 2

The prediction error of model 2 is lower than the previous model because this model uses both radiation and ambient temperature as input but model 1 uses only radiation or ambient temperature to forecast the energy produced by PV power system. It can assume that the forecasting using more input variables provides higher accuracy than the less one.

3.5.3 Model 3

One factor applied to create model 3 is the strength of the correlation between weather parameter and PV module generated energy. Due to the results of section 3.4, the first step uses ambient temperature as input variable to estimate solar irradiance. After that PV power system production is forecasted by using the predicted solar irradiance in the second step as show in Fig. 3.3.

Data sets of this model are divided differently from the other models. Twelve months of ambient temperature and solar irradiance data sets are used to estimate solar intensity through the next seven months in the first step. The next step is applying data sets of four months to estimate solar irradiance to fit the best line with PV power system production. Then, the other three months data sets are conducted to test the performance of model.

The best lines for both steps conducted to gather the future output are applied by Simple Linear Regression same as the first model. Simple regression equation in the first step obtained by using ambient temperature for solar irradiance estimation is expressed as follow:

$$y = -3.1718 + 0.2532x \qquad (37)$$

Simple regression equation in the second step gathered by using predicted solar irradiance from the first step to forecast the output from PV system is presented as

$$y = -19.8966 + 10.8857x \qquad (38)$$

The correlation between actual and forecasted PV module system production displaying the major error of the model is presented in Fig. 3.9 and the model performance in term of MSE shown in Table 3.5 is also indicated that this model might not be most suitable to adopt.
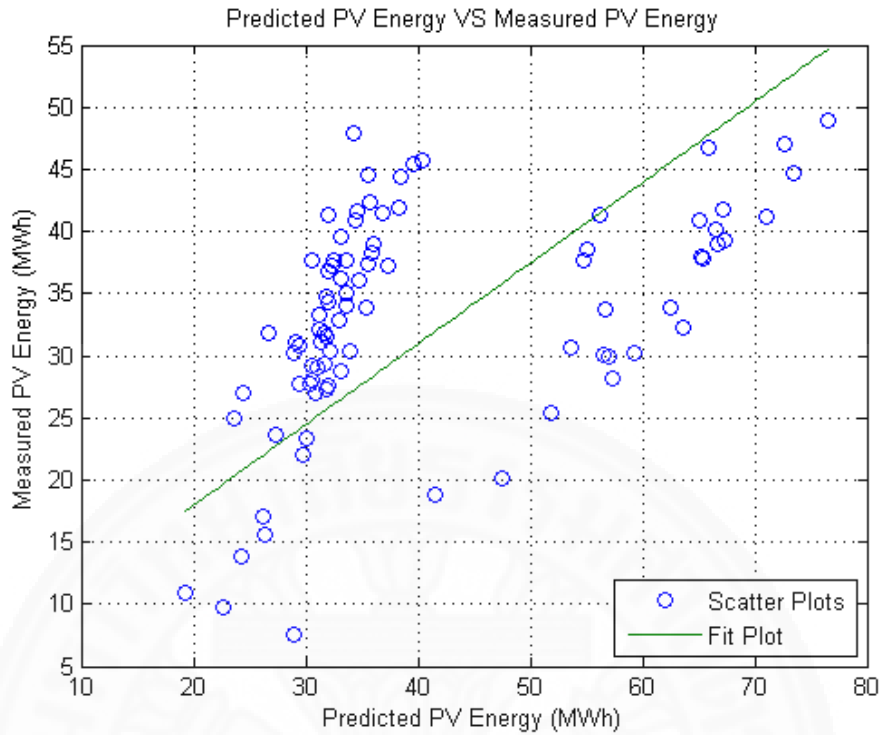
Figure 3.9: The correlation between measured and predicted energy production of Model 3

Table 3.5: MSE of actual and predicted PV system production of Model 3

Input	Output	MSE
Estimated solar irradiance by using ambient temperature	PV system generated energy	220.1535

One reason affected to the accuracy of Model 3 is the strength of the correlation between solar irradiance and ambient temperature which is displayed in Fig. 3.10. Their relationship seems to be rather poor. It is also indicated in term of the coefficient of determination, R^2, shown in Table 3.6 that ambient temperature is not suitable to apply for solar irradiance prediction.
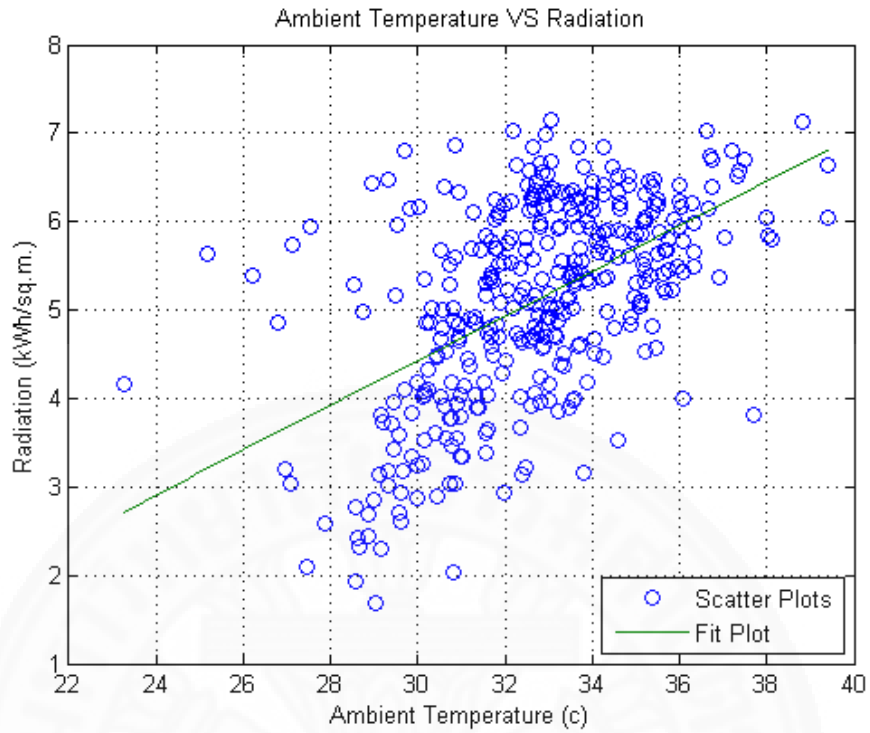
Figure 3.10: The correlation between ambient temperature and solar irradiance

Table 3.6: R^2 coefficient between ambient temperature and solar irradiance

Input	Output	R^2 Coefficient
Ambient temperature	Solar irradiance	0.2876

The experiments using linear algorithm method to forecast the production generated by PV power system provide results in the acceptable error. They indicate that the main factor affected to the result accuracy is solar irradiance but it is not obtained automatically from Thai Meteorological Department. Weather forecasted information used as input variable is not enough to make a good experiment. Moreover, the effect of increasing input variable type also displays the better of the model performance. Therefore, it can assume that the suitable model should be designed for Thailand. Additionally, Solar radiation should be forecasted by another approaches or add more related and known parameters in the model to improve the prediction accuracy.

Chapter 4
Non-linear Analysis

In linear algorithm, it suggests that the suitable model should be designed for Thailand since weather forecasted information gathered from Meteorological Department is not enough to achieve the good results. PV modules generally orientation in solar power plant are always optimized according to the local weather conditions. That affects to all panels have the same azimuth and inclination angle, including total solar radiation. Therefore, the other approaches which are applied to know the actual solar radiation and used to achieve the production from solar power plant are also presented in this chapter.

4.1 Step of Procedure

1. Collect data from solar power plant: hourly system production, hourly solar irradiance and the site details

2. Collect weather parameters affecting to PV system production: Humidity, Wind Speed, Ambient Temperature and Sky Condition

3. Find hourly solar irradiance by calculation method

4. Estimate the actual solar irradiance by using weather factor in step 2 combines with calculated solar irradiance in step 3 in model 1

5. Then, predict the production generated by PV power system from the actual solar in step 5

6. In model 2, use calculated solar irradiance in step 3 and weather parameters in step 2 as inputs to predict the outcome from solar power plant

7. Compare the result accuracy between model 1 and model 2 to evaluate the model performance

4.2 Data Description

4.2.1 Data Collection

The fundamental time series data sets are obtained from the same solar power plant in Chapter 3 and collected from May 2012 to February 2014. They consist of the hourly information of solar intensity stroke on PV module and the output generated by the

plant and they are recorded between 07.00 a.m. and 05.00 p.m. The plant also provides its location and PV module installation data.
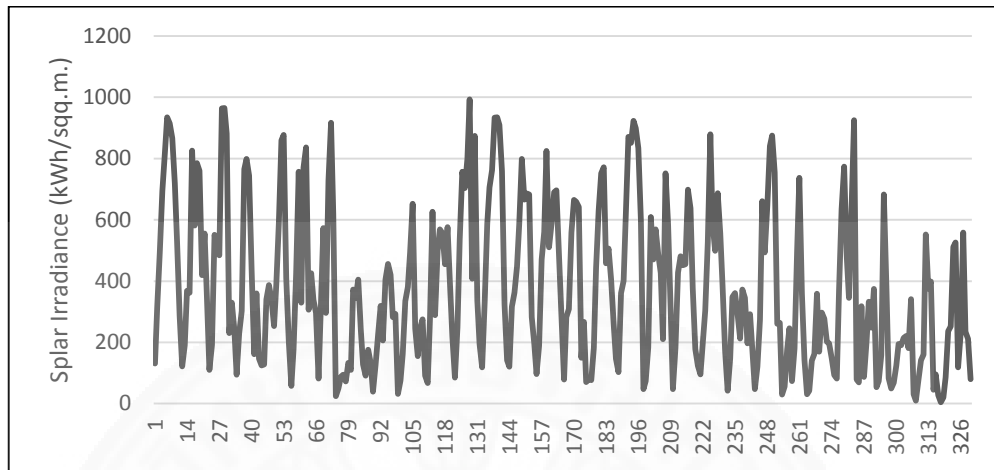
Figure 4.1: Example of hourly solar irradiance in July 2013
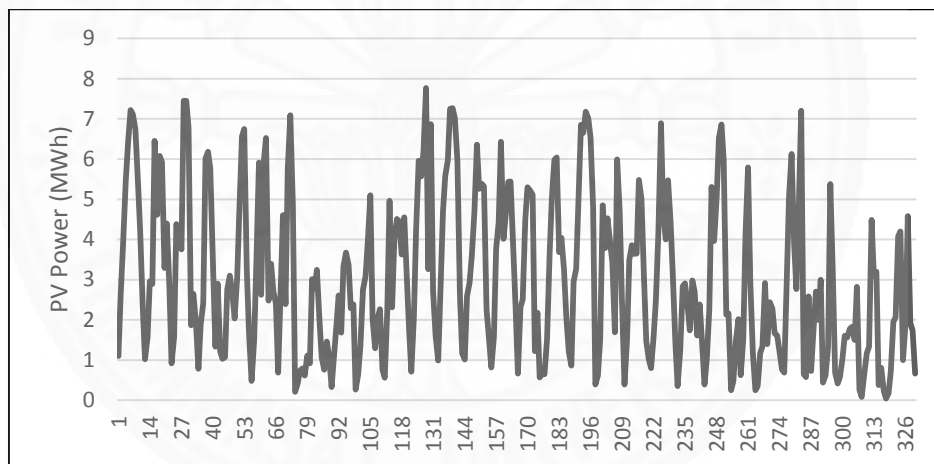
Figure 4.2: Example of hourly PV power system production in July 2013

Since the production and irradiance are recorded between 2012 and 2014, the historical meteorological data sets are downloaded from a public weather forecast website, www.wunderground.com. The weather data are gathered from Srakeaw province meteorological station instead of using data from Prachinburi province because the power plant location is nearer Srakeaw province to Prachinburi province. In this experiment, they consist of ambient temperature, humidity, wind speed and sky condition. Example of the weather parameter data sets obtained from Srakeaw province meteorological station are presented in Fig. 4.3.

Daily Weather History & Observations

2013	Temp. [°F]			Dew Point [°F]			Humidity [%]			Sea Level Press. [in]			Visibility [mi]			Wind [mph]			Precip. [in]	Events
Jul	high	avg	low	high	avg	low	high	avg	low	high	avg	low	high	avg	low	high	avg	high	sum	
7	88	80	77	78	77	77	95	90	76	29.76	29.75	29.73	7.0	5.5	5.0	0	0	-	0.00	Rain
8	84	78	76	77	76	75	96	88	79	29.81	29.78	29.75	5.0	4.8	4.0	0	0	-	0.00	Rain
9	84	80	74	78	76	74	94	88	75	29.81	29.76	29.71	6.0	5.5	4.0	0	0	-	0.00	Rain
10	84	80	75	76	75	75	97	90	72	29.77	29.75	29.71	6.0	5.2	4.0	0	0	-	0.00	Rain
11	89	82	75	78	76	75	99	87	61	29.84	29.78	29.73	6.0	4.9	4.0	2	0	-	0.00	Rain , Thunderstorm
12	90	82	75	79	77	76	96	78	59	29.82	29.77	29.70	6.0	5.5	5.0	5	1	-	0.00	
13	91	84	77	79	77	74	97	74	48	29.74	29.68	29.60	7.0	5.9	5.0	9	1	-	0.00	
14	79	-	79	77	77	77	92	92	92	29.68	29.68	29.68	5.0	5.0	5.0	0	0	-	0.08	Thunderstorm

Figure 4.3: Example of meteorological data sets from Srakeaw Province

Sky Condition is an amount of cloud observation which cover the sky on each day. It directly affects to solar intensity that is the main factor to predict the output from solar power plant. It can be identified as a number, Cloudy Index, adopted to use in the experiment. Cloudy Index can be defined in proportion as a random number relating to the sky environment. It is specified in range [0, 1] which is easy to apply in this research.

There are five types of sky condition relating to the obtained data at Srakeaw province: Clear sky, Cloudy sky, Thunderstrom, Fog and Rain. They are separated to three groups in order to define Cloudy Index. When sky is clear or cloudy, it can be assumed that Cloudy Index equals to *0.9* or *0.6*, respectively. Furthermore, Cloudy Index of the rest of Sky Condition is equal to *0.3*. The summary of Cloudy Index conducted to use in this study is presented in Table 4.1.

Table 4.1: Cloudy Index from Srakeaw province's sky condition

Sky Condition	Cloudy Index
Clear	0.9
Cloudy	0.6
Thunderstorm, Rain, Fog	0.3

4.2.2 Data Pre-processing

In order to obtain the better performance results and allow the operation finishing its procedure, data preprocessing is important to decrease noise and variable distribution by input and output variables analysis and transformation.

Although the raw data sets from the solar power plant are recorded every hour, there are some data missing or being irregular that might occur from disabled sensors or/and the error of data transmission. In this work, the missing or irregular data are estimated by interpolation approach, which is the method to get the value between two points of data.

Furthermore, each kind of time series data sets are normalized between a range [0, 1] before applying to ANN model. This process adjusts and converts the different scale value to a common scale value. The data normalization is defined as the following equation:

$$x_{normalized} = \frac{x - x_{min}}{x_{max} - x_{min}} \tag{39}$$

where x_{max} and x_{min} are the maximum and minimum points of the time series data sets, respectively.

After obtaining the forecasted solar power plant production, the data set is denormalized and compared with the actual power data to evaluate the performance of the model.

4.3 Solar Irradiance Calculation

The equation (6) – (19) in Chapter 2 (Section 2.3) are used to calculate solar irradiance following to Hottel's solar radiation model. The calculated answer is an estimated solar radiation from 7.00 a.m. to 5.00 p.m. of the whole year (1st Jan to 31st Dec) which is based on clear sky condition. Parameters used to calculate solar irradiance are displayed in Table 4.2 and the examples of calculated solar irradiance are presented in Fig. 4.4.

Table 4.2: The parameters use to calculate solar radiation

Parameter	Value
1. Local longitude of standard time meridian (LSTM)	$105°$
2. Longitude of site location (Long)	$101.84°$
3. Latitude of site location (ϕ)	$13.96°$
4. Inclination angle of solar panel installation (β)	$15°$
5. Azimuth angle of solar panel installation (α)	$0°$
6. Altitude of solar panel installation (A)	0.04 km.
7. Climate correction factors (r_0, r_1 and r_k)	0.95, 0.98, 1.12
8. The average reflectance of the ground (ρ)	0.2
9. Solar constant (G_{on})	1,367 W/m^2
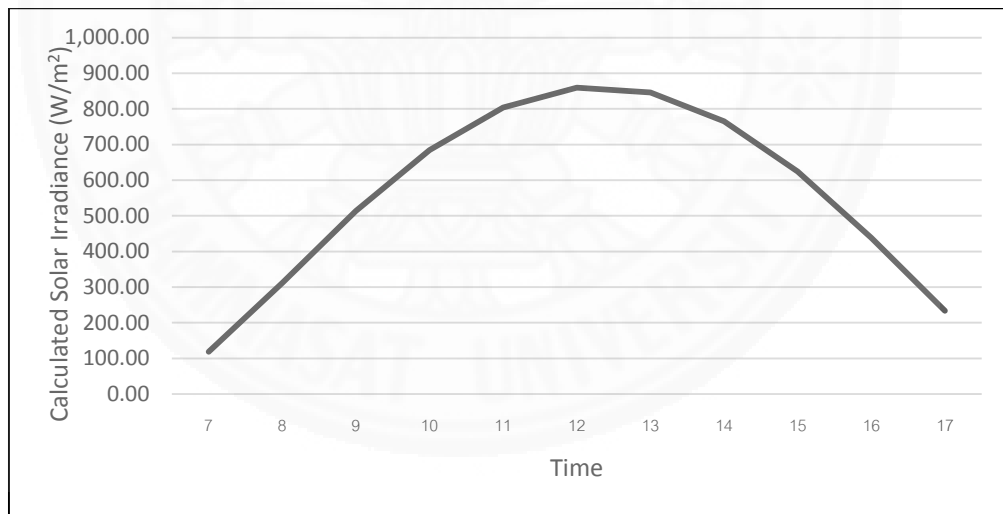
Figure 4.4: Example of calculated solar irradiance

When compare the calculated solar irradiance and the actual obtained from the solar power plant as presented in Fig. 4.5, it seems that the actual one has less value than the calculated one because the calculation is based on the clear sky condition that does not consider the factors affecting to solar irradiance. Therefore, the factors should be considered in order to achieve high efficiency of prediction.
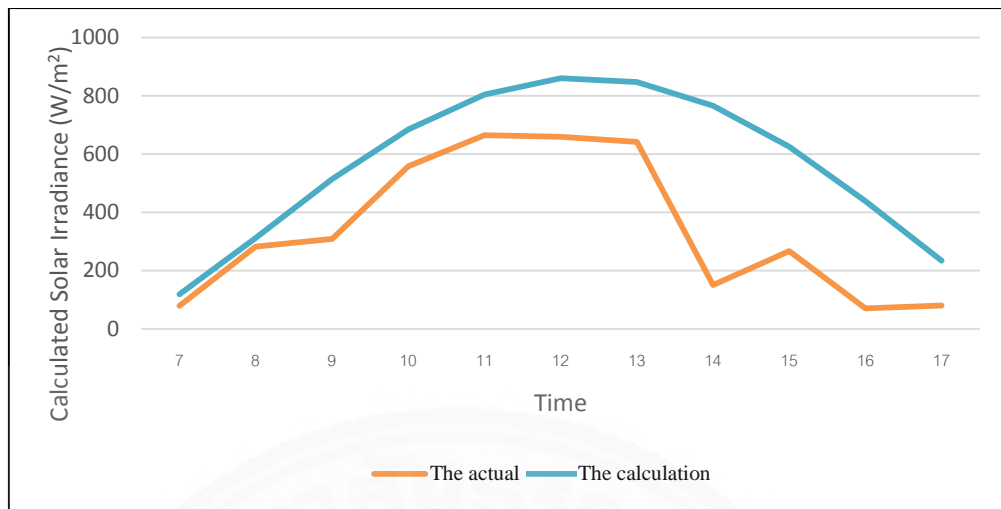
Figure 4.5: Comparing the actual and calculated solar irradiance

4.4 Experimental Model and Methodology

In nonlinear algorithm, the new model is designed to improve the prediction accuracy when compare to the previous model in Thailand. It is divided to two stages: the estimation of actual solar irradiance and the forecasting of PV power system production as shows in Fig. 4.6.
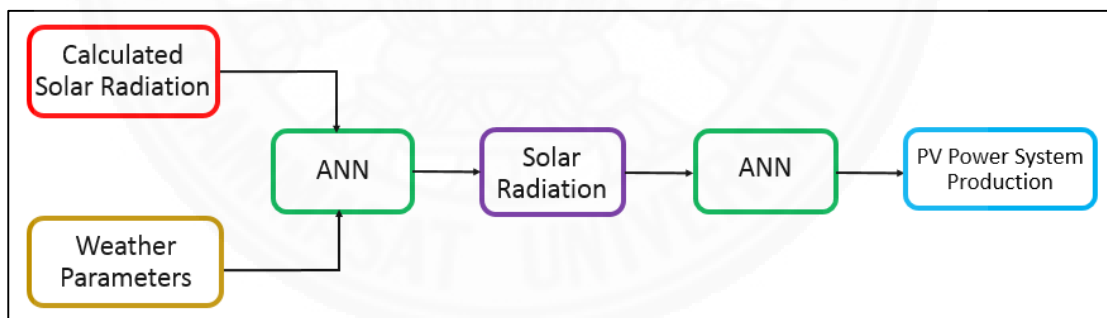
Figure 4.6: The designed model for non-linear algorithm

Weather parameter obtained from Section 4.2 and calculated solar irradiance from Section 4.3 which also already normalized by equation (34) are taken part as inputs variable of the model to estimate the actual solar irradiance in the first stage. After that solar power plant production is forecasted in the second stage by the estimated solar irradiance. Fig. 4.7 and Fig. 4.8 respectively present the details of the both stages.
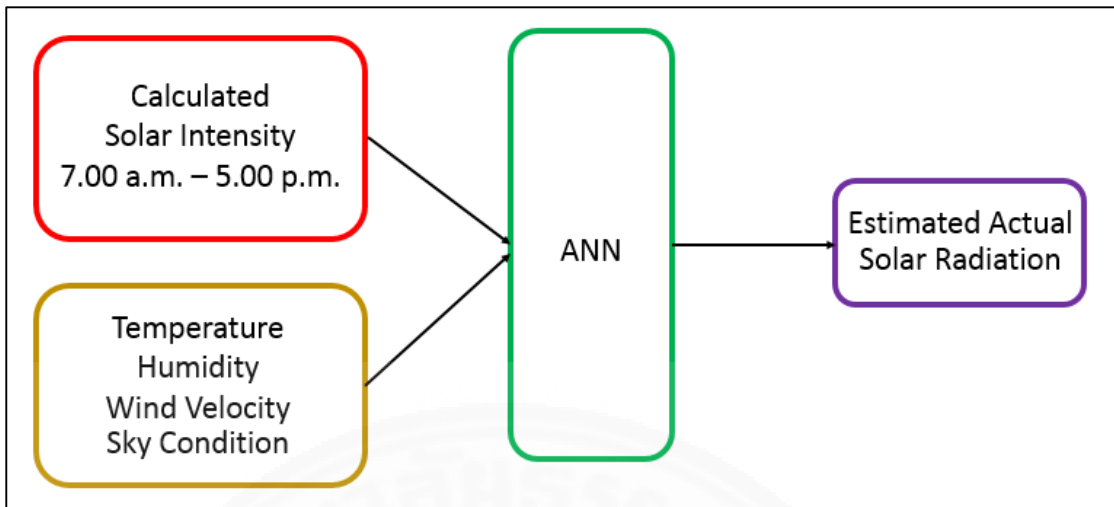
Figure 4.7: Detail of the first stage in non-linear algorithm model

Figure 4.8: Detail of the second stage in non-linear algorithm model

Thailand previous model used to compare the model performance with the designed model is displayed in Fig. 4.9.
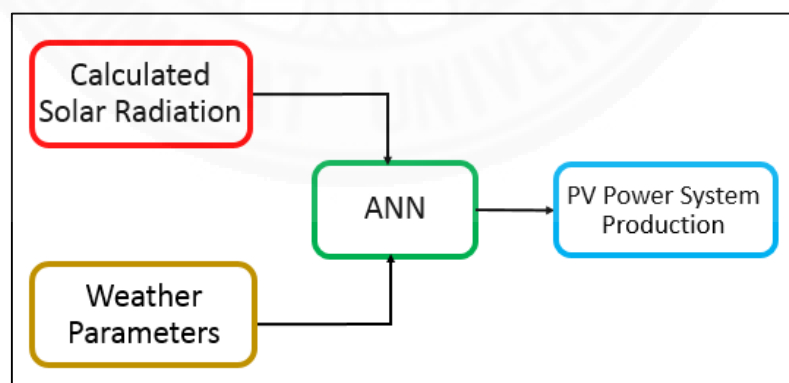
Figure 4.9: The compared model for non-linear algorithm

Two approaches based on Artificial Neural Network (ANN) are applied to predict the actual solar irradiance and the outputs generated from PV power plant between 7.00 a.m. and 5.00 p.m. in the next day, Feedforward Neural Network (FFNN) and Nonlinear Autoregressive Network with Exogenous Input (NARX).

4.4.1 Feedforward Neural Network

There are 19 variables in the input layer: solar radiation data calculate between 7.00 a.m. and 5.00 p.m. in the next day; maximum, minimum and average value of the forecasted temperature and humidity; maximum wind speed and cloudy index. The time series data sets are randomly divided to three groups for training, validation and testing. They are set to the range 70% for training, 15% for stopping the training before overfitting and remaining 15% for evaluation of the approximation quality.

The results of this study are the next day prediction of production generated by solar power plant, so the 11 hours PV power output between 7.00 a.m. and 5.00 p.m. are taken part as the output neurons. FFNN model applied in MATLAB@2013a is presented in Fig.4.10. It has only one hidden layer because the increasing of hidden layer affects to the possibility of overfitting and computation time but the appropriate number of hidden neurons are determined by the trial and error method.
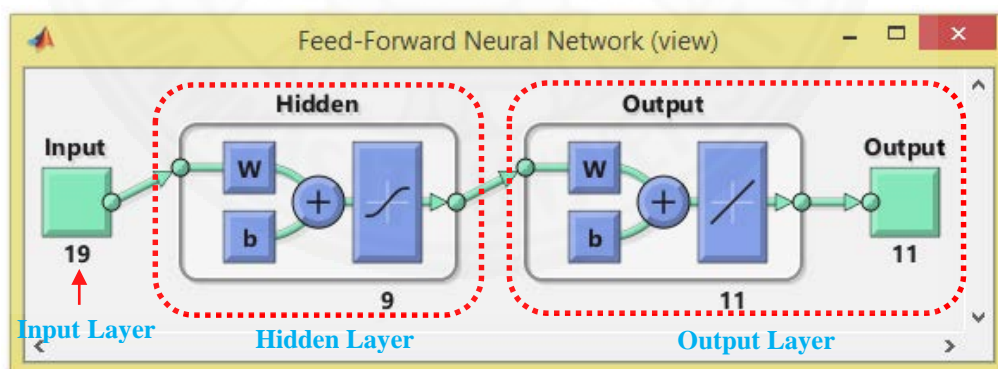
Figure 4.10: Feedforward Neural Network model

Transfer function in hidden layer and output layer is adopted by hyperbolic tangent function and linear function, respectively. The training algorithm used in this model is Backpropagation based on a Levenberg-Marquardt minimization approach.

4.4.2 Nonlinear Autoregressive Network with Exogenous Input

Input layer in this method uses estimated solar irradiance and 6 weather parameters: maximum, minimum, average temperature, humidity, maximum wind speed and sky condition as input variables. Although the input variables are divided to three groups same as FFNN approach, the process and the number of data are different. It uses *divideblock* function to divides the first 60% of the samples to the training set, the next 20% for validation and the last 20% for testing. The outcome in the output layer are also the prediction of the next day production generated by PV power system from 7.00 a.m. to 5.00 p.m.

For this study, the number of hidden layers and output neurons are same as the previous approach due to the same reason. Levenberg-Marquardt is used as a training function and Sigmoid transfer function is used in the hidden layer including with a linear transfer function is used in the output layer. Fig.4.11 displays NARX model applied in MATLAB@2013a. The number of delays and hidden neurons are varied to evaluate the performance of model.
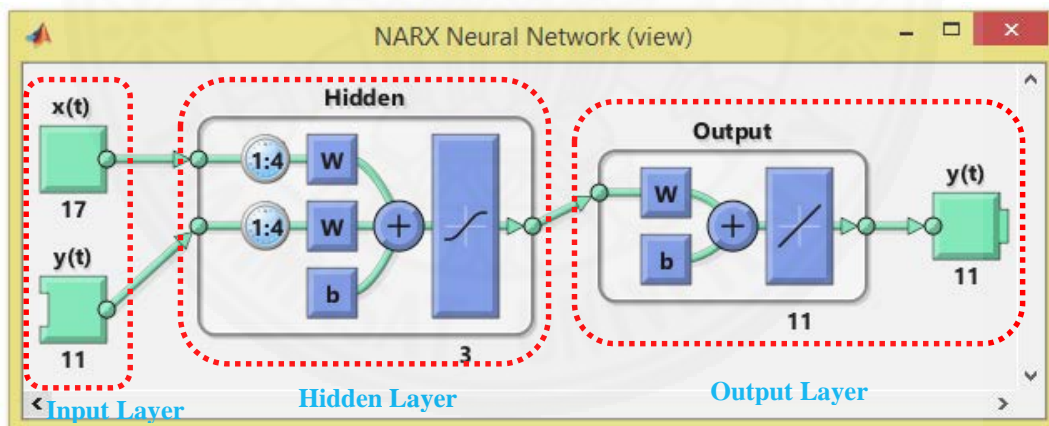
Figure 4.11: NARX model

4.5 Experiment Result and Discussion

There are two approaches applied to test the performance of model, FFNN and NARX. The designed model performance is evaluated and compared to Thailand previous model. The experiment results are divided according to the applied approach to present the prediction accuracy of model. FFNN result is displayed in the first section following with NARX result in the next section.

41

4.5.1 Feedforward Neural Network

The network training data sets are the data sets from 11 May 2012 to 10 Feb 2014. Model format including input variables and the output are explained in Section 4.4.1. Then, the data used to verify the model performance are the next three days from the last day of training. In order to compare the prediction accuracy of model, the compared model displayed in Fig. 4.9 is also used to forecast the same output.

For both models, due to the random start of neural network initial weights, the outcomes from the experiment will be differ every time when the program is run. So, the initial random value is set to gather the same output every time when the program is simulated.

The number of hidden neurons are varied by trial and error method to find the best model performance. Table4.3 presents the designed model in Fig. 4.6 errors between solar power plant predicted production and the actual generated production. Table 4.4 displayed the experiment results of the compared model.

Table 4.3: Results of the designed model by using Feedforward Neural Network approach

No. of Hidden Neurons		MAPE	MSE
H1	H2		
5	5	32.5562	0.0081
8	18	24.3440	0.0082
10	10	28.8567	0.0089
10	15	26.1949	0.0090
15	15	24.9549	0.0064
15	20	24.6523	0.0063
15	25	25.0416	0.0065
18	18	131.2432	0.5020
18	28	160.5218	1.6057
19	19	20.3124	0.0067
19	20	19.6776	0.0066
19	21	22.5813	0.0083
19	23	19.9351	0.0068
19	25	19.5641	0.0065

19	26	19.0691	0.0061
19	27	31.9310	0.0517
19	28	17.6936	0.0056
19	29	19.7997	0.0064
19	30	21.3264	0.0084
20	10	25.2490	0.0121
20	20	22.8128	0.0120
20	25	22.6801	0.0120
25	10	33.7619	0.0400
25	15	54.5712	0.0421
25	20	31.7946	0.0412
25	25	31.8021	0.0391

Table 4.4: Results of the compared model by using Feedforward Neural Network approach

No. of Hidden Neurons	MAPE	MSE
5	27.1095	0.0108
6	25.2819	0.0094
7	24.4528	0.0083
8	20.2657	0.0057
9	26.6903	0.0086
10	21.9917	0.0079
11	26.7712	0.0124
12	22.1695	0.0094
13	27.8413	0.0108
14	33.6972	0.0416
15	22.5157	0.0086
16	27.7176	0.0123
17	24.9583	0.0795
18	31.6525	0.0130
19	43.1470	0.0225
20	36.6192	0.0220
21	33.5759	0.0507

22	46.3155	0.0434
23	27.5639	0.0175
24	43.9279	0.0648
25	29.6615	0,0134

In the designed model, it provides the lowest error, *MAPE = 17.6936* or *MSE = 0.0056*, when the number of hidden neurons in the first stage (H1) equals to 19 and the second stage (H2) equals to 28. The lowest error in the compared model, *MAPE = 20.2657* or *MSE = 0.0057*, is evaluated at the number of hidden neurons (H) equals to 8. Fig. 4.12 and Fig. 4.13 show the best result of each model when compare the forecasted power output with the measured power output in the next three days by applying on the designed and compared model, respectively
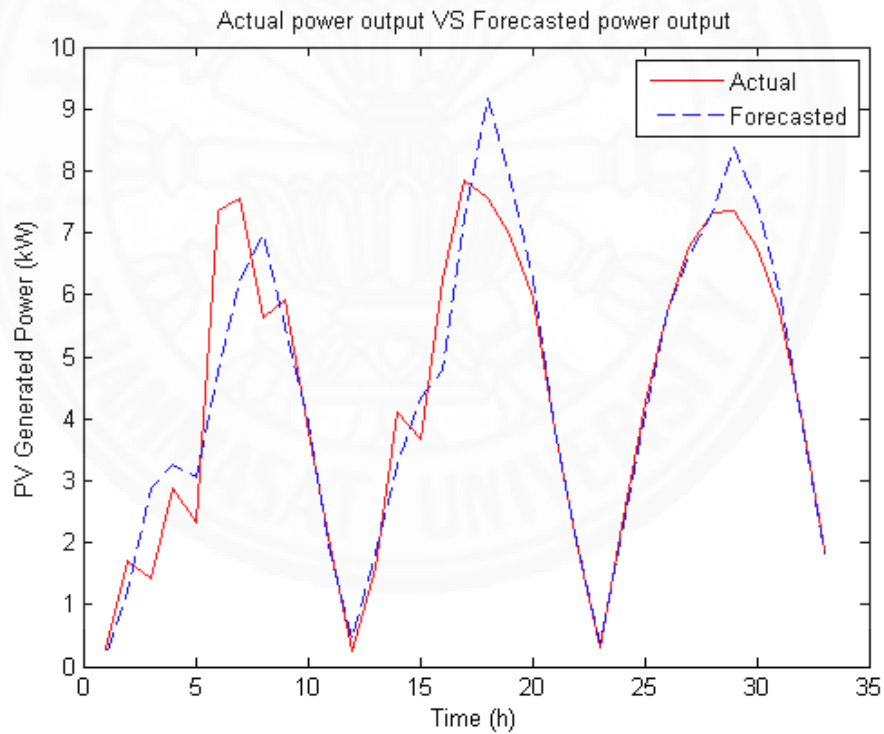
Figure 4.12: Compare the actual and forecasted power output by using the designed model
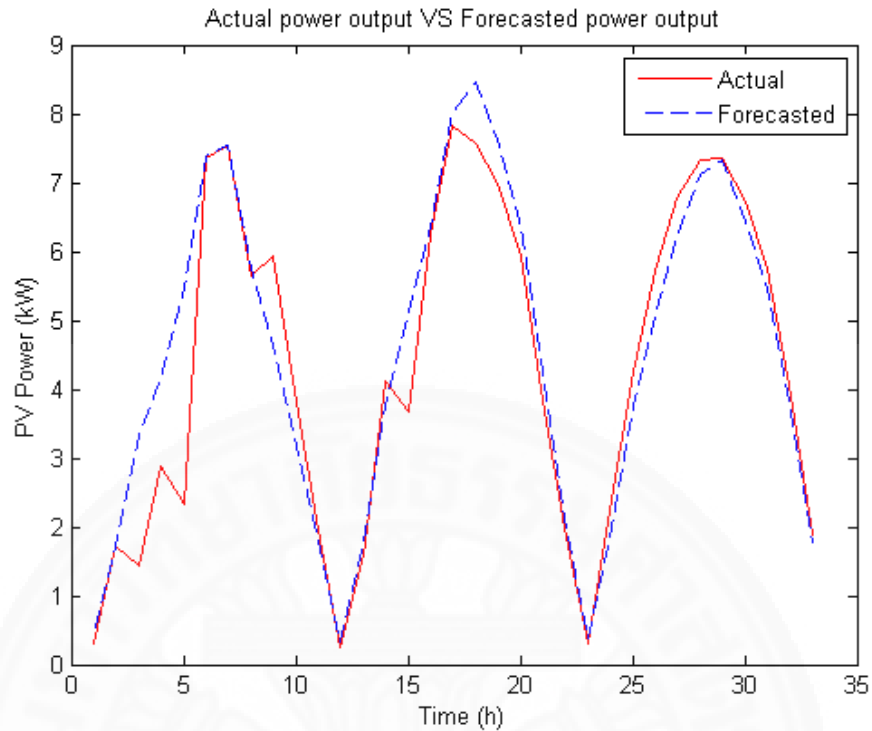
Figure 4.13: Compare the actual and forecasted power output by using the compared model

4.5.2 Nonlinear Autoregressive Network with Exogenous Input

In this research, there is another approach, NARX, applied to the designed model and the compared model to test the performance of each model. Then, they are being compared between each other in order to present the results which expected to provide the same trend as the previous approach. Both of them are conducted with the same methodology to get initial weight of neural network in order to obtain the same target when simulating the program and use *MSE* to evaluate the performance.

For the designed model, the number of delays (D) are varied from 2 to 4 and they are determined that they are same in the first and second stage. The number of hidden neurons in the first stage (H1) are defined as: 1, 3, 5, 8, 13, 15, 18, 20, 25, 30, 35 and 40. In each number of hidden neurons, the number of hidden neurons in the second stage (H2) are also defined same as the first stage. When the model is tested, one model performance value, *MSE = 0.0210*, is specified as a reference for seeking trend of the model performance. The number of hidden neurons in the second stage will be increased 2 steps and decreased 2 steps from the neurons that MSE less than the

45

reference. Table 4.5 shows the detail of increasing and decreasing the number of hidden neurons in order to find the performance trend.

Table 4.5: The detail of increasing and decreasing the number of hidden neurons

Delay	H1	H2	MSE
2	5	10	
		13	0.0315
		14	0.0213
		15	0.0175
		16	0.0412
		17	0.0803
		18	
		20	

In the compared model, the number of delays are also varied from 2 to 4 and the number of hidden neurons (H) are also defined as: 1, 3, 5, 8, 13, 15, 18, 20, 25, 30, 35 and 40 on each delay. The model performance reference value is also same as the designed model to find the model performance trend. When the error meets the reference value, H will be increased 2 steps and decreased 2 steps

The experiment results are the next three days prediction errors between the actual and predicted PV power system production. Table 4.6 to 4.8 display the results that use the designed model in the experiment and vary the number of delay from 1:2 to 1:4, respectively. The experiment results by using the compared model and varying the number of delay is presented in Table 4.9.

Table 4.6: Results of the designed model by using NARX Network approach when Delay = 1:2

H2 \ 1	1	3	5	8	10	13	15	18	20	25	30	35	40
1	0.4332	0.0582	0.0311	0.0210	0.0189	0.0253	0.0224	0.0535	0.0552	0.0483	0.0521	0.0579	0.0613
2	0.0159	-	-	-	0.2444	-	-	-	-	0.0417	-	-	-
3	0.0204	0.0279	0.0275	0.0467	0.0197	0.0498	0.0216	0.0215	0.0342	0.0179	0.0255	0.0424	0.0412
4	0.0180	-	-	0.0235	0.0345	0.0226	-	-	-	0.0218	0.0237	-	-
5	0.0204	0.0230	0.0261	0.0206	0.0247	0.1795	0.0243	0.0239	0.0284	0.0259	0.0150	0.0213	0.0258
6	0.0169	-	-	0.0181	-	0.0246	0.0315	-	-	-	0.0277	-	0.0259
7	0.0226	-	-	0.0177	0.0247	0.0184	0.0172	0.0224	0.0279	-	0.0175	-	0.0138
8	0.0168	0.0234	0.0217	0.0282	0.0256	0.0252	0.0204	-	-	0.0296	0.0402	0.0393	0.0192
9	0.0188	-	-	0.0214	0.0180	0.0314	0.0166	-	-	-	0.0347	-	0.0174
10	0.0233	0.0360	0.0225	0.0200	0.0149	0.0233	0.0195	0.0272	0.0377	0.0242	0.0375	0.0224	0.0214
11	0.0325	-	-	0.0258	0.0164	-	0.0154	-	-	-	-	0.0300	0.0242
12	-	-	-	0.0457	0.0256	-	0.0273	-	-	-	-	0.0280	-
13	0.0368	0.0287	0.0315	0.0298	0.0283	0.0253	0.0436	0.0631	0.0534	0.0486	0.0228	0.0181	0.0351
14	-		0.0213	-	-	-	-	-	-	-	-	0.0154	-
15	0.0406	0.0334	0.0175	0.0246	0.0283	0.0215	0.0279	0.0665	0.0382	0.0298	0.0222	0.0307	0.0495
16	-	-	0.0412	-	-	-	-	-	-	-	-	0.0342	-
17	-	-	0.0803	-	-	-	-	-	-	-	-	0.0381	-
18	0.0218	0.0248	0.0402	0.0504	0.0300	0.0341	0.0542	0.0351	0.0406	0.0291	0.0579	0.0187	0.0334
19	-	-	-	-	-	-	-	-	-	-	-	0.0438	-
20	0.0497	0.0551	0.0476	0.0530	0.0489	0.0247	0.0388	0.0317	0.0421	0.0304	0.0854	0.0411	0.0542

Table 4.7: Results of the designed model by using NARX Network approach when Delay = 1:3

H2 \ H1	1	3	5	8	10	13	15	18	20	25	30	35	40
1	0.4332	0.0221	0.0235	0.0425	0.0949	0.0245	0.0264	0.0505	0.0961	0.0418	0.0263	0.0289	0.0762
2	0.0197	0.0163	-	0.0207	0.0320	0.0219	-	-	0.0342	0.0217	0.2954	-	-
3	0.0125	0.0152	0.0309	0.0167	0.0187	0.0209	0.0561	0.0268	0.0700	0.0207	0.0207	0.0494	0.0353
4	0.0128	0.0266	-	0.0258	0.0203	0.0262	-	-	0.0200	0.0184	0.0185	-	0.0994
5	0.0250	0.0201	0.0417	0.0200	0.0205	0.0509	0.0394	0.0335	0.0181	0.0131	0.0150	0.0221	0.0206
6	0.0121	0.0123	-	0.0247	0.0207	-	-	-	0.0162	0.0178	0.0143	0.0215	0.0645
7	0.0184	0.0220	-	0.0362	0.0252	-	-	-	0.0243	0.0206	0.0257	0.0108	0.0555
8	0.0225	0.0182	0.0271	0.0241	0.0157	0.0241	0.0369	0.0225	0.0399	0.0234	0.0142	0.0145	0.0270
9	0.0137	0.0205	-	0.0154	0.0257	-	-	-	-	0.0286	0.0150	0.0283	-
10	0.0202	0.0165	0.0362	0.0191	0.0203	0.0238	0.0282	0.0256	0.0264	0.0199	0.0324	0.0259	0.0808
11	0.0226	0.0228	-	0.0192	0.0243	-	-	-	-	0.0160	0.0287	-	-
12	0.0155	0.0340	-	0.0302	0.0147	-	-	-	-	0.0189	-	-	-
13	0.0241	0.0240	0.0295	0.0204	0.0293	0.0235	0.0231	0.0280	0.0298	0.0220	0.0290	0.0231	0.0288
14	0.0281	-	-	0.0337	0.0171	-	-	-	0.0476	0.0479	0.0244	0.0222	
15	0.0292	0.0287	0.0473	0.0274	0.0583	0.0393	0.0322	0.0388	0.0149	0.0414	0.0200	0.0157	0.0578
16	-	-	-	0.0409	0.0358	-	-	-	0.0196	-	0.0205	0.0353	-
17	-	-	-	0.0338	-	-	-	-	0.0219	-	0.0357	0.0254	-
18	0.0233	0.0410	0.0312	0.0208	0.0472	0.0332	0.0271	0.0321	0.0220	0.0688	0.0152	0.0421	0.0792
19				0.0216	-	-	-	-	-	-	0.0160	-	-
20	0.0332	0.0302	0.0669	0.0173	0.0323	0.0337	0.0310	0.0333	0.0412	0.0544	0.0452	0.0375	0.0914
21	-	-	-	0.0389	-	-	-	-	-	-	0.0332	-	-
22	-	-	-	0.0283	-	-	-	-	-	-	-	-	-

Table 4.8: Results of the designed model by using NARX Network approach when Delay = 1:4

H2 \ H1	1	3	5	8	10	13	15	18	20	25	30	35	40
1	1.0596	0.1190	0.0138	0.3394	0.0369	0.0472	0.2076	0.2031	0.0160	0.0323	0.0151	0.1859	0.1302
2	0.0204	0.0245	0.0075	0.0959	-	0.0194	0.0229	0.1669	0.0271	-	0.0247	-	-
3	0.0256	0.0221	0.0284	0.0159	0.0332	0.0256	0.0223	0.0299	0.0212	0.0779	0.0238	0.0135	0.0260
4	0.0179	-	0.0231	0.0362	-	0.0165	-	0.0265	0.0153	0.0416	0.0202	0.0235	-
5	0.0137	0.0227	0.0144	0.0118	0.0233	0.0171	0.0245	0.0211	0.0164	0.0189	0.0207	0.0216	0.0388
6	0.0125	-	0.0209	0.0164	0.0346	0.0198	-	-	0.0212	0.0178	0.0151	0.0284	-
7	0.0155	-	0.0198	0.0105	0.0199	0.0290	-	-	0.0136	0.0262	0.0145	0.0431	-
8	0.0203	0.0288	0.0260	0.0148	0.0197	0.0200	0.0285	0.0279	0.0164	0.0161	0.0126	0.0179	0.0244
9	0.0103	0.0242	0.0112	0.0340	0.0221	0.0240	0.0239	-	0.0174	0.0181	0.0259	0.0141	-
10	0.0166	0.0189	0.0156	0.0197	0.0166	0.0372	0.0251	0.0266	0.0227	0.0242	0.0228	0.0926	0.0514
11	0.0166	0.0218	0.0162	0.0224	0.0247	0.0184	0.0190	-	0.0190	0.0433	0.0236	0.0221	-
12	0.0109	0.0388	0.0215	0.0161	0.0167	0.0179	0.0413	-	0.0205	0.0200	0.0123	-	-
13	0.0284	0.0254	0.0271	0.0198	0.0236	0.0164	0.0183	0.0236	0.0146	0.0169	0.0139	0.0315	0.0846
14	0.0353	-	-	0.0188	0.0163	0.0202	0.0167	-	0.0148	0.0316	0.0179	0.0349	-
15	0.0576	0.0230	0.0308	0.0275	0.0354	0.0140	0.0206	0.0293	0.0266	0.0433	0.0270	0.0187	0.0630
16	-	-	-	0.0151	0.0310	0.0313	0.0254	-	0.0147	-	0.0197	0.0265	-
17	-	-	-	0.0381	-	0.0219	0.0237	-	0.0128	-	0.0264	0.0650	-
18	0.0211	0.0211	0.0218	0.0212	0.0227	0.0313	0.0346	0.0585	0.0248	0.0699	0.0273	0.0599	0.0913
19	-	-	-	-	-	-	-	-	0.0163	-	-	-	-
20	0.0360	0.0249	0.0298	0.0400	0.0291	0.0244	0.0236	0.0272	0.0349	0.0848	0.0380	0.0411	0.0426
21	-	-	-	-	-	-	-	-	0.0380	-	-	-	-

Table 4.9: Results of the compared model by using NARX Network approach

Delay	H	MSE	Delay	H	MSE	Delay	H	MSE
2	1	0.0216	3	1	0.0213	4	1	0.0168
	3	0.0246		3	0.0257		2	0.0221
	5	0.0406		5	0.0232		3	0.0163
	8	0.0256		8	0.0231		4	0.0205
	9	0.0225		10	0.0384		5	0.0233
	10	0.0169		13	0.0244		8	0.0239
	11	0.0253		15	0.0261		10	0.0273
	12	0.0183		18	0.0355		11	0.0225
	13	0.0255		20	0.0266		12	0.0243
	14	0.032		25	0.0388		13	0.0173
	15	0.0242		30	0.0254		14	0.0415
	18	0.022		33	0.0209		15	0.0258
	20	0.0489		34	0.042		18	0.0472
	25	0.0298		35	0.0197		19	0.0304
	27	0.0291		36	0.0449		20	0.0194
	28	0.0247		37	0.0322		21	0.0307
	29	0.0193		40	0.0507		22	0.0297
	30	0.0196					25	0.0213
	31	0.0405					30	0.0355
	32	0.0208					35	0.0317
	35	0.0268					40	0.0308
	40	0.0316						

The best result in the designed model, *MSE = 0.0075*, is obtained when delay in both stages equals to 4, the number of hidden neurons in the first stage and the second stage equal to 5 and 2, respectively. Fig. 4.14 shows the comparing between the actual power output obtained by measuring and the forecasted production by using the designed model when the error is lowest.
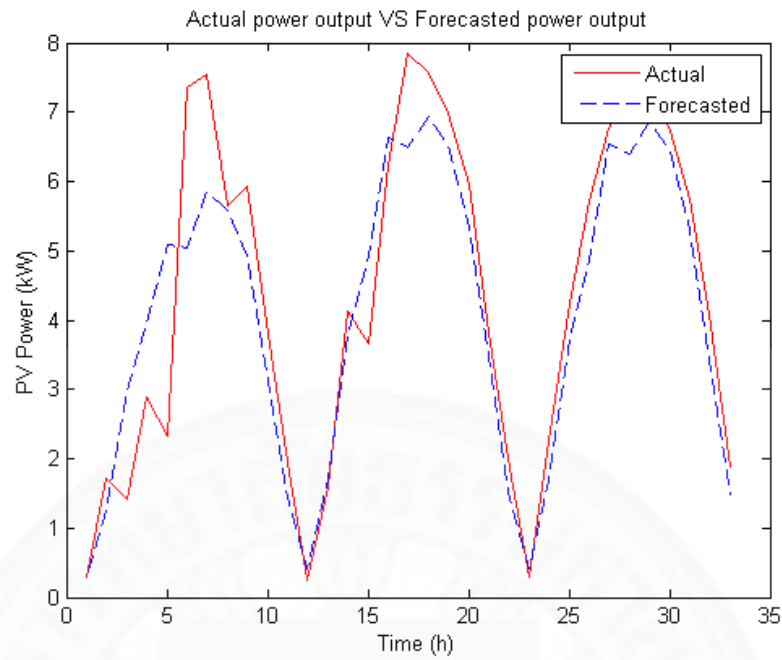
Figure 4.14: Compare the actual and forecasted power output by using the designed model

In the compared model, the number of delay equals to 4 and the number of hidden neurons equals to 3 provides the best performance of model, *MSE = 0.0163*. Fig. 4.15 displays the comparing of the actual power output and the estimated power output at the lowest error point by using the compared model.
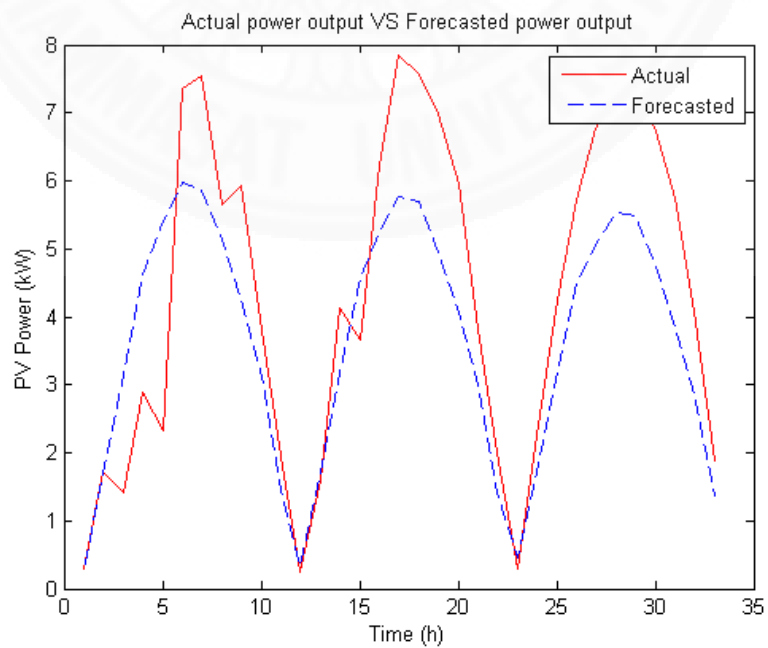
Figure 4.15: Compare the actual and forecasted power output by using the compared model

Both ANN approaches provide results in the same trend. In any case, either using FFNN or NARX, the new designed model used to forecast the production still show more accurate prediction comparing to the old model. This fact is presented because the designed model has two stages conducted to forecast the production generated by PV modules system. Since solar irradiance has the rather high effect to the power output which presented in Chapter 3, the first stage improves solar irradiance from the calculation in the clear sky condition with weather parameters in order to obtain nearly the actual solar irradiance. After that the estimated solar irradiance will used to predict the output in the second stage.

It is different in the compared model. Only one stage is directly used to forecast the production generated by PV modules system by combining the calculated solar irradiance and weather parameters as input variables.

Moreover, when compare each number of delay between both models, $D = 2, 3$ and 4, it also present in Fig. 4.16 to Fig. 4.18 that the errors of designed model in the left are less than the other model in the right. Therefore, it can conclude that the compared model does not fine enough to estimate the outcome when compare to the designed model due to its process.
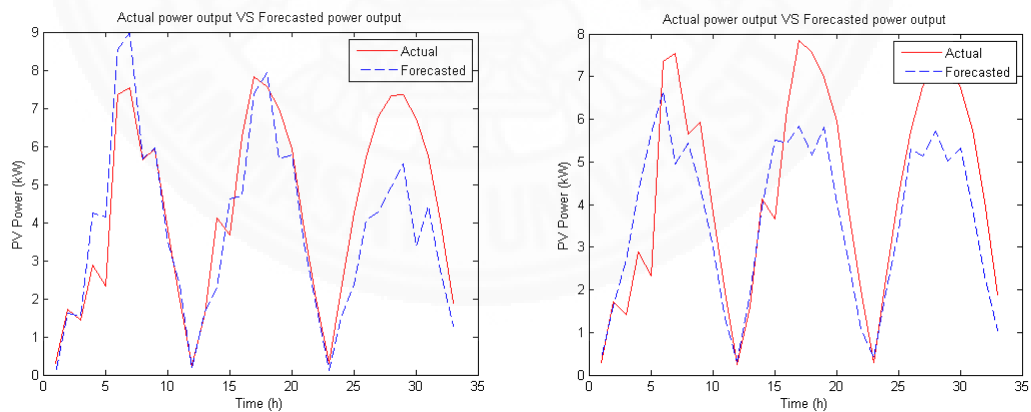
Figure 4.16: Compare the actual and forecasted power output, Delay = 1:2
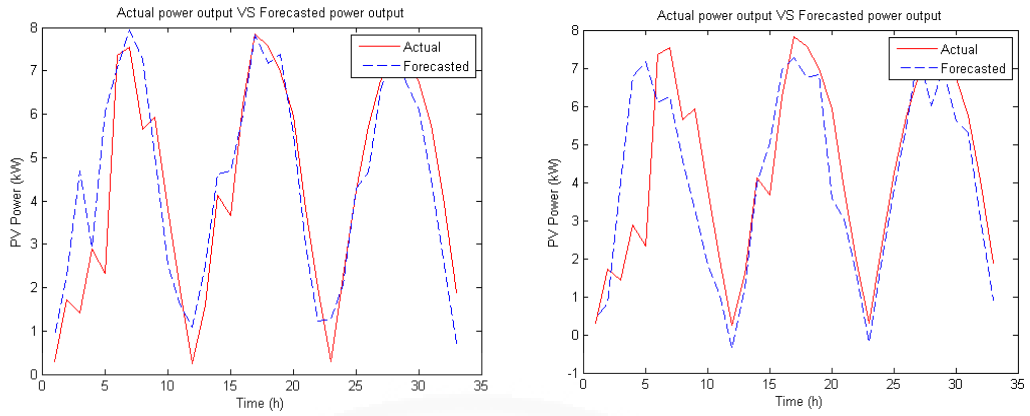
Figure 4.17: Compare the actual and forecasted power output, Delay = 1:3
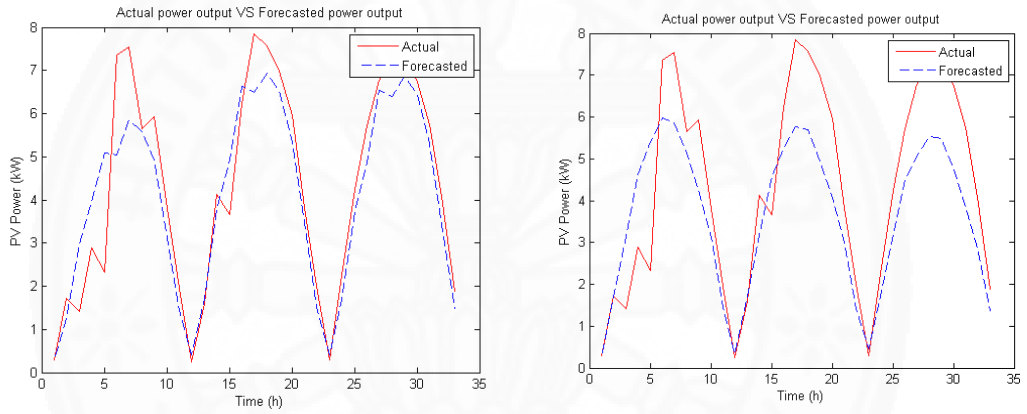
Figure 4.18: Compare the actual and forecasted power output, Delay = 1:4

Chapter 5
Conclusions and Recommendations

5.1 Conclusion

Due to a support of using renewable energy resources to generate electricity, the penetration of renewable energy power plant is rapidly occurred. Solar power is used widely in Thailand in order to generate electricity and connect to the main power grid system. However, the fluctuation and intermittence of solar power affecting to the generating of photovoltaic (PV) power system production still being the cause of problem in the main power system particularly in its power quality and stability. Hence, a good model and approach is necessary to apply for the forecasting of solar power plant output that can be used to manage the power system efficiently and to reduce the operating cost.

This study provides the suitable model for Thailand and approaches to forecast the production of PV power system in the next day, both linear algorithm and non-linear algorithm. Linear Regression Analysis is applied to predict the output in daily in linear algorithm and Artificial Neural Network (ANN) is conducted in non-linear algorithm to forecast the production in hourly.

In linear algorithm, solar radiation and ambient temperature are used as input variables to predict the daily generated energy in three experimental models. The second model using both weather parameters as inputs presents the best performance, *MSE = 2.5794*. Moreover, the experimental result indicates that the correlation between energy produced by solar power plant and solar radiation is better than ambient temperature. The last model possesses a large number of the prediction errors because the input data automatically gathered from Thailand Meteorological Department does not enough. Thus, the suitable model for Thailand is designed to forecast the PV power system production.

The other approaches conducted to predict the hourly outcome in non-linear algorithm base on the designed model and ANN. FFNN and NARX are the approaches applied to compare the designed model to the previous model in the prediction accuracy. Solar radiation in this algorithm is obtained by calculation and weather

parameters are gathered from public website and they are also used as input variables. Both FFNN and NARX verify that the designed model performance is better than the compared previous model. In FFNN, the designed model error is *MAPE = 17.6936* and the compared model error is *MAPE = 20.2657*. The errors of designed and compared model in NARX are *MSE = 0.0075* and *0.0163*, respectively. Additionally, when considering in each delay of NARX, it also emphasizes that the designed model has the prediction accuracy more than the compared model. For that reason, the designed model has one more stage to adjust the calculated solar radiation in order to have it being approximated to the actual for estimating the power output in the next stage.

5.2 Recommendation

The main factor affecting to the PV power system production is solar irradiance. It is obtained in this study by calculation that is suitable for the clear sky condition affecting to the mistakes might easily occur when apply. Therefore, the solar irradiance prediction by using the higher accuracy approaches might provide the better result in the forecasting of solar power plant output.

References

1.   Provincial Electricity Authority (2012). *About the Provincial Electricity Authority (PEA).* https://www.pea.co.th/en/introduction/Pages/History.aspx

2.   RENEW Wisconsin (2004). *An Introduction to Distributed Generation Interconnection*. http://www.renewwisconsin.org/wind/Toolbox-Applications%20and %20forms/Interconnection/Introduction%20to%20Distributed%20Generation.pdf

3.   Khatib, T., Mohamed, A., Sopian, K., Mahmoud, M. (2012). Assessment of Artificial Neural Networks for Hourly Solar Radiation Prediction. *International Journal of Photoenergy*, *2012*(946890), 1-7.

4.   Department of Alternative Energy Development and Efficiency of Thailand (1999). *Solar Radiation Map of Thailand*. http://www2.dede.go.th/dede/renew/solar_p.htm

5.   Huang, Y., Lu, J., Liu, C., Xu, X., Wang, W., Zhou, X. (2010). Comparative study of power forecasting methods for PV stations. *International Conference on Power System Technology (POWERCON)* (pp. 1-6). Hangzhou, China: IEEE.

6.   Agbo, G. A., Alfa, B., Ibeh, G. F., Adamu, I. S. (2013). Application of Regression and Multiple Correlation Analysis to Morning Hours Solar Radiation in Lapai. *International Journal of Physical Sciences, 8*(27), 1437-1441.

7.   Oudjana, S. H., Hellal, A., & Mahamed, I. H. (2012). Short Term Photovoltaic Power Generation Forecasting Using Neural Network. *11th International Conference on Environment and Electrical Engineering (EEEIC)* (pp. 706-711). Venice, Italy: IEEE.

8.   De Giorgi, M. G., Congedo, P. M., Malvoni, M., Tarantino M. (2013). Short-Term Power Forecasting by Statistical Methods for Photovoltaic Plants in South Italy. *4th Imeko TC19 Symposium on Environmental Instrumentation and Measurements Protecting Environment, Climate Changes and Pollution Control, Proceeding of a symposium held in Lecce, Italy, 3-4 June 2013* (pp. 171-175). New York, USA: Curran Associates, Inc.

9.   Mekhilef, S., Saidur, R., & Kamalisarvestani, M. (2012). Effect of Dust, Humidity and Air Velocity on Efficiency of Photovoltaic Cells. *Renewable and Sustainable Energy Reviews*, *16*(5), 2920-2925.

10.   Bacher, P., Madsen, H. & Nielsen, H.A. (2009). Online Short-Term Solar Power Forecasting. *Solar Energy*, *83*(10), 1772-1783.

11.   Yadav, A. K., & Chandel, S. S. (2014). Solar Radiation Prediction using Artificial Neural Network Techniques, A Review. *Renewable and Sustainable Energy Reviews*, *33*, 772-781.

12.   Elminir, H. K., Azzam, Y. A., & Younes, F. I. (2007). Prediction of Hourly and Daily Diffuse Fraction using Neural Network, as Compared to Linear Regression Models. *Energy*, *32*(8), 1513-1523.

13.   Mellit, A. (2008). Artificial Intelligence Technique for Modelling and Forecasting of Solar Radiation Data: A Review. *International Journal of Artificial Intelligence and Soft Computing, 1*(1), 52-76.

14.   Reddy, K. S., & Ranjan, M. (2003). Solar Resource Estimation using Artificial Neural Networks and Comparison with Other Correlation Models. *Energy Conversion and Management*, *44*(15), 2519-2530.

15.   Chaouachi, A., Kamel, R. M., Ichikawa, R., Hayashi, H., Nagasaka, K. (2009). Neural Network Ensemble-based Solar Power Generation Short-Term Forecasting. *World Academy of Science, Engineering and Technology*, *3*(6), 41-46.

16.   Saberian, A., Hizam, H., Radzi, M. A. M., Ab Kadir, M. Z. A., Mirzaei, M. (2014). Modelling and Prediction of Photovoltaic Power Output Using Artificial Neural Networks. *International Journal of Photoenergy*, *2014*(469701), 1-10.

17.   Al-Messabi, N., Li, Y., El-Amin, I. Goh, C. (2012). Forecasting of Photovoltaic Power Yield Using Dynamic Neural Networks. *The 2012 International Joint Conference on Neural Networks (IJCNN)* (pp. 1-5). Brisbane, Australia: IEEE.

18.   Tao, C., Shanxu, D., & Changsong, C. (2010). Forecasting Power Output for Grid-Connected Photovoltaic Power System without using Solar Radiation Measurement. *2nd IEEE International Symposium on Power Electronics for Distributed Generation Systems (PEDG)* (pp. 773-777). Hefei, China: IEEE

19.   Markvart, T. (2000). *Solar Electricity Second Edition*. England: JohnWiley &Sons LTD.

20.   Chapra, S. C. (2012). *Applied Numerical Methods with MATLAB for Engineers and Scientists*. New York: McGraw-Hill.

21.   Pham, H. T., Tran, V. T., & Yang, B.S. (2010). A Hybrid of Nonlinear Autoregressive Model with Exogenous Input and Autoregressive Moving Average

Model for Long-Term Machine State Forecasting. *Expert Systems with Applications, 37*(4), 3310-3317

22.   MathWorks® (2015). *Design Time Series NARX Feedback Neural Networks*. http://www.mathworks.com/help/nnet/ug/design-time-series-narx-feedback-neural-networks.html

23.   Vanguard Software Corporation (2014). *Mean Absolute Percent Error*. http://www.vanguardsw.com/business-forecasting-101/mean-absolute-percent-error-mape/

24.   Meebunsmer, P., & Charoenlarpnopparut, C. (2014). Forecasting of Solar Power Plant Production under the Effect of Weather Condition. *Regional Conference on Computer and Information Engineering 2014* (pp.229-233). Yogyakarta, Indonesia: Universitas Gadjah Mada.

25.   Mellit, A., & Pavan, A. M. (2010). A 24-h forecast of solar irradiance using artificial neural network: Application for performance prediction of a grid-connected PV plant at Trieste, Italy. *Solae Energy*, *84*(5), 807-821.

26.   Zhang, W., Wang, Y., Wang, J., Liang, J. (2009). Electricity Demand Forecasting Based on Feedforward Neural Network Training by A Novel Hybrid Evolutionary Algorithm. *International Conference on Computer Engineering and Technology*, *1*, 98-102.

27.   SAS Institute Inc. (2009). *SAS/STAT® 9.2 User's Guide (Second Edition)*. Retrieved from September, 2009, http://support.sas.com/documentation/cdl/en/statug/63033/PDF/default/statug.pdf

28.   Provincial Electricity Authority (2012). *PEA Smart Grid Roadmap*. https://www.pea.co.th/en/introduction/Pages/PEA%20smart%20grid%20roadmap.aspx

Appendices
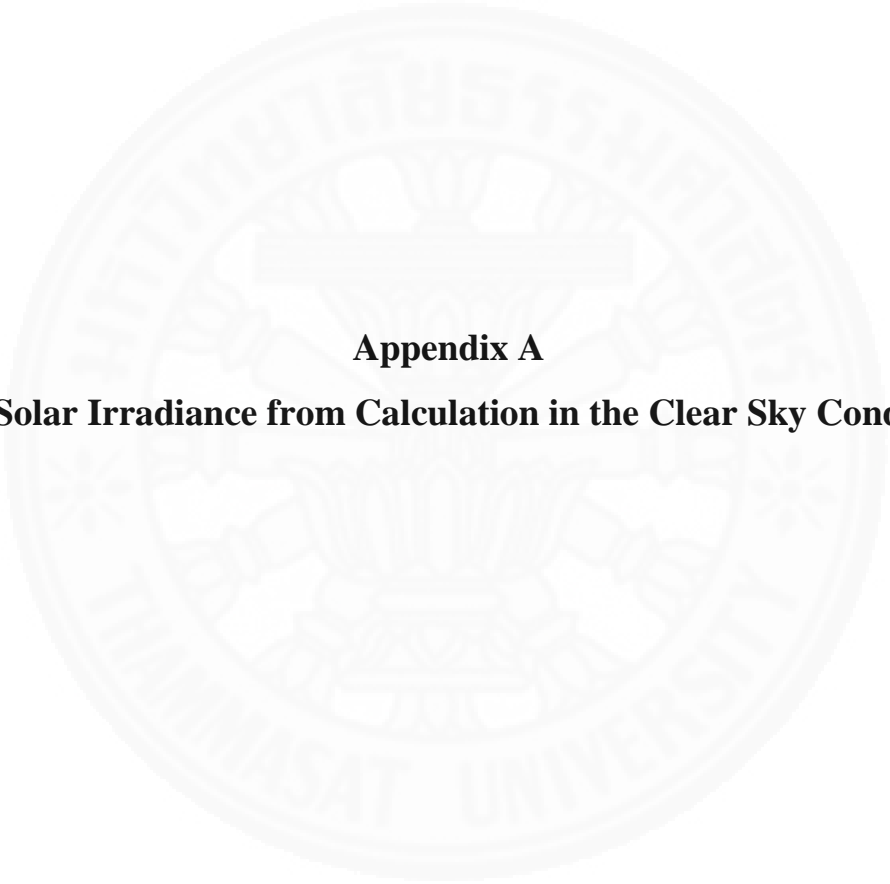
Appendix A

The Solar Irradiance from Calculation in the Clear Sky Condition

Date	Day Time	7.00	8.00	9.00	10.00	11.00	12.00	13.00	14.00	15.00	16.00	17.00
1	1-Jan	58.8068	251.5701	475.1001	662.5955	790.9103	848.2911	829.9487	737.3915	578.5891	369.6479	146.3361
2	2-Jan	58.0200	250.3194	474.1045	662.0739	790.9507	848.9165	831.1312	739.0575	580.6186	371.8474	148.2011
3	3-Jan	57.2586	249.1173	473.1626	661.6081	791.0464	849.5942	832.3608	740.7634	582.6797	374.0709	150.0881
4	4-Jan	56.5227	247.9648	472.2754	661.1986	791.1973	850.3236	833.6363	742.5077	584.7707	376.3164	151.9955
5	5-Jan	55.8125	246.8627	471.4436	660.8455	791.4032	851.1039	834.9565	744.2887	586.8897	378.5820	153.9217
6	6-Jan	55.1282	245.8119	470.6678	660.5490	791.6637	851.9344	836.3201	746.1049	589.0349	380.8657	155.8650
7	7-Jan	54.4698	244.8134	469.9487	660.3095	791.9786	852.8143	837.7260	747.9546	591.2043	383.1656	157.8236
8	8-Jan	53.8377	243.8678	469.2868	660.1270	792.3474	853.7426	839.1727	749.8361	593.3959	385.4795	159.7959
9	9-Jan	53.2320	242.9759	468.6828	660.0016	792.7699	854.7185	840.6590	751.7477	595.6079	387.8055	161.7800
10	10-Jan	52.6529	242.1384	468.1369	659.9333	793.2454	855.7410	842.1833	753.6876	597.8382	390.1415	163.7742
11	11-Jan	52.1007	241.3561	467.6498	659.9221	793.7734	856.8090	843.7442	755.6540	600.0848	392.4853	165.7765
12	12-Jan	51.5756	240.6295	467.2217	659.9678	794.3534	857.9214	845.3402	757.6451	602.3456	394.8350	167.7851
13	13-Jan	51.0779	239.9592	466.8530	660.0705	794.9846	859.0772	846.9698	759.6589	604.6185	397.1883	169.7981
14	14-Jan	50.6079	239.3458	466.5440	660.2298	795.6665	860.2751	848.6314	761.6937	606.9016	399.5432	171.8136
15	15-Jan	50.1659	238.7897	466.2948	660.4455	796.3981	861.5140	850.3233	763.7474	609.1926	401.8975	173.8296
16	16-Jan	49.7521	238.2914	466.1057	660.7173	797.1789	862.7925	852.0439	765.8180	611.4894	404.2491	175.8442
17	17-Jan	49.3669	237.8514	465.9768	661.0448	798.0078	864.1093	853.7914	767.9037	613.7899	406.5958	177.8555
18	18-Jan	49.0106	237.4700	465.9080	661.4277	798.8839	865.4631	855.5641	770.0023	616.0920	408.9355	179.8613
19	19-Jan	48.6834	237.1476	465.8995	661.8654	799.8064	866.8524	857.3602	772.1119	618.3933	411.2659	181.8598
20	20-Jan	48.3859	236.8843	465.9512	662.3575	800.7742	868.2758	859.1779	774.2303	620.6919	413.5851	183.8490
21	21-Jan	48.1181	236.6805	466.0629	662.9033	801.7862	869.7318	861.0154	776.3555	622.9854	415.8907	185.8269
22	22-Jan	47.8805	236.5364	466.2345	663.5022	802.8413	871.2189	862.8708	778.4854	625.2717	418.1808	187.7916

Date	Day\Time	7.00	8.00	9.00	10.00	11.00	12.00	13.00	14.00	15.00	16.00	17.00
23	23-Jan	47.6734	236.4521	466.4657	664.1536	803.9384	872.7354	864.7421	780.6179	627.5486	420.4531	189.7410
24	24-Jan	47.4971	236.4276	466.7563	664.8566	805.0761	874.2798	866.6275	782.7508	629.8139	422.7055	191.6732
25	25-Jan	47.3518	236.4631	467.1060	665.6105	806.2534	875.8503	868.5249	784.8819	632.0654	424.9359	193.5864
26	26-Jan	47.2379	236.5585	467.5143	666.4143	807.4689	877.4454	870.4325	787.0092	634.3010	427.1423	195.4785
27	27-Jan	47.1557	236.7139	467.9807	667.2673	808.7211	879.0632	872.3481	789.1305	636.5184	429.3226	197.3478
28	28-Jan	47.1055	236.9290	468.5049	668.1683	810.0088	880.7020	874.2698	791.2436	638.7154	431.4747	199.1923
29	29-Jan	47.0875	237.2038	469.0861	669.1165	811.3304	882.3601	876.1956	793.3463	640.8900	433.5966	201.0102
30	30-Jan	47.1020	237.5380	469.7237	670.1106	812.6845	884.0355	878.1232	795.4366	643.0400	435.6864	202.7998
31	31-Jan	47.1492	237.9314	470.4171	671.1496	814.0695	885.7265	880.0508	797.5121	645.1633	437.7420	204.5593
32	1-Feb	47.2295	238.3838	471.1655	672.2323	815.4839	887.4310	881.9762	799.5708	647.2577	439.7617	206.2870
33	2-Feb	47.3430	238.8946	471.9680	673.3575	816.9260	889.1473	883.8973	801.6106	649.3212	441.7434	207.9811
34	3-Feb	47.4900	239.4636	472.8238	674.5238	818.3942	890.8735	885.8120	803.6292	651.3518	443.6854	209.6402
35	4-Feb	47.6708	240.0901	473.7320	675.7298	819.8868	892.6074	887.7183	805.6246	653.3474	445.5858	211.2625
36	5-Feb	47.8856	240.7738	474.6915	676.9743	821.4021	894.3472	889.6139	807.5946	655.3061	447.4429	212.8467
37	6-Feb	48.1346	241.5141	475.7013	678.2558	822.9383	896.0909	891.4968	809.5372	657.2259	449.2551	214.3913
38	7-Feb	48.4180	242.3102	476.7603	679.5727	824.4935	897.8364	893.3650	811.4503	659.1049	451.0205	215.8947
39	8-Feb	48.7361	243.1615	477.8673	680.9235	826.0660	899.5818	895.2163	813.3318	660.9412	452.7378	217.3558
40	9-Feb	49.0891	244.0672	479.0210	682.3067	827.6539	901.3250	897.0485	815.1798	662.7330	454.4053	218.7732
41	10-Feb	49.4773	245.0265	480.2202	683.7206	829.2553	903.0639	898.8598	816.9923	664.4786	456.0215	220.1457
42	11-Feb	49.9007	246.0385	481.4635	685.1635	830.8683	904.7966	900.6479	818.7672	666.1762	457.5850	221.4723
43	12-Feb	50.3598	247.1023	482.7496	686.6337	832.4910	906.5209	902.4108	820.5028	667.8241	459.0946	222.7517
44	13-Feb	50.8546	248.2169	484.0769	688.1295	834.1213	908.2348	904.1466	822.1971	669.4207	460.5488	223.9831

Date	Day	Time 7.00	8.00	9.00	10.00	11.00	12.00	13.00	14.00	15.00	16.00	17.00
45	14-Feb	51.3853	249.3813	485.4439	689.6490	835.7574	909.9363	905.8532	823.8482	670.9645	461.9465	225.1655
46	15-Feb	51.9523	250.5942	486.8491	691.1904	837.3971	911.6233	907.5286	825.4544	672.4539	463.2866	226.2981
47	16-Feb	52.5555	251.8546	488.2909	692.7518	839.0386	913.2937	909.1709	827.0140	673.8876	464.5679	227.3800
48	17-Feb	53.1953	253.1612	489.7676	694.3314	840.6797	914.9456	910.7782	828.5252	675.2641	465.7896	228.4107
49	18-Feb	53.8718	254.5127	491.2775	695.9273	842.3184	916.5769	912.3485	829.9865	676.5822	466.9506	229.3895
50	19-Feb	54.5850	255.9078	492.8187	697.5373	843.9528	918.1856	913.8801	831.3962	677.8405	468.0501	230.3160
51	20-Feb	55.3351	257.3451	494.3897	699.1596	845.5806	919.7697	915.3711	832.7527	679.0380	469.0874	231.1896
52	21-Feb	56.1221	258.8231	495.9884	700.7922	847.2000	921.3272	916.8197	834.0547	680.1736	470.0619	232.0100
53	22-Feb	56.9460	260.3402	497.6129	702.4329	848.8088	922.8562	918.2242	835.3008	681.2463	470.9729	232.7770
54	23-Feb	57.8068	261.8950	499.2615	704.0799	850.4050	924.3548	919.5830	836.4895	682.2550	471.8199	233.4903
55	24-Feb	58.7045	263.4858	500.9321	705.7309	851.9865	925.8211	920.8944	837.6197	683.1991	472.6025	234.1499
56	25-Feb	59.6388	265.1109	502.6226	707.3840	853.5514	927.2533	922.1569	838.6901	684.0776	473.3204	234.7558
57	26-Feb	60.6096	266.7687	504.3312	709.0369	855.0975	928.6495	923.3689	839.6995	684.8900	473.9734	235.3080
58	27-Feb	61.6165	268.4573	506.0557	710.6877	856.6230	930.0079	924.5290	840.6471	685.6356	474.5612	235.8067
59	28-Feb	62.6593	270.1749	507.7941	712.3343	858.1258	931.3268	925.6358	841.5317	686.3140	475.0840	236.2522
60	1-Mar	63.7376	271.9198	509.5443	713.9744	859.6040	932.6045	926.6879	842.3524	686.9246	475.5415	236.6447
61	2-Mar	64.8507	273.6900	511.3041	715.6061	861.0556	933.8393	927.6841	843.1086	687.4671	475.9341	236.9847
62	3-Mar	65.9981	275.4836	513.0714	717.2273	862.4788	935.0297	928.6232	843.7993	687.9414	476.2618	237.2727
63	4-Mar	67.1793	277.2986	514.8442	718.8358	863.8716	936.1742	929.5040	844.4240	688.3471	476.5251	237.5092
64	5-Mar	68.3933	279.1331	516.6201	720.4296	865.2322	937.2711	930.3255	844.9821	688.6844	476.7242	237.6948
65	6-Mar	69.6393	280.9850	518.3971	722.0066	866.5589	938.3191	931.0867	845.4731	688.9531	476.8596	237.8304
66	7-Mar	70.9166	282.8523	520.1730	723.5648	867.8498	939.3169	931.7867	845.8966	689.1535	476.9320	237.9167

Date	Day\Time	7.00	8.00	9.00	10.00	11.00	12.00	13.00	14.00	15.00	16.00	17.00
67	8-Mar	72.2239	284.7329	521.9457	725.1022	869.1032	940.2630	932.4247	846.2523	689.2856	476.9418	237.9545
68	9-Mar	73.5602	286.6248	523.7129	726.6169	870.3176	941.1563	933.0000	846.5400	689.3499	476.8900	237.9449
69	10-Mar	74.9243	288.5257	525.4726	728.1067	871.4912	941.9956	933.5118	846.7596	689.3466	476.7772	237.8888
70	11-Mar	76.3151	290.4337	527.2226	729.5699	872.6225	942.7797	933.9595	846.9109	689.2762	476.6045	237.7873
71	12-Mar	77.7310	292.3466	528.9607	731.0045	873.7100	943.5077	934.3427	846.9941	689.1394	476.3726	237.6415
72	13-Mar	79.1708	294.2622	530.6848	732.4087	874.7522	944.1786	934.6610	847.0093	688.9367	476.0828	237.4527
73	14-Mar	80.6329	296.1784	532.3930	733.7807	875.7478	944.7915	934.9140	846.9566	688.6688	475.7361	237.2221
74	15-Mar	82.1157	298.0932	534.0830	735.1187	876.6954	945.3455	935.1015	846.8365	688.3367	475.3337	236.9510
75	16-Mar	83.6178	300.0043	535.7529	736.4210	877.5937	945.8401	935.2233	846.6493	687.9412	474.8769	236.6407
76	17-Mar	85.1373	301.9096	537.4007	737.6859	878.4416	946.2744	935.2793	846.3955	687.4832	474.3670	236.2928
77	18-Mar	86.6727	303.8071	539.0244	738.9119	879.2380	946.6480	935.2696	846.0757	686.9639	473.8055	235.9086
78	19-Mar	88.2220	305.6946	540.6221	740.0974	879.9817	946.9603	935.1943	845.6905	686.3843	473.1937	235.4896
79	20-Mar	89.7837	307.5701	542.1918	741.2408	880.6719	947.2110	935.0535	845.2407	685.7457	472.5333	235.0374
80	21-Mar	91.3557	309.4315	543.7318	742.3408	881.3075	947.3998	934.8475	844.7271	685.0494	471.8258	234.5535
81	22-Mar	92.9362	311.2768	545.2403	743.3960	881.8879	947.5263	934.5768	844.1507	684.2968	471.0729	234.0396
82	23-Mar	94.5235	313.1040	546.7155	744.4051	882.4122	947.5905	934.2416	843.5123	683.4892	470.2763	233.4972
83	24-Mar	96.1155	314.9111	548.1557	745.3669	882.8798	947.5924	933.8427	842.8132	682.6281	469.4376	232.9281
84	25-Mar	97.7103	316.6963	549.5593	746.2803	883.2901	947.5319	933.3805	842.0544	681.7152	468.5586	232.3338
85	26-Mar	99.3060	318.4575	550.9248	747.1441	883.6426	947.4091	932.8558	841.2371	680.7520	467.6413	231.7161
86	27-Mar	100.9008	320.1931	552.2505	747.9573	883.9368	947.2242	932.2694	840.3627	679.7402	466.6874	231.0767
87	28-Mar	102.4926	321.9011	553.5352	748.7191	884.1726	946.9776	931.6222	839.4324	678.6815	465.6988	230.4173
88	29-Mar	104.0796	323.5798	554.7774	749.4285	884.3496	946.6696	930.9150	838.4479	677.5777	464.6774	229.7395

Date	Day	Time	7.00	8.00	9.00	10.00	11.00	12.00	13.00	14.00	15.00	16.00	17.00
89	30-Mar		105.6599	325.2276	555.9758	750.0849	884.4676	946.3007	930.1490	837.4104	676.4307	463.6253	229.0452
90	31-Mar		107.2315	326.8428	557.1292	750.6875	884.5266	945.8713	929.3251	836.3216	675.2422	462.5443	228.3360
91	1-Apr		108.7927	328.4238	558.2364	751.2357	884.5265	945.3822	928.4447	835.1832	674.0142	461.4365	227.6136
92	2-Apr		110.3415	329.9691	559.2963	751.7291	884.4676	944.8339	927.5088	833.9967	672.7487	460.3038	226.8797
93	3-Apr		111.8763	331.4771	560.3079	752.1670	884.3499	944.2273	926.5188	832.7639	671.4476	459.1483	226.1361
94	4-Apr		113.3952	332.9467	561.2703	752.5494	884.1738	943.5632	925.4762	831.4865	670.1129	457.9719	225.3844
95	5-Apr		114.8965	334.3762	562.1827	752.8757	883.9395	942.8427	924.3823	830.1665	668.7467	456.7768	224.6263
96	6-Apr		116.3785	335.7646	563.0442	753.1459	883.6475	942.0665	923.2386	828.8056	667.3511	455.5648	223.8633
97	7-Apr		117.8395	337.1107	563.8543	753.3599	883.2983	941.2359	922.0466	827.4058	665.9280	454.3382	223.0972
98	8-Apr		119.2781	338.4132	564.6121	753.5176	882.8924	940.3520	920.8081	825.9690	664.4796	453.0987	222.3295
99	9-Apr		120.6926	339.6712	565.3174	753.6192	882.4307	939.4161	919.5247	824.4971	663.0081	451.8486	221.5618
100	10-Apr		122.0815	340.8836	565.9695	753.6647	881.9137	938.4293	918.1980	822.9923	661.5154	450.5897	220.7956
101	11-Apr		123.4435	342.0497	566.5682	753.6544	881.3424	937.3930	916.8299	821.4564	660.0038	449.3240	220.0324
102	12-Apr		124.7771	343.1684	567.1131	753.5886	880.7176	936.3087	915.4222	819.8917	658.4753	448.0535	219.2737
103	13-Apr		126.0811	344.2392	567.6041	753.4677	880.0403	935.1778	913.9766	818.3001	656.9321	446.7801	218.5210
104	14-Apr		127.3541	345.2613	568.0410	753.2922	879.3115	934.0019	912.4952	816.6837	655.3763	445.5058	217.7755
105	15-Apr		128.5951	346.2342	568.4238	753.0627	878.5323	932.7824	910.9797	815.0447	653.8100	444.2323	217.0387
106	16-Apr		129.8028	347.1572	568.7526	752.7797	877.7039	931.5211	909.4322	813.3851	652.2353	442.9616	216.3119
107	17-Apr		130.9763	348.0300	569.0275	752.4439	876.8276	930.2196	907.8546	811.7072	650.6542	441.6955	215.5963
108	18-Apr		132.1146	348.8523	569.2487	752.0563	875.9046	928.8796	906.2490	810.0130	649.0689	440.4358	214.8932
109	19-Apr		133.2167	349.6237	569.4165	751.6175	874.9363	927.5029	904.6174	808.3046	647.4814	439.1841	214.2038
110	20-Apr		134.2818	350.3440	569.5312	751.1285	873.9240	926.0913	902.9618	806.5842	645.8937	437.9423	213.5291

Date	Day Time	7.00	8.00	9.00	10.00	11.00	12.00	13.00	14.00	15.00	16.00	17.00
111	21-Apr	135.3091	351.0131	569.5933	750.5903	872.8693	924.6465	901.2842	804.8540	644.3078	436.7119	212.8704
112	22-Apr	136.2980	351.6310	569.6033	750.0039	871.7737	923.1706	899.5868	803.1159	642.7256	435.4946	212.2285
113	23-Apr	137.2477	352.1976	569.5618	749.3704	870.6386	921.6653	897.8717	801.3722	641.1492	434.2920	211.6046
114	24-Apr	138.1578	352.7131	569.4693	748.6911	869.4658	920.1326	896.1408	799.6249	639.5803	433.1056	210.9996
115	25-Apr	139.0278	353.1776	569.3267	747.9671	868.2569	918.5745	894.3964	797.8760	638.0210	431.9369	210.4143
116	26-Apr	139.8571	353.5914	569.1347	747.1997	867.0135	916.9928	892.6405	796.1277	636.4730	430.7874	209.8497
117	27-Apr	140.6456	353.9547	568.8942	746.3902	865.7375	915.3896	890.8752	794.3820	634.9381	429.6583	209.3065
118	28-Apr	141.3929	354.2680	568.6061	745.5401	864.4304	913.7669	889.1026	792.6408	633.4180	428.5511	208.7854
119	29-Apr	142.0987	354.5317	568.2713	744.6507	863.0942	912.1267	887.3247	790.9062	631.9146	427.4670	208.2873
120	30-Apr	142.7630	354.7462	567.8909	743.7236	861.7306	910.4711	885.5437	789.1801	630.4294	426.4072	207.8127
121	1-May	143.3856	354.9122	567.4659	742.7602	860.3414	908.8019	883.7616	787.4644	628.9641	425.3730	207.3622
122	2-May	143.9666	355.0303	566.9975	741.7621	858.9287	907.1213	881.9803	785.7610	627.5203	424.3655	206.9365
123	3-May	144.5059	355.1011	566.4869	740.7309	857.4941	905.4313	880.2021	784.0718	626.0995	423.3857	206.5359
124	4-May	145.0038	355.1255	565.9353	739.6681	856.0396	903.7339	878.4288	782.3986	624.7032	422.4346	206.1611
125	5-May	145.4603	355.1041	565.3439	738.5756	854.5672	902.0312	876.6624	780.7432	623.3327	421.5133	205.8124
126	6-May	145.8757	355.0379	564.7142	737.4549	853.0786	900.3251	874.9048	779.1072	621.9896	420.6226	205.4902
127	7-May	146.2502	354.9278	564.0473	736.3077	851.5760	898.6176	873.1581	777.4925	620.6751	419.7633	205.1949
128	8-May	146.5843	354.7746	563.3448	735.1358	850.0611	896.9108	871.4241	775.9006	619.3906	418.9363	204.9267
129	9-May	146.8783	354.5795	562.6081	733.9409	848.5360	895.2066	869.7047	774.3333	618.1372	418.1424	204.6858
130	10-May	147.1326	354.3433	561.8386	732.7248	847.0025	893.5071	868.0017	772.7919	616.9161	417.3822	204.4725
131	11-May	147.3478	354.0673	561.0377	731.4893	845.4627	891.8140	866.3169	771.2782	615.7284	416.6563	204.2870
132	12-May	147.5243	353.7524	560.2071	730.2361	843.9183	890.1294	864.6521	769.7935	614.5753	415.9653	204.1293

Date	Day Time	7.00	8.00	9.00	10.00	11.00	12.00	13.00	14.00	15.00	16.00	17.00
133	13-May	147.6628	353.3999	559.3482	728.9670	842.3714	888.4551	863.0090	768.3393	613.4577	415.3099	203.9996
134	14-May	147.7639	353.0110	558.4627	727.6839	840.8239	886.7931	861.3894	766.9169	612.3766	414.6904	203.8978
135	15-May	147.8282	352.5867	557.5520	726.3885	839.2776	885.1451	859.7947	765.5278	611.3330	414.1073	203.8241
136	16-May	147.8565	352.1285	556.6177	725.0827	837.7345	883.5130	858.2268	764.1731	610.3276	413.5610	203.7783
137	17-May	147.8495	351.6375	555.6616	723.7682	836.1963	881.8986	856.6871	762.8541	609.3613	413.0518	203.7604
138	18-May	147.8080	351.1150	554.6851	722.4469	834.6651	880.3036	855.1772	761.5721	608.4348	412.5800	203.7703
139	19-May	147.7328	350.5623	553.6899	721.1206	833.1425	878.7297	853.6985	760.3280	607.5488	412.1458	203.8078
140	20-May	147.6247	349.9809	552.6777	719.7910	831.6304	877.1787	852.2525	759.1231	606.7040	411.7495	203.8729
141	21-May	147.4846	349.3719	551.6500	718.4600	830.1306	875.6522	850.8406	757.9583	605.9010	411.3911	203.9652
142	22-May	147.3134	348.7368	550.6085	717.1292	828.6448	874.1518	849.4642	756.8347	605.1403	411.0708	204.0845
143	23-May	147.1120	348.0770	549.5549	715.8005	827.1748	872.6791	848.1244	755.7530	604.4224	410.7886	204.2306
144	24-May	146.8813	347.3938	548.4908	714.4757	825.7223	871.2356	846.8227	754.7143	603.7477	410.5445	204.4031
145	25-May	146.6224	346.6886	547.4177	713.1563	824.2890	869.8228	845.5602	753.7194	603.1167	410.3385	204.6017
146	26-May	146.3362	345.9629	546.3374	711.8442	822.8764	868.4422	844.3380	752.7689	602.5296	410.1705	204.8262
147	27-May	146.0236	345.2180	545.2515	710.5409	821.4863	867.0951	843.1572	751.8637	601.9868	410.0403	205.0759
148	28-May	145.6857	344.4553	544.1615	709.2483	820.1202	865.7830	842.0190	751.0044	601.4885	409.9479	205.3507
149	29-May	145.3236	343.6763	543.0691	707.9678	818.7795	864.5072	840.9243	750.1916	601.0349	409.8929	205.6499
150	30-May	144.9381	342.8823	541.9759	706.7012	817.4659	863.2690	839.8740	749.4258	600.6261	409.8752	205.9731
151	31-May	144.5305	342.0747	540.8833	705.4500	816.1809	862.0695	838.8691	748.7077	600.2622	409.8945	206.3199
152	1-Jun	144.1017	341.2551	539.7931	704.2157	814.9257	860.9100	837.9104	748.0376	599.9433	409.9504	206.6896
153	2-Jun	143.6527	340.4247	538.7066	702.9999	813.7019	859.7916	836.9988	747.4159	599.6693	410.0426	207.0818
154	3-Jun	143.1847	339.5849	537.6255	701.8042	812.5107	858.7154	836.1349	746.8430	599.4403	410.1707	207.4958

Date	Day	Time 7.00	8.00	9.00	10.00	11.00	12.00	13.00	14.00	15.00	16.00	17.00
155	4-Jun	142.6987	338.7372	536.5512	700.6298	811.3535	857.6825	835.3195	746.3193	599.2561	410.3342	207.9311
156	5-Jun	142.1957	337.8829	535.4853	699.4784	810.2316	856.6938	834.5533	745.8450	599.1166	410.5327	208.3869
157	6-Jun	141.6769	337.0233	534.4291	698.3513	809.1461	855.7503	833.8367	745.4202	599.0216	410.7657	208.8628
158	7-Jun	141.1432	336.1599	533.3841	697.2499	808.0983	854.8529	833.1705	745.0451	598.9709	411.0326	209.3578
159	8-Jun	140.5958	335.2940	532.3518	696.1755	807.0893	854.0025	832.5550	744.7199	598.9642	411.3328	209.8715
160	9-Jun	140.0356	334.4268	531.3335	695.1294	806.1202	853.1998	831.9906	744.4446	599.0012	411.6657	210.4030
161	10-Jun	139.4638	333.5598	530.3306	694.1129	805.1921	852.4455	831.4779	744.2192	599.0815	412.0307	210.9516
162	11-Jun	138.8813	332.6942	529.3444	693.1272	804.3058	851.7405	831.0171	744.0436	599.2047	412.4271	211.5165
163	12-Jun	138.2893	331.8312	528.3763	692.1735	803.4625	851.0853	830.6085	743.9178	599.3705	412.8542	212.0969
164	13-Jun	137.6887	330.9723	527.4274	691.2530	802.6631	850.4805	830.2523	743.8416	599.5782	413.3112	212.6921
165	14-Jun	137.0805	330.1185	526.4992	690.3668	801.9083	849.9267	829.9488	743.8148	599.8274	413.7974	213.3011
166	15-Jun	136.4658	329.2711	525.5927	689.5158	801.1990	849.4244	829.6980	743.8373	600.1174	414.3120	213.9231
167	16-Jun	135.8456	328.4315	524.7093	688.7013	800.5361	848.9740	829.5001	743.9086	600.4478	414.8540	214.5572
168	17-Jun	135.2209	327.6006	523.8500	687.9242	799.9201	848.5759	829.3550	744.0285	600.8178	415.4227	215.2026
169	18-Jun	134.5926	326.7798	523.0161	687.1854	799.3519	848.2304	829.2628	744.1966	601.2268	416.0171	215.8583
170	19-Jun	133.9616	325.9701	522.2085	686.4859	798.8320	847.9379	829.2233	744.4124	601.6739	416.6363	216.5233
171	20-Jun	133.3291	325.1728	521.4285	685.8265	798.3610	847.6986	829.2364	744.6756	602.1585	417.2794	217.1967
172	21-Jun	132.6958	324.3888	520.6770	685.2082	797.9395	847.5127	829.3020	744.9854	602.6797	417.9453	217.8775
173	22-Jun	132.0628	323.6194	519.9550	684.6315	797.5679	847.3802	829.4198	745.3415	603.2367	418.6331	218.5647
174	23-Jun	131.4309	322.8655	519.2636	684.0975	797.2467	847.3014	829.5896	745.7431	603.8286	419.3416	219.2572
175	24-Jun	130.8010	322.1283	518.6037	683.6066	796.9763	847.2762	829.8110	746.1897	604.4544	420.0698	219.9541
176	25-Jun	130.1740	321.4087	517.9762	683.1597	796.7570	847.3045	830.0836	746.6804	605.1132	420.8167	220.6543

Date	Day Time	7.00	8.00	9.00	10.00	11.00	12.00	13.00	14.00	15.00	16.00	17.00
177	26-Jun	129.5508	320.7077	517.3820	682.7573	796.5892	847.3865	830.4071	747.2145	605.8041	421.5809	221.3567
178	27-Jun	128.9323	320.0264	516.8220	682.4000	796.4730	847.5218	830.7808	747.7914	606.5258	422.3615	222.0601
179	28-Jun	128.3192	319.3657	516.2968	682.0885	796.4087	847.7104	831.2044	748.4100	607.2775	423.1572	222.7636
180	29-Jun	127.7125	318.7264	515.8075	681.8230	796.3964	847.9520	831.6771	749.0695	608.0579	423.9668	223.4659
181	30-Jun	127.1128	318.1096	515.3546	681.6043	796.4362	848.2464	832.1985	749.7690	608.8659	424.7891	224.1659
182	1-Jul	126.5210	317.5161	514.9389	681.4325	796.5283	848.5932	832.7677	750.5075	609.7003	425.6227	224.8624
183	2-Jul	125.9379	316.9467	514.5611	681.3082	796.6725	848.9921	833.3841	751.2840	610.5600	426.4665	225.5543
184	3-Jul	125.3642	316.4024	514.2218	681.2316	796.8688	849.4425	834.0470	752.0974	611.4436	427.3190	226.2404
185	4-Jul	124.8006	315.8838	513.9217	681.2030	797.1171	849.9441	834.7554	752.9466	612.3499	428.1791	226.9195
186	5-Jul	124.2479	315.3918	513.6612	681.2226	797.4174	850.4964	835.5085	753.8305	613.2776	429.0452	227.5903
187	6-Jul	123.7068	314.9272	513.4410	681.2907	797.7693	851.0987	836.3054	754.7479	614.2252	429.9161	228.2517
188	7-Jul	123.1780	314.4906	513.2615	681.4074	798.1727	851.7504	837.1451	755.6976	615.1915	430.7902	228.9024
189	8-Jul	122.6621	314.0828	513.1232	681.5728	798.6273	852.4508	838.0267	756.6782	616.1751	431.6663	229.5411
190	9-Jul	122.1598	313.7044	513.0266	681.7870	799.1326	853.1992	838.9489	757.6886	617.1744	432.5429	230.1667
191	10-Jul	121.6717	313.3561	512.9719	682.0499	799.6884	853.9949	839.9109	758.7273	618.1880	433.4185	230.7777
192	11-Jul	121.1984	313.0386	512.9596	682.3615	800.2941	854.8370	840.9113	759.7929	619.2144	434.2917	231.3731
193	12-Jul	120.7406	312.7523	512.9899	682.7217	800.9493	855.7246	841.9490	760.8841	620.2521	435.1609	231.9515
194	13-Jul	120.2988	312.4979	513.0632	683.1305	801.6535	856.6567	843.0228	761.9995	621.2996	436.0247	232.5115
195	14-Jul	119.8735	312.2759	513.1796	683.5876	802.4060	857.6326	844.1314	763.1374	622.3552	436.8815	233.0521
196	15-Jul	119.4654	312.0869	513.3393	684.0928	803.2062	858.6510	845.2734	764.2964	623.4175	437.7299	233.5718
197	16-Jul	119.0748	311.9311	513.5425	684.6458	804.0534	859.7110	846.4476	765.4750	624.4847	438.5683	234.0694
198	17-Jul	118.7025	311.8092	513.7892	685.2464	804.9468	860.8114	847.6524	766.6715	625.5552	439.3951	234.5437

Date	Day Time	7.00	8.00	9.00	10.00	11.00	12.00	13.00	14.00	15.00	16.00	17.00
199	18-Jul	118.3487	311.7215	514.0796	685.8941	805.8858	861.9510	848.8865	767.8843	626.6274	440.2088	234.9933
200	19-Jul	118.0140	311.6684	514.4136	686.5885	806.8693	863.1288	850.1484	769.1119	627.6997	441.0079	235.4170
201	20-Jul	117.6988	311.6503	514.7913	687.3291	807.8966	864.3433	851.4365	770.3525	628.7702	441.7908	235.8135
202	21-Jul	117.4036	311.6673	515.2125	688.1155	808.9667	865.5933	852.7493	771.6044	629.8374	442.5560	236.1817
203	22-Jul	117.1287	311.7199	515.6771	688.9471	810.0786	866.8775	854.0852	772.8659	630.8995	443.3018	236.5202
204	23-Jul	116.8746	311.8082	516.1849	689.8232	811.2313	868.1945	855.4426	774.1353	631.9547	444.0268	236.8279
205	24-Jul	116.6415	311.9324	516.7358	690.7432	812.4236	869.5428	856.8198	775.4108	633.0015	444.7293	237.1035
206	25-Jul	116.4299	312.0927	517.3295	691.7064	813.6545	870.9210	858.2151	776.6906	634.0379	445.4079	237.3459
207	26-Jul	116.2400	312.2892	517.9656	692.7120	814.9228	872.3276	859.6269	777.9729	635.0624	446.0610	237.5540
208	27-Jul	116.0721	312.5220	518.6439	693.7592	816.2272	873.7610	861.0532	779.2560	636.0730	446.6871	237.7265
209	28-Jul	115.9265	312.7911	519.3639	694.8470	817.5665	875.2197	862.4925	780.5379	637.0682	447.2846	237.8623
210	29-Jul	115.8034	313.0966	520.1251	695.9747	818.9393	876.7019	863.9428	781.8169	638.0462	447.8522	237.9604
211	30-Jul	115.7032	313.4383	520.9270	697.1412	820.3443	878.2062	865.4024	783.0910	639.0051	448.3882	238.0197
212	31-Jul	115.6258	313.8162	521.7691	698.3454	821.7800	879.7306	866.8694	784.3584	639.9434	448.8913	238.0392
213	1-Aug	115.5716	314.2301	522.6508	699.5864	823.2450	881.2736	868.3419	785.6173	640.8593	449.3600	238.0178
214	2-Aug	115.5406	314.6799	523.5714	700.8630	824.7379	882.8334	869.8180	786.8658	641.7510	449.7929	237.9547
215	3-Aug	115.5331	315.1654	524.5302	702.1741	826.2570	884.4082	871.2959	788.1020	642.6169	450.1887	237.8489
216	4-Aug	115.5490	315.6862	525.5264	703.5183	827.8007	885.9961	872.7736	789.3241	643.4553	450.5459	237.6995
217	5-Aug	115.5884	316.2421	526.5593	704.8944	829.3675	887.5953	874.2493	790.5301	644.2646	450.8633	237.5057
218	6-Aug	115.6513	316.8326	527.6278	706.3012	830.9557	889.2040	875.7208	791.7183	645.0430	451.1396	237.2668
219	7-Aug	115.7378	317.4574	528.7312	707.7372	832.5636	890.8202	877.1864	792.8867	645.7891	451.3735	236.9818
220	8-Aug	115.8479	318.1160	529.8684	709.2010	834.1895	892.4421	878.6441	794.0336	646.5013	451.5639	236.6503

Date	Day \ Time	7.00	8.00	9.00	10.00	11.00	12.00	13.00	14.00	15.00	16.00	17.00
221	9-Aug	115.9814	318.8078	531.0383	710.6912	835.8315	894.0676	880.0919	795.1572	647.1779	451.7095	236.2715
222	10-Aug	116.1382	319.5324	532.2400	712.2062	837.4879	895.6948	881.5278	796.2556	647.8175	451.8093	235.8448
223	11-Aug	116.3183	320.2890	533.4722	713.7445	839.1568	897.3219	882.9500	797.3270	648.4186	451.8622	235.3698
224	12-Aug	116.5215	321.0771	534.7338	715.3045	840.8364	898.9467	884.3564	798.3697	648.9797	451.8672	234.8459
225	13-Aug	116.7475	321.8958	536.0235	716.8846	842.5247	900.5673	885.7451	799.3820	649.4995	451.8234	234.2728
226	14-Aug	116.9962	322.7443	537.3401	718.4830	844.2200	902.1817	887.1143	800.3622	649.9766	451.7298	233.6501
227	15-Aug	117.2672	323.6220	538.6821	720.0981	845.9201	903.7879	888.4620	801.3085	650.4097	451.5855	232.9775
228	16-Aug	117.5604	324.5278	540.0481	721.7280	847.6232	905.3838	889.7862	802.2194	650.7975	451.3899	232.2548
229	17-Aug	117.8752	325.4608	541.4368	723.3710	849.3272	906.9675	891.0852	803.0933	651.1389	451.1421	231.4819
230	18-Aug	118.2114	326.4200	542.8467	725.0252	851.0302	908.5370	892.3571	803.9285	651.4326	450.8416	230.6586
231	19-Aug	118.5685	327.4044	544.2761	726.6889	852.7301	910.0902	893.6000	804.7237	651.6776	450.4877	229.7851
232	20-Aug	118.9461	328.4129	545.7234	728.3600	854.4249	911.6252	894.8122	805.4772	651.8729	450.0799	228.8613
233	21-Aug	119.3436	329.4443	547.1872	730.0366	856.1126	913.1400	895.9918	806.1877	652.0175	449.6178	227.8875
234	22-Aug	119.7605	330.4974	548.6656	731.7169	857.7911	914.6326	897.1372	806.8538	652.1104	449.1010	226.8637
235	23-Aug	120.1963	331.5709	550.1569	733.3987	859.4584	916.1010	898.2466	807.4743	652.1509	448.5291	225.7904
236	24-Aug	120.6502	332.6635	551.6595	735.0802	861.1124	917.5434	899.3184	808.0477	652.1382	447.9020	224.6678
237	25-Aug	121.1217	333.7740	553.1714	736.7592	862.7511	918.9578	900.3509	808.5730	652.0716	447.2195	223.4965
238	26-Aug	121.6101	334.9008	554.6908	738.4339	864.3723	920.3423	901.3427	809.0490	651.9504	446.4816	222.2769
239	27-Aug	122.1145	336.0425	556.2160	740.1020	865.9742	921.6951	902.2921	809.4747	651.7741	445.6882	221.0096
240	28-Aug	122.6341	337.1976	557.7449	741.7615	867.5546	923.0143	903.1977	809.8490	651.5423	444.8395	219.6954
241	29-Aug	123.1683	338.3645	559.2757	743.4104	869.1115	924.2982	904.0581	810.1709	651.2545	443.9356	218.3350
242	30-Aug	123.7160	339.5418	560.8063	745.0466	870.6429	925.5450	904.8720	810.4397	650.9104	442.9767	216.9291

Date	Day \ Time	7.00	8.00	9.00	10.00	11.00	12.00	13.00	14.00	15.00	16.00	17.00
243	31-Aug	124.2763	340.7276	562.3349	746.6680	872.1469	926.7531	905.6379	810.6545	650.5099	441.9633	215.4788
244	1-Sep	124.8483	341.9205	563.8594	748.2726	873.6215	927.9207	906.3548	810.8146	650.0527	440.8957	213.9850
245	2-Sep	125.4310	343.1186	565.3777	749.8582	875.0648	929.0462	907.0213	810.9194	649.5389	439.7745	212.4488
246	3-Sep	126.0234	344.3202	566.8879	751.4227	876.4748	930.1280	907.6365	810.9682	648.9683	438.6002	210.8713
247	4-Sep	126.6243	345.5236	568.3879	752.9642	877.8497	931.1647	908.1992	810.9607	648.3412	437.3735	209.2537
248	5-Sep	127.2327	346.7269	569.8756	754.4806	879.1877	932.1548	908.7085	810.8965	647.6577	436.0952	207.5973
249	6-Sep	127.8473	347.9283	571.3491	755.9698	880.4870	933.0969	909.1635	810.7751	646.9181	434.7661	205.9035
250	7-Sep	128.4670	349.1260	572.8061	757.4299	881.7458	933.9896	909.5634	810.5964	646.1228	433.3871	204.1736
251	8-Sep	129.0906	350.3181	574.2447	758.8589	882.9624	934.8317	909.9074	810.3602	645.2722	431.9592	202.4092
252	9-Sep	129.7168	351.5027	575.6628	760.2547	884.1352	935.6220	910.1949	810.0665	644.3668	430.4836	200.6119
253	10-Sep	130.3444	352.6778	577.0583	761.6156	885.2626	936.3592	910.4253	809.7152	643.4074	428.9613	198.7831
254	11-Sep	130.9719	353.8416	578.4293	762.9396	886.3430	937.0424	910.5981	809.3066	642.3945	427.3936	196.9246
255	12-Sep	131.5981	354.9922	579.7736	764.2248	887.3749	937.6706	910.7128	808.8407	641.3290	425.7819	195.0382
256	13-Sep	132.2216	356.1276	581.0893	765.4694	888.3569	938.2428	910.7692	808.3180	640.2118	424.1275	193.1256
257	14-Sep	132.8410	357.2458	582.3744	766.6718	889.2877	938.7581	910.7670	807.7386	639.0439	422.4319	191.1887
258	15-Sep	133.4549	358.3449	583.6269	767.8301	890.1658	939.2159	910.7059	807.1032	637.8262	420.6966	189.2292
259	16-Sep	134.0618	359.4230	584.8450	768.9427	890.9902	939.6153	910.5860	806.4122	636.5600	418.9232	187.2493
260	17-Sep	134.6604	360.4782	586.0266	770.0079	891.7595	939.9559	910.4073	805.6664	635.2463	417.1134	185.2508
261	18-Sep	135.2491	361.5086	587.1700	771.0243	892.4728	940.2370	910.1698	804.8663	633.8866	415.2689	183.2357
262	19-Sep	135.8266	362.5123	588.2733	771.9904	893.1290	940.4583	909.8738	804.0128	632.4821	413.3915	181.2061
263	20-Sep	136.3912	363.4873	589.3349	772.9046	893.7272	940.6194	909.5194	803.1068	631.0343	411.4830	179.1641
264	21-Sep	136.9417	364.4319	590.3528	773.7656	894.2665	940.7200	909.1071	802.1493	629.5447	409.5454	177.1118

Date	Day\Time	7.00	8.00	9.00	10.00	11.00	12.00	13.00	14.00	15.00	16.00	17.00
265	22-Sep	137.4764	365.3442	591.3255	774.5722	894.7461	940.7599	908.6372	801.1412	628.0149	407.5806	175.0512
266	23-Sep	137.9940	366.2225	592.2513	775.3231	895.1653	940.7390	908.1104	800.0838	626.4464	405.5905	172.9846
267	24-Sep	138.4929	367.0650	593.1287	776.0171	895.5235	940.6573	907.5272	798.9781	624.8411	403.5773	170.9141
268	25-Sep	138.9718	367.8699	593.9562	776.6531	895.8201	940.5150	906.8883	797.8256	623.2006	401.5431	168.8418
269	26-Sep	139.4292	368.6356	594.7323	777.2303	896.0548	940.3120	906.1945	796.6275	621.5269	399.4899	166.7699
270	27-Sep	139.8636	369.3605	595.4556	777.7475	896.2271	940.0488	905.4467	795.3853	619.8216	397.4198	164.7006
271	28-Sep	140.2738	370.0429	596.1249	778.2040	896.3368	939.7255	904.6458	794.1004	618.0869	395.3352	162.6361
272	29-Sep	140.6583	370.6814	596.7388	778.5990	896.3836	939.3428	903.7928	792.7744	616.3246	393.2383	160.5784
273	30-Sep	141.0158	371.2745	597.2962	778.9318	896.3675	938.9009	902.8887	791.4089	614.5368	391.1311	158.5299
274	1-Oct	141.3450	371.8206	597.7961	779.2019	896.2885	938.4006	901.9349	790.0056	612.7255	389.0161	156.4925
275	2-Oct	141.6446	372.3186	598.2373	779.4086	896.1465	937.8425	900.9324	788.5662	610.8929	386.8956	154.4685
276	3-Oct	141.9134	372.7671	598.6190	779.5517	895.9418	937.2273	899.8826	787.0925	609.0410	384.7717	152.4598
277	4-Oct	142.1502	373.1648	598.9403	779.6306	895.6747	936.5559	898.7870	785.5864	607.1721	382.6468	150.4686
278	5-Oct	142.3539	373.5106	599.2004	779.6453	895.3453	935.8291	897.6468	784.0496	605.2883	380.5232	148.4969
279	6-Oct	142.5233	373.8034	599.3987	779.5955	894.9542	935.0481	896.4637	782.4842	603.3919	378.4032	146.5466
280	7-Oct	142.6575	374.0422	599.5345	779.4811	894.5019	934.2137	895.2391	780.8921	601.4850	376.2891	144.6197
281	8-Oct	142.7555	374.2261	599.6072	779.3022	893.9888	933.3272	893.9748	779.2754	599.5700	374.1833	142.7181
282	9-Oct	142.8162	374.3541	599.6165	779.0589	893.4158	932.3898	892.6724	777.6360	597.6492	372.0879	140.8437
283	10-Oct	142.8389	374.4255	599.5620	778.7513	892.7835	931.4027	891.3335	775.9760	595.7247	370.0054	138.9982
284	11-Oct	142.8228	374.4396	599.4435	778.3797	892.0927	930.3672	889.9601	774.2975	593.7989	367.9379	137.1834
285	12-Oct	142.7670	374.3957	599.2607	777.9445	891.3444	929.2848	888.5538	772.6028	591.8741	365.8877	135.4010
286	13-Oct	142.6710	374.2934	599.0135	777.4460	890.5395	928.1569	887.1166	770.8938	589.9525	363.8570	133.6525

Date	Day / Time	7.00	8.00	9.00	10.00	11.00	12.00	13.00	14.00	15.00	16.00	17.00
287	14-Oct	142.5342	374.1321	598.7021	776.8850	889.6790	926.9851	885.6504	769.1728	588.0365	361.8480	131.9396
288	15-Oct	142.3559	373.9114	598.3264	776.2618	888.7642	925.7709	884.1570	767.4420	586.1282	359.8629	130.2637
289	16-Oct	142.1358	373.6312	597.8866	775.5773	887.7961	924.5159	882.6386	765.7035	584.2301	357.9038	128.6263
290	17-Oct	141.8735	373.2911	597.3830	774.8322	886.7760	923.2218	881.0970	763.9596	582.3443	355.9729	127.0286
291	18-Oct	141.5687	372.8910	596.8159	774.0273	885.7053	921.8904	879.5342	762.2124	580.4730	354.0721	125.4720
292	19-Oct	141.2210	372.4310	596.1857	773.1637	884.5854	920.5233	877.9525	760.4641	578.6186	352.2035	123.9577
293	20-Oct	140.8305	371.9110	595.4931	772.2422	883.4176	919.1225	876.3537	758.7170	576.7830	350.3691	122.4868
294	21-Oct	140.3970	371.3312	594.7385	771.2639	882.2036	917.6898	874.7400	756.9732	574.9686	348.5708	121.0603
295	22-Oct	139.9205	370.6918	593.9226	770.2300	880.9447	916.2270	873.1135	755.2349	573.1775	346.8106	119.6793
296	23-Oct	139.4011	369.9931	593.0462	769.1418	879.6427	914.7360	871.4763	753.5043	571.4117	345.0902	118.3446
297	24-Oct	138.8391	369.2354	592.1102	768.0003	878.2993	913.2189	869.8305	751.7836	569.6733	343.4114	117.0571
298	25-Oct	138.2345	368.4194	591.1153	766.8072	876.9160	911.6775	868.1783	750.0749	567.9644	341.7760	115.8175
299	26-Oct	137.5878	367.5454	590.0627	765.5636	875.4947	910.1139	866.5216	748.3802	566.2869	340.1856	114.6265
300	27-Oct	136.8994	366.6141	588.9533	764.2711	874.0371	908.5301	864.8628	746.7018	564.6427	338.6420	113.4847
301	28-Oct	136.1698	365.6263	587.7883	762.9312	872.5451	906.9281	863.2038	745.0416	563.0339	337.1466	112.3927
302	29-Oct	135.3995	364.5827	586.5689	761.5454	871.0206	905.3100	861.5468	743.4018	561.4622	335.7010	111.3509
303	30-Oct	134.5892	363.4841	585.2963	760.1154	869.4653	903.6777	859.8939	741.7843	559.9294	334.3066	110.3599
304	31-Oct	133.7396	362.3315	583.9718	758.6428	867.8814	902.0335	858.2472	740.1910	558.4373	332.9648	109.4198
305	1-Nov	132.8514	361.1259	582.5969	757.1294	866.2706	900.3793	856.6086	738.6241	556.9876	331.6770	108.5311
306	2-Nov	131.9256	359.8683	581.1730	755.5769	864.6350	898.7172	854.9804	737.0853	555.5820	330.4444	107.6939
307	3-Nov	130.9631	358.5599	579.7014	753.9871	862.9765	897.0492	853.3644	735.5765	554.2220	329.2683	106.9085
308	4-Nov	129.9649	357.2018	578.1839	752.3618	861.2972	895.3776	851.7628	734.0995	552.9093	328.1497	106.1749

Date	Day Time	7.00	8.00	9.00	10.00	11.00	12.00	13.00	14.00	15.00	16.00	17.00
309	5-Nov	128.9321	355.7954	576.6220	750.7029	859.5991	893.7042	850.1774	732.6562	551.6452	327.0897	105.4934
310	6-Nov	127.8657	354.3420	575.0173	749.0123	857.8842	892.0312	848.6102	731.2482	550.4312	326.0895	104.8639
311	7-Nov	126.7670	352.8428	573.3715	747.2919	856.1546	890.3606	847.0632	729.8773	549.2687	325.1498	104.2865
312	8-Nov	125.6372	351.2994	571.6864	745.5436	854.4123	888.6945	845.5383	728.5450	548.1590	324.2717	103.7611
313	9-Nov	124.4777	349.7133	569.9637	743.7695	852.6594	887.0348	844.0372	727.2531	547.1034	323.4559	103.2876
314	10-Nov	123.2898	348.0859	568.2052	741.9714	850.8979	885.3836	842.5619	726.0029	546.1030	322.7032	102.8661
315	11-Nov	122.0749	346.4188	566.4127	740.1515	849.1298	883.7427	841.1141	724.7961	545.1589	322.0143	102.4964
316	12-Nov	120.8344	344.7137	564.5882	738.3117	847.3573	882.1143	839.6955	723.6340	544.2722	321.3899	102.1783
317	13-Nov	119.5699	342.9723	562.7335	736.4541	845.5824	880.5002	838.3078	722.5181	543.4440	320.8305	101.9118
318	14-Nov	118.2829	341.1962	560.8506	734.5806	843.8070	878.9022	836.9527	721.4496	542.6751	320.3366	101.6966
319	15-Nov	116.9750	339.3871	558.9413	732.6934	842.0333	877.3224	835.6319	720.4299	541.9665	319.9087	101.5326
320	16-Nov	115.6477	337.5469	557.0077	730.7944	840.2631	875.7624	834.3469	719.4601	541.3189	319.5472	101.4196
321	17-Nov	114.3026	335.6773	555.0517	728.8859	838.4986	874.2242	833.0991	718.5414	540.7331	319.2524	101.3574
322	18-Nov	112.9415	333.7803	553.0754	726.9696	836.7417	872.7095	831.8902	717.6750	540.2097	319.0246	101.3458
323	19-Nov	111.5660	331.8575	551.0806	725.0479	834.9943	871.2201	830.7215	716.8618	539.7495	318.8639	101.3845
324	20-Nov	110.1777	329.9109	549.0696	723.1225	833.2584	869.7576	829.5944	716.1028	539.3529	318.7706	101.4734
325	21-Nov	108.7783	327.9425	547.0442	721.1957	831.5358	868.3238	828.5103	715.3990	539.0204	318.7447	101.6122
326	22-Nov	107.3696	325.9540	545.0064	719.2694	829.8285	866.9201	827.4703	714.7513	538.7525	318.7862	101.8007
327	23-Nov	105.9531	323.9475	542.9585	717.3455	828.1383	865.5484	826.4758	714.1604	538.5496	318.8952	102.0388
328	24-Nov	104.5307	321.9249	540.9023	715.4262	826.4670	864.2100	825.5280	713.6271	538.4119	319.0716	102.3261
329	25-Nov	103.1039	319.8881	538.8398	713.5133	824.8164	862.9065	824.6278	713.1520	538.3397	319.3151	102.6624
330	26-Nov	101.6744	317.8390	536.7732	711.6089	823.1883	861.6393	823.7765	712.7359	538.3332	319.6257	103.0475

Date	Day\Time	7.00	8.00	9.00	10.00	11.00	12.00	13.00	14.00	15.00	16.00	17.00
331	27-Nov	100.2438	315.7797	534.7044	709.7148	821.5844	860.4098	822.9750	712.3792	538.3924	320.0031	103.4812
332	28-Nov	98.8138	313.7121	532.6354	707.8330	820.0063	859.2195	822.2242	712.0826	538.5176	320.4470	103.9633
333	29-Nov	97.3859	311.6382	530.5683	705.9654	818.4558	858.0695	821.5251	711.8463	538.7085	320.9570	104.4934
334	30-Nov	95.9617	309.5598	528.5049	704.1137	816.9345	856.9613	820.8786	711.6709	538.9653	321.5328	105.0714
335	1-Dec	94.5426	307.4790	526.4474	702.2799	815.4438	855.8959	820.2853	711.5565	539.2878	322.1738	105.6970
336	2-Dec	93.1303	305.3977	524.3975	700.4657	813.9854	854.8746	819.7461	711.5036	539.6757	322.8796	106.3699
337	3-Dec	91.7260	303.3178	522.3573	698.6730	812.5607	853.8984	819.2616	711.5123	540.1289	323.6496	107.0900
338	4-Dec	90.3312	301.2413	520.3287	696.9034	811.1713	852.9685	818.8324	711.5828	540.6470	324.4831	107.8568
339	5-Dec	88.9471	299.1700	518.3136	695.1586	809.8184	852.0858	818.4591	711.7151	541.2298	325.3796	108.6701
340	6-Dec	87.5751	297.1059	516.3138	693.4404	808.5034	851.2513	818.1421	711.9093	541.8767	326.3384	109.5296
341	7-Dec	86.2163	295.0508	514.3311	691.7503	807.2277	850.4659	817.8820	712.1653	542.5873	327.3585	110.4350
342	8-Dec	84.8720	293.0066	512.3675	690.0900	805.9925	849.7305	817.6791	712.4830	543.3612	328.4394	111.3859
343	9-Dec	83.5431	290.9751	510.4247	688.4611	804.7990	849.0458	817.5337	712.8624	544.1976	329.5800	112.3819
344	10-Dec	82.2307	288.9582	508.5043	686.8650	803.6484	848.4126	817.4462	713.3031	545.0960	330.7794	113.4226
345	11-Dec	80.9357	286.9575	506.6083	685.3032	802.5419	847.8315	817.4166	713.8050	546.0557	332.0369	114.5077
346	12-Dec	79.6591	284.9750	504.7383	683.7771	801.4804	847.3032	817.4452	714.3676	547.0760	333.3512	115.6366
347	13-Dec	78.4016	283.0122	502.8959	682.2883	800.4651	846.8283	817.5320	714.9907	548.1559	334.7214	116.8088
348	14-Dec	77.1640	281.0710	501.0827	680.8380	799.4968	846.4073	817.6771	715.6738	549.2948	336.1464	118.0238
349	15-Dec	75.9470	279.1530	499.3005	679.4275	798.5766	846.0405	817.8805	716.4163	550.4916	337.6250	119.2811
350	16-Dec	74.7513	277.2599	497.5507	678.0581	797.7051	845.7286	818.1421	717.2177	551.7455	339.1560	120.5800
351	17-Dec	73.5772	275.3933	495.8350	676.7311	796.8834	845.4717	818.4616	718.0775	553.0553	340.7383	121.9198
352	18-Dec	72.4255	273.5547	494.1546	675.4475	796.1121	845.2702	818.8391	718.9949	554.4201	342.3705	123.3000

Date	Day Time	7.00	8.00	9.00	10.00	11.00	12.00	13.00	14.00	15.00	16.00	17.00
353	19-Dec	71.2964	271.7458	492.5113	674.2087	795.3920	845.1243	819.2740	719.9693	555.8388	344.0513	124.7196
354	20-Dec	70.1905	269.9681	490.9063	673.0155	794.7237	845.0342	819.7663	720.9998	557.3101	345.7793	126.1780
355	21-Dec	69.1079	268.2229	489.3410	671.8691	794.1078	845.0000	820.3155	722.0856	558.8330	347.5532	127.6742
356	22-Dec	68.0491	266.5119	487.8169	670.7705	793.5448	845.0218	820.9211	723.2259	560.4060	349.3715	129.2074
357	23-Dec	67.0143	264.8364	486.3351	669.7206	793.0353	845.0995	821.5827	724.4197	562.0280	351.2327	130.7766
358	24-Dec	66.0036	263.1978	484.8969	668.7204	792.5797	845.2332	822.2997	725.6660	563.6975	353.1353	132.3808
359	25-Dec	65.0173	261.5974	483.5036	667.7706	792.1784	845.4227	823.0716	726.9638	565.4132	355.0776	134.0190
360	26-Dec	64.0556	260.0365	482.1564	666.8720	791.8317	845.6678	823.8977	728.3119	567.1736	357.0581	135.6900
361	27-Dec	63.1185	258.5165	480.8563	666.0254	791.5399	845.9684	824.7772	729.7093	568.9772	359.0752	137.3926
362	28-Dec	62.2062	257.0385	479.6045	665.2316	791.3032	846.3241	825.7095	731.1548	570.8226	361.1271	139.1257
363	29-Dec	61.3187	255.6037	478.4020	664.4911	791.1218	846.7347	826.6937	732.6471	572.7081	363.2121	140.8880
364	30-Dec	60.4563	254.2133	477.2498	663.8046	790.9959	847.1996	827.7289	734.1848	574.6321	365.3284	142.6781
365	31-Dec	59.6190	252.8685	476.1489	663.1725	790.9254	847.7186	828.8142	735.7668	576.5930	367.4743	144.4946

Appendix B

Non-Linear Algorithm Equation Coefficient
Feedforward Neural Network

A) Compared Model
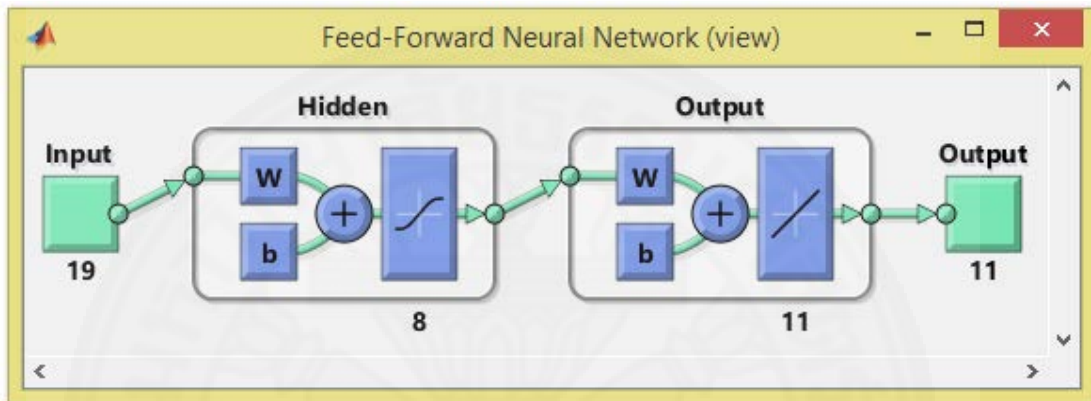
The output, y_n, is a function of Layer Weight, *LW*, and the result from Hidden Layer, *h*, that it can display in term of

$$y_n = (LW*h) + b_2$$

where $h = \text{tansig} ((IW*x_n) + b_1)$

Initial Weight is denoted as *IW* and the input is denoted as x_n.

The value of b_1 in the hidden layer is presented as follow:

b_1 = [41.1143 ; 54.4324 ; 40.5287 ; -40.2529 ; 38.0478 ; -70.2440 ; 33.9122 ; 10.2175]

For b_2 in the output layer, it can show as

b_2 = [-0.7320 ; -0.4733 ; -0.2379 ; -0.2891 ; -0.3083 ; 0.1235 ; 0.2334 ; 0.1008 ; 0.2047 ; -0.0082 ; 0.0147]

The last two coefficients of Compare Model, *LW* and *IW*, are described, respectively.

Layer Weight, LW(i,j) =

i \ j	1	2	3	4	5	6	7	8
1	-0.0199	1.8042	0.4540	-4.3092	-1.6989	-0.0170	-4.2839	-0.6496
2	0.0058	13.4173	0.3587	-19.8113	-13.3358	-0.0377	-19.7496	-0.9121
3	-0.0130	2.0489	0.1879	-27.7346	-2.0068	-0.0634	-27.5745	-0.6830
4	-0.0360	60.0913	0.3524	-35.9742	-60.0880	-0.0289	-35.8895	-1.1201
5	0.0084	17.0547	0.1866	-41.3241	-17.0951	-0.0787	-41.1373	-0.9072
6	0.2524	123.2457	-1.1696	-60.8428	-123.1729	0.2136	-60.2948	0.9473
7	0.2533	234.9227	-1.5364	-61.3716	-234.8684	0.2481	-60.7200	1.6378
8	0.1080	243.1228	-1.3489	-50.0061	-243.0656	0.2611	-49.4794	1.5871
9	-0.0144	189.9109	-1.3066	-42.4741	-189.8626	0.1443	-41.7904	1.9802
10	-0.0742	145.2277	-0.9514	-25.2337	-145.2473	0.1171	-24.6248	1.6424
11	0.0074	82.5222	-0.9630	-25.7025	-82.5031	0.0449	-25.0819	1.9573

Initial Weight, IW(i,j) =

i\j	1	2	3	4	5	6	7	8	9	10
1	192.365	-559.767	637.239	631.841	-200.983	-848.970	-511.913	361.287	1,074.137	1,010.259
2	-15.030	-411.779	616.992	358.012	-496.300	-257.641	213.969	28.967	294.380	-184.833
3	46.574	-445.487	610.012	88.080	-221.952	-178.734	-26.686	149.550	329.110	-285.204
4	-11.666	69.634	-76.097	-205.994	82.462	337.495	-87.960	-218.566	-258.385	304.436
5	-15.170	-422.552	783.758	-131.070	-22.644	-222.481	-258.058	342.803	292.041	-221.774
6	-521.852	-1,268.520	879.812	1,430.022	707.204	-483.403	-1,040.988	-812.329	-110.900	642.848
7	11.610	-72.445	107.830	146.974	-89.692	-198.515	-131.539	378.076	201.108	-294.812
8	14.915	-145.041	157.552	34.487	0.710	-40.427	-115.160	-0.723	269.966	-182.398

i\j	11	12	13	14	15	16	17	18	19
1	-1,211.174	-32.877	8.474	11.382	-4.618	16.681	-20.453	-3.007	-1.346
2	-4.481	11.855	9.928	-14.761	-0.118	-0.698	9.024	6.209	2.072
3	34.049	-1.386	0.209	-0.310	-0.553	1.402	-0.714	-0.212	-0.331
4	-14.080	-0.602	2.248	-0.206	-0.296	1.426	1.818	-0.089	-0.330
5	-1.626	11.857	9.936	-14.778	-0.118	-0.700	9.039	6.210	2.073
6	789.182	34.688	20.843	-98.673	-36.105	33.948	56.444	-3.946	-6.205
7	13.030	0.581	-2.266	0.220	0.306	-1.447	-1.831	0.091	0.337
8	33.055	-0.570	0.083	0.211	0.096	0.133	0.059	-0.091	-0.151

B) Designed Model

Stage1
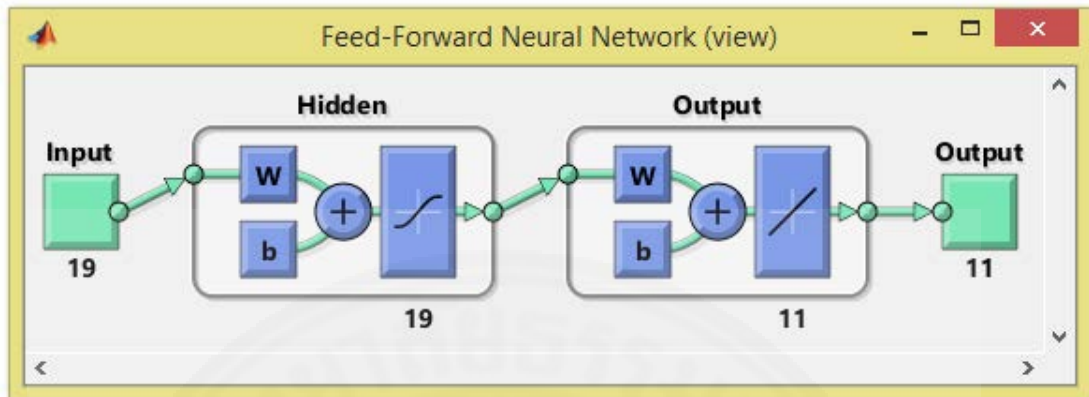
Coefficients in stage 1 of Designed Model consist of Initial Weight, *IW*, Layer Weight, *LW*, b_1 and b_2 same as Compared Model. They can be denoted as follow:

b_1 = [-4.7837 ; -7.7997 ; -13.7174 ; -46.5198 ; -32.0543 ; 3.0448 ; -1.1174 ; 2.6446 ; 0.3938 ; -55.7725 ; -1.6369 ; -7.5940 ; -2.5363 ; -1.2426 ; 56.7795 ; -21.2398 ; 2.8826 ; -1.1795 ; -3.3930]

b_2 = [-1.1989 ; -0.9757 ; -0.8530 ; -0.9910 ; -1.0838 ; -0.5135 ; -0.5552 ; 0.4937 ; -0.4795 ; -0.1952 ; -0.5455]

Layer Weight 1, $LW_1(i,j) =$

i\j	1	2	3	4	5	6	7	8	9	10
1	-0.145	-0.328	-0.072	0.088	-0.024	-0.012	1.018	1.022	0.006	0.080
2	-0.309	-0.025	-0.070	0.071	0.014	0.163	1.701	1.646	0.002	0.095
3	-0.346	-0.111	-0.090	0.115	0.009	0.232	2.744	2.685	0.001	0.117
4	-0.500	-0.169	-0.117	0.107	-0.028	0.238	1.197	1.048	-0.050	0.105
5	-0.612	0.008	-0.084	0.090	-0.150	0.210	-1.121	-1.402	0.059	0.143
6	-0.790	1.224	-0.212	-0.034	-0.081	0.548	5.529	5.506	0.172	0.272
7	-0.649	0.903	-0.220	0.069	0.119	0.803	12.803	13.240	0.179	0.188
8	-0.142	1.319	-0.126	0.194	0.169	0.678	14.718	15.389	0.032	0.067
9	-0.410	0.513	-0.066	0.188	0.169	0.506	7.775	8.249	0.212	-0.043
10	-0.278	0.611	0.013	0.046	0.067	0.284	3.682	3.964	0.170	-0.039
11	-0.199	0.385	-0.044	0.007	0.067	0.339	5.956	6.363	0.088	-0.005

Layer Weight 1, $LW_1(i,j) =$

i \ j	11	12	13	14	15	16	17	18	19
1	0.215	0.031	2.960	-0.201	-0.045	0.066	3.002	-0.336	-0.374
2	0.153	0.005	5.434	-0.261	-0.056	0.132	5.530	-0.350	-0.535
3	0.125	0.023	8.348	-0.236	-0.086	0.134	8.456	-0.267	-0.636
4	0.253	0.002	7.203	-0.355	-0.017	0.231	7.276	-0.335	-0.620
5	0.317	-0.102	10.455	-0.492	0.104	0.263	10.515	-0.397	-0.647
6	0.216	0.016	10.837	-0.363	-0.177	0.173	10.944	-0.579	-1.077
7	0.330	0.241	9.958	-0.520	-0.407	0.205	10.150	-0.797	-0.984
8	0.572	0.252	3.575	-0.634	-0.270	0.075	3.761	-0.517	-0.668
9	0.655	0.173	3.832	-0.783	-0.213	0.046	4.053	-0.506	-0.626
10	0.490	0.130	1.222	-0.496	-0.172	0.016	1.384	-0.224	-0.498
11	0.450	0.133	0.722	-0.397	-0.079	-0.014	0.895	-0.336	-0.369

Initial Weight 1, $IW_1(i,j) =$

i \ j	1	2	3	4	5	6	7	8	9	10
1	14.475	85.872	-47.297	-81.774	-40.668	33.343	72.067	53.620	-15.155	-108.882
2	-17.990	-2.129	8.569	11.991	9.081	1.981	-2.380	-5.398	-5.440	-5.331
3	-30.023	-21.036	-8.521	13.846	32.546	32.330	8.789	-27.694	-67.744	-92.668
4	-7.137	30.386	33.510	31.234	19.869	1.582	-13.206	-25.291	-31.418	-27.844
5	115.040	-93.546	-47.852	0.307	23.534	22.793	8.635	-9.299	-26.985	-43.161
6	15.641	40.370	-41.844	-53.842	-19.461	32.097	55.041	35.348	-24.107	-104.908
7	-3.281	-58.038	32.479	45.761	19.596	-15.792	-28.656	-20.069	-1.612	18.903
8	3.355	34.641	-9.864	-30.430	-23.642	3.583	23.510	24.175	4.265	-13.880
9	47.417	0.275	2.959	1.073	-4.465	-7.666	-3.536	7.914	23.267	36.706
10	69.226	-22.095	-8.409	4.490	11.043	10.911	8.326	1.504	-6.761	-18.491
11	31.658	-53.033	-15.332	14.166	23.618	17.044	4.118	-9.372	-30.060	-57.362
12	-58.835	76.452	34.691	-5.423	-26.954	-25.603	-5.318	15.092	31.537	36.276
13	17.667	-7.371	-15.750	-11.640	1.910	12.453	13.599	1.170	-23.145	-2.141
14	22.906	-48.967	-6.794	13.566	25.828	17.852	-5.189	-27.132	-29.976	-5.067
15	10.830	5.564	-2.042	-15.012	-24.281	-19.652	-1.026	24.562	52.043	63.341
16	-104.163	39.649	24.913	13.143	1.006	-9.871	-18.798	-30.338	-43.936	-51.617
17	-16.492	1.935	26.178	7.630	-8.401	-14.391	-1.749	6.900	0.469	10.042
18	-14.819	25.623	1.065	-7.302	-9.886	-5.488	2.873	9.309	12.002	7.014
19	1.008	-7.085	-5.130	-1.036	12.065	13.821	-4.599	-22.561	-15.753	27.899

Initial Weight 1, $IW_1(i,j) =$

i \ j	11	12	13	14	15	16	17	18	19
1	29.272	-0.990	0.024	0.500	-0.870	1.042	-1.783	-0.642	-0.131
2	11.125	-0.837	-1.778	-1.973	0.456	-2.950	0.494	0.663	-0.797
3	121.799	-24.638	20.112	2.446	-11.569	-3.827	15.526	-13.126	-1.599
4	42.798	154.471	-74.877	-32.506	-3.861	-9.934	68.699	-17.978	19.013
5	-26.524	33.169	-23.496	35.856	55.195	-66.408	90.982	-14.417	-12.544
6	47.666	-0.691	0.621	-0.292	-1.475	2.166	-1.448	-0.252	0.318
7	19.395	-1.280	3.439	-1.931	-1.377	3.824	-1.935	-1.057	0.380
8	-19.890	1.232	-3.257	1.826	1.274	-3.513	1.775	1.004	-0.345
9	-33.486	-23.579	-122.313	92.345	28.499	-64.039	-90.248	-17.916	-2.524
10	-78.000	-4.015	6.304	99.465	-68.531	135.442	-71.899	-44.276	-22.862
11	65.518	2.507	1.417	-6.236	6.034	-10.098	10.929	-0.969	1.769
12	-34.606	-3.508	24.953	-3.916	7.445	-19.263	3.383	-4.202	-3.838
13	1.333	-1.420	3.496	0.941	5.527	-3.164	3.332	-0.943	-2.610
14	36.455	-0.206	0.992	-4.264	3.389	-5.899	8.564	0.199	1.913
15	-101.933	16.091	-1.514	33.168	-48.041	10.056	-32.627	6.898	-11.491
16	95.891	56.737	-25.576	-3.080	-17.836	-5.449	14.855	-1.679	7.447
17	-0.518	1.302	-3.271	-1.040	-5.331	2.966	-3.214	0.945	2.540
18	-20.597	0.318	0.332	0.909	-1.371	1.559	-1.249	0.059	0.652
19	-1.502	-1.320	0.739	-1.694	0.508	0.912	0.171	0.180	0.018

Stage 2
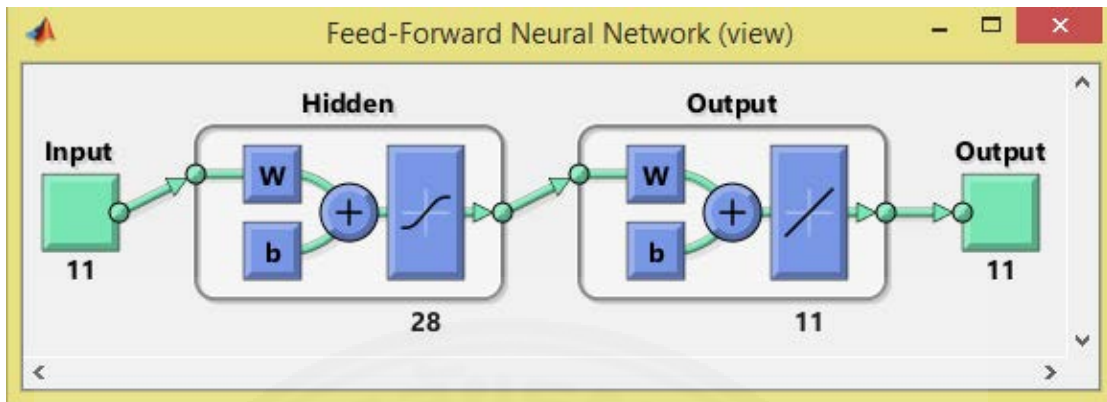
In the second stage, type of Coefficients will be denoted same as the first stage which are displayed as follow:

b_1 = [9.3551 ; 11.6969 ; 0.3520 ; 2.2035 ; 9.9308 ; 0.1979 ; -0.3987 ;

-0.1103 ; -0.3467 ; -0.0855 ; -0.0288 ; -0.0285 ; 0.2009 ; -0.7801 ;

0.0081 ; 0.0092 ; -0.0640 ; -0.0277 ; 2.9027 ; 0.1511 ; 1.2298 ;

-3.6791 ; 4.1575 ; -15.2126 ; -1.3121 ; -0.7086 ; 3.8056 ; -3.8267]

b_2 = [2.4056 ; 1.1520 ; 0.4911 ; 0.0487 ; -1.4353 ; -2.1804 ; -1.2297 ;

-0.4246 ; 0.8376 ; -0.0780 ; -1.8138]

Layer Weight 2, $LW_2(i,j)$ =

i＼j	1	2	3	4	5	6	7	8	9	10
1	0.237	0.590	0.178	-0.315	-0.330	1.104	-1.707	0.360	1.141	-3.734
2	0.254	-0.209	-0.138	-0.049	-0.306	0.462	-2.344	0.897	1.911	-1.719
3	0.596	-0.567	0.508	-0.342	-0.713	1.808	-3.292	2.768	1.457	-3.430
4	0.991	-0.662	1.531	-0.430	-1.196	2.391	-3.557	3.790	1.242	-5.614
5	1.066	-0.587	2.038	-1.040	-1.266	4.857	-3.349	6.309	0.253	-4.024
6	1.441	-0.937	2.376	-1.233	-1.763	5.542	-4.440	5.408	-6.306	-4.375
7	1.137	-0.933	2.109	-0.940	-1.453	4.705	-4.573	3.601	3.483	-3.580
8	0.828	-1.115	1.751	-0.606	-0.936	3.152	-6.845	3.684	2.424	-1.866
9	0.845	-0.844	2.424	-0.555	-0.991	3.091	-3.953	1.236	2.511	-3.448
10	0.456	-0.514	1.092	-0.433	-0.532	2.561	-1.665	-1.177	2.934	-0.842
11	0.443	-0.363	-0.136	-0.553	-0.524	2.741	-1.212	-0.890	-0.169	-2.939

Layer Weight 2, $LW_2(i,j)$ =

i/j	11	12	13	14	15	16	17	18	19	20
1	-3.693	-1.144	-2.729	-0.734	5.940	-4.195	1.207	-1.807	-0.002	-0.459
2	-2.301	-0.534	-0.547	-0.711	1.247	-0.278	-1.267	-0.923	-0.004	1.649
3	-4.885	-2.796	0.170	-1.056	-3.203	0.045	-1.329	-1.294	-0.009	3.131
4	-2.618	-3.879	0.345	-1.751	-4.513	-0.061	-2.030	-3.355	-0.013	4.937
5	-4.924	-6.111	6.478	-1.957	-4.360	-0.161	-1.772	-4.427	-0.014	5.797
6	-5.306	-7.583	-0.705	-2.406	-5.757	-0.265	-2.571	-6.046	-0.015	6.622
7	-3.594	-7.022	-0.880	-1.777	-6.263	0.205	-2.986	-5.099	-0.013	5.077
8	-1.554	-3.551	1.199	-2.562	-4.736	-0.016	-3.272	-4.368	-0.013	2.110
9	-6.146	-2.758	-0.711	-2.005	-3.694	-0.071	-2.700	-4.337	-0.013	4.341
10	-1.429	-2.179	-2.805	-1.155	-3.235	0.123	-1.651	-0.716	-0.010	6.360
11	-1.858	-1.046	1.364	-0.750	-1.444	-0.013	-1.016	-2.300	-0.005	-1.218

Layer Weight 2, $LW_2(i,j)$ =

i \ j	21	22	23	24	25	26	27	28		
1	-0.160	0.013	0.014	2.939	0.082	1.035	0.029	0.017		
2	-0.224	0.325	0.113	1.234	-0.119	1.031	0.325	0.118		
3	-0.318	0.563	0.209	0.785	0.267	1.516	0.561	0.218		
4	-0.330	0.742	0.260	0.448	0.865	2.521	0.734	0.272		
5	-0.307	0.794	0.308	0.152	1.142	2.817	0.784	0.323		
6	-0.414	0.791	0.390	0.214	1.339	3.439	0.782	0.408		
7	-0.437	0.780	0.383	-1.842	1.177	2.417	0.774	0.398		
8	-0.647	0.535	0.281	-0.470	0.953	3.719	0.532	0.291		
9	-0.375	0.814	0.301	0.567	1.364	2.888	0.807	0.314		
10	-0.155	0.576	0.233	-0.720	0.632	1.629	0.572	0.244		
11	-0.105	0.335	0.162	-1.374	-0.094	1.089	0.333	0.166		

Initial Weight 2, $IW_2(i,j)$ =

i \ j	1	2	3	4	5	6	7	8	9	10	11
1	1.965	-3.232	2.335	-0.522	0.063	-4.661	-3.431	1.888	0.271	-1.767	1.266
2	-3.505	-0.772	-3.434	-0.900	-0.817	2.344	-3.887	0.275	-1.893	-6.044	-2.369
3	-0.225	-0.124	-0.253	0.160	0.072	-0.008	0.250	0.006	0.477	-0.077	-0.232
4	0.225	-0.216	0.326	0.483	0.141	0.043	-0.434	0.003	0.204	-0.699	-0.619
5	0.058	0.575	1.960	-3.070	1.069	-2.380	-2.745	2.514	-1.610	-1.950	4.020
6	-0.075	0.049	-0.066	-0.158	-0.027	-0.001	0.163	0.001	-0.059	0.154	0.214
7	0.051	-0.096	-0.054	0.031	0.059	-0.122	-0.245	-0.197	-0.032	-0.004	0.071
8	0.009	0.028	0.028	-0.013	-0.044	-0.047	-0.013	-0.027	-0.084	-0.063	-0.045
9	0.011	-0.006	-0.006	-0.007	0.002	-0.109	0.025	-0.013	-0.005	0.008	0.000
10	0.065	-0.061	0.049	-0.257	0.027	0.012	-0.054	0.063	-0.027	0.033	-0.075
11	-0.020	0.030	-0.184	0.140	-0.012	0.001	0.064	0.057	-0.094	0.045	0.011
12	0.066	-0.045	-0.035	-0.002	-0.103	-0.041	-0.028	0.037	0.049	0.056	0.090
13	0.017	-0.011	-0.009	0.003	0.154	-0.033	-0.003	0.028	0.010	-0.002	0.008
14	0.075	0.157	-0.038	-0.092	-0.036	-0.008	0.982	-0.134	0.053	-0.123	-0.070

Initial Weight 2, $IW_2(i,j)$ =

i \ j	1	2	3	4	5	6	7	8	9	10	11
15	-0.120	0.344	-0.216	0.006	0.043	0.055	0.036	-0.039	0.071	-0.030	-0.038
16	-0.423	0.483	-0.251	0.074	-0.126	0.189	-0.051	-0.054	0.216	-0.119	0.009
17	-0.064	-0.276	0.038	0.010	-0.133	0.178	-0.180	0.138	0.045	0.024	-0.052
18	-0.146	-0.047	0.222	0.025	0.091	-0.064	-0.051	0.016	-0.026	0.118	-0.034
19	-2.509	3.765	-6.392	4.110	-3.407	-3.669	1.831	1.688	-3.551	-0.695	8.598
20	0.051	0.094	-0.063	0.025	0.028	0.044	0.014	-0.018	-0.039	0.106	-0.056
21	0.253	-0.355	-0.208	0.101	0.263	-0.430	-0.860	-0.656	-0.129	0.003	0.283
22	-3.348	2.686	-2.217	0.746	-2.892	4.630	-0.131	0.178	1.521	-1.054	-0.900
23	3.389	5.821	-1.300	0.433	2.155	-3.411	4.596	-3.005	0.040	0.203	-0.638
24	-3.598	8.575	3.671	2.490	-2.803	4.243	4.774	-6.366	-4.133	3.059	0.984
25	-0.316	-0.158	-0.369	0.230	0.103	-0.050	0.344	-0.003	0.641	-0.107	-0.331
26	-0.059	-0.119	0.021	0.078	0.024	-0.009	-0.805	0.094	-0.047	0.093	0.058
27	3.443	-2.759	2.274	-0.773	3.009	-4.808	0.177	-0.167	-1.548	1.080	0.936
28	-3.054	-5.470	1.268	-0.372	-2.048	3.171	-4.268	2.791	-0.003	-0.178	0.538

Appendix C

Non-Linear Algorithm Equation Coefficient
Nonlinear Autoregressive Network with Exogenous Inputs

A) Compared Model
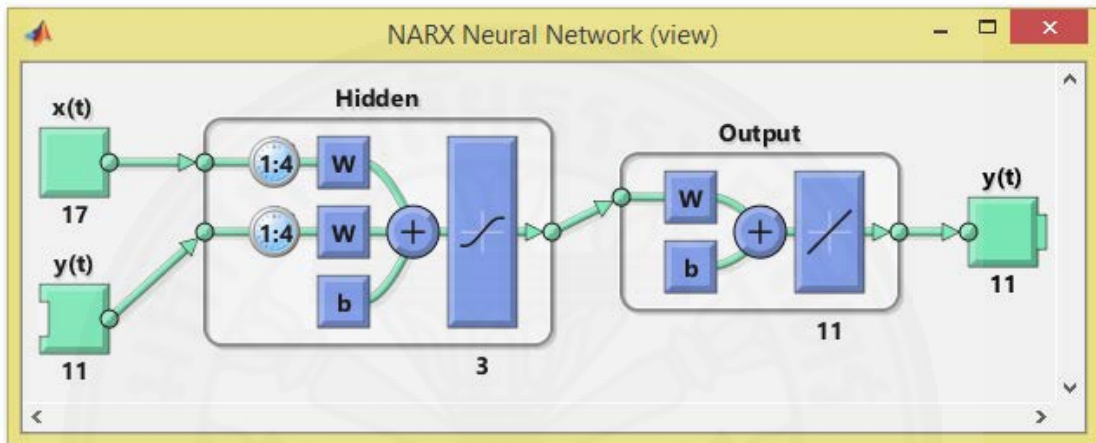
b_1 in hidden layer = [1.4236 ; 0.2827 ; 1.3476]

b_2 in output layer = [-0.5748 ; 0.4605 ; 0.0567 ; 0.7180 ; 0.7620 ; 0.9281 ;

0.0743 ; 0.4223 ; 0.6834 ; -0.1891 ; -0.0366]

Layer Weight in the output layer, $LW(i,j)$ =

i \ j	1	2	3
1	-0.1556	-0.4411	0.1715
2	-0.2932	-0.0133	-0.4907
3	-0.1378	-0.0640	0.0948
4	-0.3870	0.1489	-0.3683
5	-0.3270	0.3303	-0.5402
6	-0.1201	0.3732	-0.8640
7	-0.0613	0.2871	0.0231
8	0.2050	0.3268	-0.8229
9	-0.0394	0.4315	-0.7549
10	0.1385	0.3124	-0.0684
11	-0.6843	0.2478	0.4964

Initial Weight of input x(t), IW_1 (i,j) =

i\j	1	2	3	4	5	6	7	8	9	10
1	-0.2191	0.0867	-0.0110	-0.1601	-0.1138	-0.1634	0.2160	0.1489	-0.2337	0.1794
2	0.1090	0.1647	-0.1706	0.1009	0.0282	0.1966	0.1052	0.1858	0.1887	0.0465
3	0.1374	-0.0361	-0.1242	0.0578	-0.1109	0.0641	0.0536	0.2224	0.0271	-0.0530

i\j	11	12	13	14	15	16	17	18	19	20
1	0.0598	0.2016	0.1700	0.0603	0.1596	0.1299	-0.0206	-0.2455	0.1043	0.0409
2	-0.1460	-0.1140	-0.0730	-0.2618	-0.0996	0.0983	0.0616	0.2717	-0.1312	-0.2117
3	-0.0545	0.0439	-0.1175	0.1077	-0.0400	0.1238	-0.0614	0.0217	0.0681	0.0994

i\j	21	22	23	24	25	26	27	28	29	30
1	-0.0499	-0.1025	-0.1140	0.0917	0.0996	-0.0339	0.1203	-0.2017	0.0047	-0.0550
2	-0.1908	-0.1328	-0.0899	-0.0675	0.0248	-0.1461	0.2038	-0.0056	-0.0396	-0.3326
3	0.0423	-0.0928	-0.1763	0.0467	0.0356	0.0048	-0.1063	0.0670	0.0008	-0.2774

i\j	31	32	33	34	35	36	37	38	39	40
1	-0.1391	-0.1938	0.0641	0.1278	0.0468	-0.0916	0.1826	-0.0571	-0.1709	0.2035
2	0.0882	0.0986	0.0454	0.1604	0.1063	-0.1638	-0.0855	0.0005	0.1913	-0.0316
3	0.1076	-0.0309	-0.0015	-0.0754	-0.0997	-0.1622	-0.0398	0.1244	0.0794	0.0187

Initial Weight of input x(t), IW_1 (i,j) =

i \ j	41	42	43	44	45	46	47	48	49	50
1	-0.1661	-0.0656	0.2002	0.1752	-0.1014	-0.1984	-0.2666	-0.2201	0.1325	-0.1867
2	-0.1357	0.1857	0.0201	-0.0940	0.0581	0.0610	-0.1990	-0.0529	0.0337	0.0128
3	0.1112	-0.1521	0.1149	-0.0274	0.1632	-0.2659	-0.0545	0.2076	0.0088	-0.0143

i \ j	51	52	53	54	55	56	57	58	59	60
1	-0.0057	-0.1527	0.1450	-0.1927	0.2119	-0.0262	0.2836	-0.1503	0.0200	-0.1934
2	-0.0183	-0.0864	-0.1937	-0.0111	-0.1062	0.0367	-0.0169	-0.0666	0.1258	-0.1983
3	-0.0929	-0.0917	-0.0817	-0.1974	-0.1671	-0.1707	-0.0839	-0.1985	0.0766	0.1470

i \ j	61	62	63	64	65	66	67	68		
1	0.1363	0.0608	0.0822	0.0590	0.1075	-0.0017	0.1747	-0.0807		
2	0.0025	-0.1642	0.1213	0.1209	0.2262	-0.0349	-0.0295	0.0825		
3	-0.1619	-0.0666	-0.4509	0.1216	0.2220	-0.1839	0.0208	0.0518		

Initial Weight of output $y(t)$, $IW_2\,(i,j)\ =$

i \ j	1	2	3	4	5	6	7	8	9
1	-0.1567	-0.2994	0.0767	-0.2431	0.0188	0.0727	0.1603	-0.1124	0.3181
2	-0.0980	0.2261	0.0620	0.1017	-0.0725	0.0575	0.1852	-0.0910	0.1342
3	0.0066	0.2082	-0.1693	0.3270	-0.2214	-0.1322	0.2437	-0.1048	0.2032

i \ j	10	11	12	13	14	15	16	17	18
1	-0.0685	0.1992	0.0587	0.0711	0.0170	0.1672	0.0981	0.1981	-0.2067
2	-0.0984	0.0701	-0.1353	0.0071	-0.1987	-0.0259	-0.0030	0.0606	-0.1929
3	0.0078	-0.1345	-0.2293	-0.0290	-0.0368	0.0905	-0.1103	-0.0099	-0.0275

i \ j	19	20	21	22	23	24	25	26	27
1	0.0063	0.0055	-0.0918	-0.0509	0.0672	0.0258	-0.0337	0.1435	-0.1657
2	-0.0146	-0.0074	0.0826	-0.0220	0.0669	0.0388	-0.0822	-0.0266	0.1139
3	0.0435	-0.1051	-0.0445	-0.0244	-0.1182	-0.1480	0.0009	-0.1867	0.1815

i \ j	28	29	30	31	32	33	34	35	36
1	-0.2350	-0.0148	-0.0138	-0.0400	-0.1739	-0.0469	-0.0928	-0.0437	-0.0196
2	-0.1412	0.1737	-0.0274	-0.0317	-0.1396	-0.0525	0.0252	-0.0740	-0.0104
3	0.1552	-0.0101	-0.0110	0.0265	-0.1091	-0.0497	0.1822	0.0520	0.0834

Initial Weight of output $y(t)$, IW_2 (i,j) =

i \ j	37	38	39	40	41	42	43	44	
1	0.0071	-0.0453	-0.1053	0.0407	0.0723	0.1169	0.0397	-0.1302	
2	-0.1289	0.1529	-0.1563	-0.0272	0.0674	-0.0892	-0.0357	0.1053	
3	-0.0143	0.0747	-0.0193	-0.0408	0.1331	-0.0693	0.0434	0.1379	

B) Designed Model

Stage1
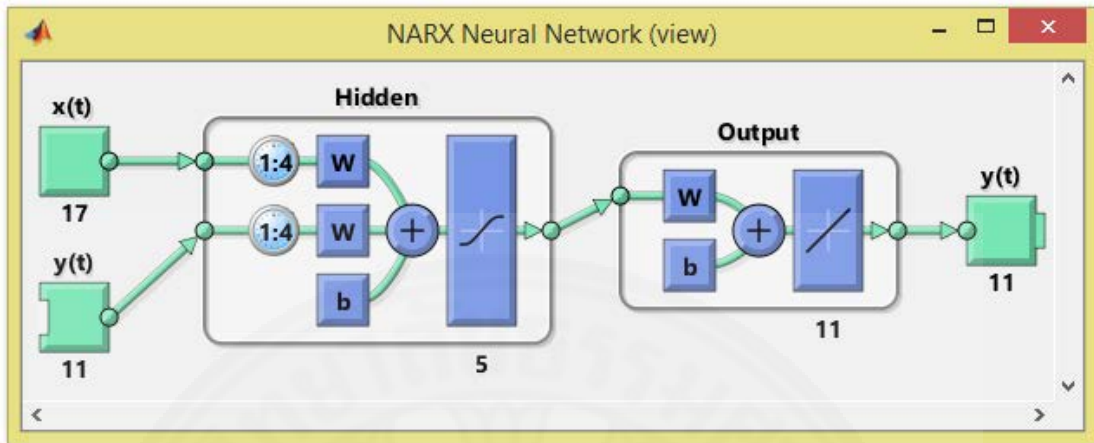
b_1 in the hidden layer = [1.0844 ; 0.6355 ; 0.3788 ; -0.9617 ; -1.4550]

b_2 in the output layer= [-1.1832 ; -0.0274 ; 0.1902 ; -0.0886 ; 0.2457 ;

0.2272 ; 0.5177 ; 0.2394 ; 0.0772 ; 0.2923 ;

-0.5975]

Layer Weight in the output layer, $LW_1(i,j)$ =

i \ j	1	2	3	4	5
1	-0.0152	0.3237	0.5516	-0.7469	-0.2577
2	-0.1848	-0.4356	0.1977	-0.0562	-0.1173
3	-0.3776	0.4145	0.1438	0.1396	0.0818
4	-0.2368	0.1647	0.3613	-0.3395	-0.0539
5	-0.4202	0.4862	0.5540	-0.6065	0.5147
6	-0.2231	0.4048	0.5119	-0.5424	0.5099
7	-0.4942	0.0706	0.3585	-0.2066	0.2008
8	-0.6392	0.5341	0.2047	-0.1264	0.2042
9	0.0876	-0.5726	0.3073	-0.2704	-0.1574
10	-0.4075	-0.4750	0.1299	-0.1767	0.0012
11	0.2517	0.1441	0.1783	0.1302	-0.3163

Initial Weight of input x(t), IW_{11} (i,j) =

i \ j	1	2	3	4	5	6	7	8	9	10
1	0.0415	-0.0111	-0.0506	-0.2662	-0.1020	0.0838	-0.0280	0.2370	-0.1137	-0.0031
2	-0.0703	0.0987	-0.1792	-0.0350	-0.1967	0.0715	-0.2697	-0.1389	-0.1788	0.2680
3	-0.0647	-0.0367	0.0160	0.2010	0.2342	0.0365	0.1703	0.0336	-0.1087	0.0091
4	-0.2294	0.0756	-0.0151	-0.0272	-0.1990	-0.0014	0.0544	0.0864	-0.0825	0.1273
5	0.0415	-0.0111	-0.0506	-0.2662	-0.1020	0.0838	-0.0280	0.2370	-0.1137	-0.0031

i \ j	11	12	13	14	15	16	17	18	19	20
1	-0.2217	-0.1429	-0.0147	0.0981	0.0398	-0.1439	-0.2730	-0.2227	0.0598	-0.1134
2	0.2356	-0.1692	-0.0923	0.0207	-0.0243	-0.0629	-0.1607	0.2932	0.1364	-0.1599
3	-0.0197	-0.2317	-0.2789	-0.1321	-0.2941	-0.0879	0.1643	-0.1552	0.1160	-0.3038
4	0.1000	0.0064	0.0143	0.1528	-0.1182	-0.0037	0.1863	0.1007	0.1145	-0.1474
5	-0.0492	-0.3408	0.1753	0.1087	-0.1095	0.0825	0.2192	0.1511	-0.2629	-0.0235

i \ j	21	22	23	24	25	26	27	28	29	30
1	0.2266	0.0515	-0.1949	0.0068	-0.0262	0.2144	-0.1616	0.1136	-0.2914	-0.1759
2	-0.0692	0.2195	-0.0650	0.1422	-0.1442	-0.0334	-0.1350	-0.2178	-0.0264	0.1586
3	-0.1115	0.0979	0.0946	0.0520	0.1310	0.2308	-0.0286	0.1763	0.1264	-0.2255
4	0.2346	-0.1164	-0.0625	-0.0457	0.1680	-0.0847	0.0454	0.1726	0.1504	-0.1867
5	0.1555	0.0470	-0.0381	0.0752	-0.0171	0.0201	0.1990	0.1578	-0.1511	-0.0899

Initial Weight of input x(t), IW_{11} (i,j) =

i\j	31	32	33	34	35	36	37	38	39	40
1	0.0894	0.0454	-0.0296	-0.0338	0.1067	0.0253	-0.1520	0.0569	0.0274	-0.1573
2	0.0039	-0.2313	-0.0509	-0.1351	-0.0870	0.1867	-0.0580	-0.0559	0.1718	0.0583
3	0.1251	-0.1657	0.2538	0.0403	0.0151	0.0797	0.1362	0.1564	-0.0708	0.2322
4	0.2097	-0.1218	0.3446	0.0961	-0.1892	0.0407	0.2137	-0.1991	0.0461	-0.0768
5	-0.1931	0.2644	0.1662	0.3685	0.0072	0.1133	0.0516	0.0915	0.1733	-0.0424

i\j	41	42	43	44	45	46	47	48	49	50
1	0.0257	0.0909	0.2447	-0.0998	-0.1373	-0.0374	-0.1057	0.1208	-0.3689	-0.0409
2	-0.0259	0.2275	-0.1935	0.0807	-0.1224	-0.0507	0.0801	-0.0607	0.2091	0.0390
3	0.1124	-0.0950	-0.0745	0.0601	-0.0925	0.0905	-0.2027	-0.0870	0.1913	0.2964
4	-0.1192	0.1008	0.0355	0.0190	-0.0918	-0.1124	0.0937	0.0622	-0.1505	0.2076
5	0.0464	0.1628	-0.0665	0.0987	0.0679	0.1549	0.0764	0.0378	-0.0297	-0.0743

i\j	51	52	53	54	55	56	57	58	59	60
1	0.0176	-0.1532	-0.0368	-0.0559	-0.0327	-0.3420	-0.0902	-0.0612	-0.0531	0.0759
2	0.1749	-0.0163	-0.1814	-0.1910	0.1102	-0.0839	-0.1336	0.2516	0.0504	-0.0806
3	-0.0068	-0.0547	0.1322	-0.1070	0.1915	0.1505	0.2665	0.1320	-0.1077	-0.1865
4	-0.1875	-0.0566	-0.1538	0.1050	-0.2662	-0.0084	0.0030	0.0563	0.0491	-0.0482
5	-0.1211	-0.1593	0.1403	0.1099	-0.0862	0.2265	-0.0330	0.0387	0.0598	-0.0279

Initial Weight of input x(t), IW_{11} (i,j) =

i j	61	62	63	64	65	66	67	68		
1	0.1871	0.1481	0.1381	-0.0006	-0.1626	-0.0044	-0.0202	0.0692		
2	0.0980	-0.1634	0.1245	0.0875	-0.0119	0.1630	-0.0838	0.0125		
3	0.0522	0.0875	0.4512	0.0096	-0.0345	0.1103	-0.0741	0.0066		
4	-0.1779	0.2916	0.0719	-0.0353	0.0893	0.0688	-0.0698	-0.1981		
5	-0.2182	-0.1613	0.2791	-0.0064	0.1959	0.2183	0.0992	-0.0268		

Initial Weight of output y(t), IW_{12} (i,j) =

i j	1	2	3	4	5	6	7	8	9
1	-0.2032	0.1005	-0.1131	-0.0897	0.1001	-0.1567	0.0031	-0.0369	-0.0196
2	0.0637	0.0303	0.2419	-0.0250	0.1053	-0.0976	-0.1336	0.1746	0.0215
3	0.1832	0.0775	0.1908	0.1757	0.0345	0.4176	0.0420	0.0885	-0.1298
4	-0.0093	-0.1010	-0.0634	0.1335	-0.0231	0.0889	0.0299	0.1641	-0.0775
5	-0.1862	-0.1445	-0.1108	-0.2848	-0.0477	-0.0014	0.2254	-0.0270	-0.0302

Initial Weight of output y(t), IW_{12} (i,j) =

i \ j	10	11	12	13	14	15	16	17	18
1	-0.1808	0.0849	0.1834	-0.0274	-0.1249	0.1562	-0.0613	0.2628	0.0397
2	-0.1513	0.0761	-0.1524	-0.0994	0.0569	0.1448	-0.0057	0.1107	0.0792
3	0.0598	0.1184	-0.0472	-0.1541	-0.3125	-0.0839	0.0316	-0.1072	0.0486
4	0.0076	0.0523	-0.0395	-0.1350	-0.3342	-0.0337	0.1014	0.0432	0.1231
5	-0.0673	0.0588	0.0678	0.1529	-0.1791	0.1776	0.1982	0.1632	-0.0357

i \ j	19	20	21	22	23	24	25	26	27
1	-0.1577	-0.1209	-0.0857	0.0989	0.2963	-0.1015	0.1452	-0.1228	0.3166
2	-0.2264	-0.0597	0.0954	-0.0294	0.0449	-0.1314	0.0444	0.0684	0.0766
3	0.0876	-0.0335	0.0023	-0.0435	0.3813	0.1613	0.0951	-0.0289	-0.1618
4	0.1873	-0.0621	-0.0324	-0.1301	0.2924	-0.0604	0.0639	0.0874	-0.0345
5	-0.0889	0.0078	-0.0809	-0.0073	0.2062	-0.0791	-0.2806	-0.0343	0.0123

Initial Weight of output y(t), IW_{12} (i,j) =

i \ j	28	29	30	31	32	33	34	35	36
1	0.1655	-0.0531	-0.0830	-0.0080	0.0239	0.0672	0.1086	0.0017	-0.0611
2	-0.0327	-0.0741	-0.0455	0.1257	-0.1541	0.0526	0.1122	0.0945	-0.0168
3	-0.1617	0.0023	0.1728	0.0265	0.1167	-0.2340	-0.1128	0.1522	0.0794
4	-0.1784	-0.2598	0.1167	-0.0132	0.2378	-0.1691	-0.1032	0.0090	0.0623
5	-0.0761	-0.0583	-0.0223	-0.1080	0.1673	-0.0640	0.1182	-0.0055	0.1432

i \ j	37	38	39	40	41	42	43	44
1	0.0998	-0.1193	-0.0983	-0.1891	0.0071	-0.0080	-0.2407	-0.1468
2	0.0124	0.0382	0.0275	-0.0679	-0.1293	0.0949	-0.2374	-0.0248
3	-0.2081	0.0195	-0.1449	-0.0099	0.0517	-0.2350	0.0415	0.2047
4	0.0395	0.0397	-0.0485	0.0849	-0.0360	-0.1894	0.0430	0.1852
5	0.1634	-0.2199	-0.2532	0.0253	-0.2111	0.0435	-0.1887	-0.1137

Stage 2
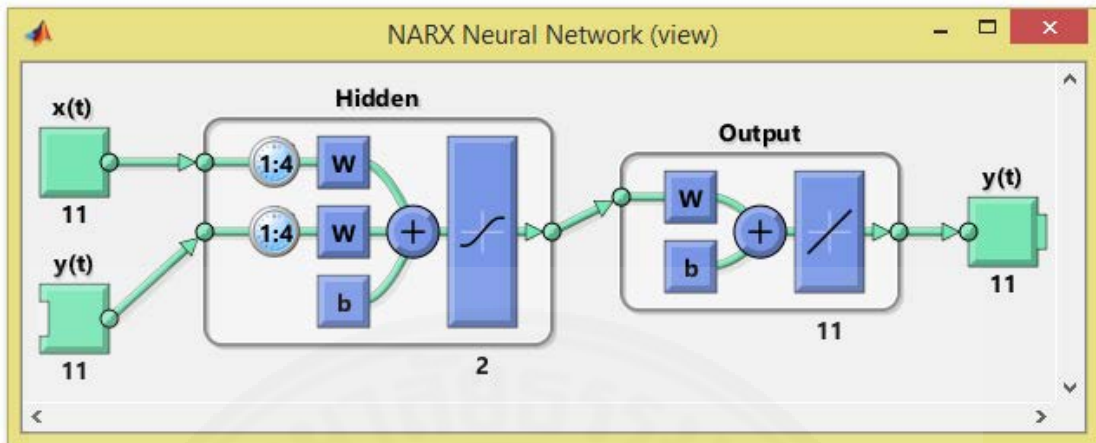
In the second stage, type of Coefficients will be denoted same as the first stage which are displayed as follow:

b_1 in the hidden layer = [0.7195 ; 1.8053]

b_2 in the output layer = [-0.8692 ; -0.6971 ; -0.3838 ; -0.3550 ; -0.3923 ;

-0.3526 ; -0.1230 ; -0.1942 ; 0.1058 ; -0.1520 ;

-0.1777]

Layer Weight in the output layer, $LW_2(i,j)$

i \ j	1	2
1	0.2477	0.2123
2	0.5297	0.1542
3	0.5800	-0.0425
4	0.5948	0.0582
5	0.8087	-0.1141
6	0.7139	-0.0427
7	0.4827	-0.2450
8	0.3866	-0.2825
9	0.1792	-0.4183
10	0.2075	-0.2948
11	0.0518	-0.1781

Initial Weight of input x(t), IW_{21} (i,j) =

i\j	1	2	3	4	5	6	7	8	9
1	0.0548	0.3996	-0.1238	0.3424	0.4528	0.1026	-0.2588	0.1782	0.0548
2	0.3206	-0.0903	-0.1950	-0.5356	-0.4746	0.6847	0.0177	-0.1378	0.3206

i\j	10	11	12	13	14	15	16	17	18
1	0.0843	-0.2351	-0.1883	0.0843	-0.0030	0.1360	0.0148	0.2101	0.0352
2	0.0032	0.2680	-0.0493	0.2261	0.2739	0.1730	0.1426	0.0840	-0.0955

i\j	19	20	21	22	23	24	25	26	27
1	0.0209	-0.0318	0.0851	0.2080	0.1820	0.1312	0.0286	0.2319	0.1285
2	-0.2198	0.0495	-0.2066	0.1311	-0.7894	-0.7035	-0.3772	-0.6708	-0.4259

i\j	28	29	30	31	32	33	34	35	36
1	0.2972	0.1010	0.4219	0.3610	0.1873	0.3119	-0.1360	0.3237	0.6179
2	-0.3279	0.2580	-0.3078	-0.5142	0.3694	0.0123	0.7240	-0.0684	-0.1509

i\j	37	38	39	40	41	42	43	44	
1	0.4554	0.2278	0.2424	-0.1054	0.1324	0.2908	-0.2407	-0.2131	
2	0.2413	-0.4805	-0.3866	-0.7926	0.1895	-0.1711	-0.1430	-0.3316	

Initial Weight of output y(t), IW_{22} (i,j) =

i \ j	1	2	3	4	5	6	7	8	9
1	-0.3849	0.2553	0.0004	-0.0155	-0.3339	-0.0655	0.0089	0.3367	-0.2643
2	0.5820	0.6016	0.1927	-0.1782	0.2679	-0.1457	-0.3512	-0.2529	0.2075

i \ j	10	11	12	13	14	15	16	17	18
1	-0.0517	0.0707	-0.0395	-0.2361	-0.0319	0.0037	0.1596	-0.2518	-0.0259
2	-0.7432	-0.3982	0.1922	-0.2385	-0.0606	0.0311	-0.1786	0.1495	-0.0776

i \ j	19	20	21	22	23	24	25	26	27
1	-0.1232	0.0024	0.0620	-0.0620	-0.3332	0.2712	-0.1347	-0.2606	-0.4323
2	0.4326	-0.2472	-0.2834	0.0960	1.4673	-0.0026	0.0882	0.5360	0.4386

i \ j	28	29	30	31	32	33	34	35	36
1	-0.4045	-0.0159	-0.3841	-0.2464	-0.3038	-0.4985	0.4957	-0.3031	-0.3500
2	1.0894	-0.4572	0.1577	0.5768	-0.2661	-0.2258	0.1541	0.0378	0.1127

i \ j	37	38	39	40	41	42	43	44	
1	-0.3493	-0.2821	0.2276	-0.1972	-0.0159	-0.4107	0.2308	0.1239	
2	0.3529	0.1069	0.7099	0.1780	-0.0687	0.4037	-0.1197	0.3977	